

2.5 GEOLOGY AND SEISMOLOGY

This section presents the findings of the regional and site-specific geologic and seismologic investigations of the Diablo Canyon Power Plant (DCPP) site. Information presented is in compliance with the criteria in Appendix A of 10 CFR 100 and meets the format and content recommendations of Regulatory Guide 1.70, Revision 1⁽³⁹⁾.

Location of earthquake epicenters within 200 miles of the plant site, and faults and earthquake epicenters within 75 miles of the plant site for either magnitudes or intensities, respectively, are shown in Figures 2.5-2, 2.5-3, and 2.5-4. A geologic and tectonic map of the region surrounding the site is given in two sheets of Figure 2.5-5, and detailed information about site geology is presented in Figures 2.5-8 through 2.5-16. Geology and seismology are discussed in detail in Sections 2.5.1 through 2.5.4. Additional information on site geology is contained in References 1 and 2.

On November 2, 1984, the NRC issued the Diablo Canyon Unit 1 Facility Operating License DPR-80. In DPR-80, License Condition Item 2.C.(7), the NRC stated, in part:

"PG&E shall develop and implement a program to reevaluate the seismic design bases used for the Diablo Canyon Power Plant."

PG&E's reevaluation effort in response to the license condition was titled the "Long Term Seismic Program" (LTSP). PG&E prepared and submitted to the NRC the "Final Report of the Diablo Canyon Long Term Seismic Program" in July 1988⁽⁴⁰⁾. Between 1988 and 1991, the NRC performed an extensive review of the Final Report, and PG&E prepared and submitted written responses to formal NRC questions. In February 1991, PG&E issued the "Addendum to the 1988 Final Report of the Diablo Canyon Long Term Seismic Program"⁽⁴¹⁾. In June 1991, the NRC issued Supplement Number 34 to the Diablo Canyon Safety Evaluation Report (SSER)⁽⁴²⁾, in which the NRC concluded that PG&E had satisfied License Condition 2.C.(7) of Facility Operating License DPR-80. In the SSER the NRC requested certain confirmatory analyses from PG&E, and PG&E subsequently submitted the requested analyses. The NRC's final acceptance of the LTSP is documented in a letter to PG&E dated April 17, 1992⁽⁴³⁾.

The LTSP contains extensive data bases and analyses that update the basic geologic and seismic information in this section of the FSAR Update. However, the LTSP material does not address or alter the current design licensing basis for the plant, and thus is not included in the FSAR Update. A complete listing of bibliographic references to the LTSP reports and other documents may be found in References 40, 41 and 42.

Detailed supporting data pertaining to this section are presented in Appendices 2.5A, 2.5B, 2.5C, and 2.5D of Reference 27 in Section 2.3. Geologic and seismic information from investigations that responded to Nuclear Regulatory Commission (NRC) licensing review questions are presented Appendices 2.5E and 2.5F of the same reference. A brief synopsis of the information presented in Reference 27 (Section 2.3) is given below.

DCPP UNITS 1 & 2 FSAR UPDATE

The DCP site is located in San Luis Obispo County approximately 190 miles south of San Francisco and 150 miles northwest of Los Angeles, California. It is adjacent to the Pacific Ocean, 12 miles west-southwest of the city of San Luis Obispo, the county seat. The plant site location and topography are shown in Figure 2.5-1.

The site is located near the mouth of Diablo Creek which flows out of the San Luis Range, the dominant feature to the northeast. The Pacific Ocean is southwest of the site. Facilities for the power plant are located on a marine terrace that is situated between the mountain range and the ocean.

The terrace is bedrock overlain by surficial deposits of marine and nonmarine origin. Seismic Category I structures at the site are situated on bedrock that is predominantly stratified marine sedimentary rocks and volcanics, all of Miocene age. A more extensive discussion of the regional geology is presented in Section 2.5.1.1 and site geology in Section 2.5.1.2.

Several investigations were performed at the site and in the vicinity of the site to determine: potential vibratory ground motion characteristics, existence of surface faulting, and stability of subsurface materials and cut slopes adjacent to Seismic Category I structures. Details of these investigations are presented in Sections 2.5.2 through 2.5.5. Consultants retained to perform these studies included: Earth Science Associates (geology and seismicity), John A. Blume and Associates (seismic design and foundation materials dynamic response), Harding-Lawson and Associates (stability of cut slope), Woodward-Clyde-Sherard and Associates (soil testing), and Geo-Recon, Incorporated (rock seismic velocity determinations). The findings of these consultants are summarized in this section and the detailed reports are included in Appendices 2.5A, 2.5B, 2.5C, 2.5D, 2.5E, and 2.5F of Reference 27 in Section 2.3.

Geologic investigation of the Diablo Canyon coastal area, including detailed mapping of all natural exposures and exploratory trenches, yielded the following basic conclusions:

- (1) The area is underlain by sedimentary and volcanic bedrock units of Miocene age. Within this area, the power plant site is underlain almost wholly by sedimentary strata of the Monterey Formation, which dip northward at moderate to very steep angles. More specifically, the reactor site is underlain by thick-bedded to almost massive Monterey sandstone that is well indurated and firm. Where exposed on the nearby hillslope, this rock is markedly resistant to erosion.
- (2) The bedrock beneath the main terrace area, within which the power plant site has been located, is covered by 3 to 35 feet of surficial deposits. These include marine sediments of Pleistocene age and nonmarine sediments of Pleistocene and Holocene age. In general, they are thickest in the vicinity of the reactor site.

DCPP UNITS 1 & 2 FSAR UPDATE

- (3) The interface between the unconsolidated terrace deposits and the underlying bedrock comprises flat to moderately irregular surfaces of Pleistocene marine planation and intervening steeper slopes that also represent erosion in Pleistocene time.
- (4) The bedrock beneath the power plant site occupies the southerly flank of a major syncline that trends west to northwest. No evidence of a major fault has been recognized within or near the coastal area, and bedrock relationships in the exploratory trenches positively indicate that no such fault is present within the area of the power plant site.
- (5) Minor surfaces of disturbance, some of which plainly are faults, are present within the bedrock that underlies the power plant site. None of these breaks offsets the interface between bedrock and the cover of terrace deposits, and none of them extends upward into the surficial cover. Thus, the latest movements along these small faults must have antedated erosion of the bedrock section in Pleistocene time.
- (6) No landslide masses or other gross expressions of ground instability are present within the power plant site or on the main hillslope east of the site. Some landslides have been identified in adjacent ground, but these are minor features confined to the naturally oversteepened walls of Diablo Canyon.
- (7) No water of subsurface origin was encountered in the exploratory trenches, and the level of permanent groundwater beneath the main terrace area probably is little different from that of the adjacent lower reaches of the deeply incised Diablo Creek.

2.5.1 BASIC GEOLOGIC AND SEISMIC INFORMATION

This section presents the basic geologic and seismic information for DCPD site and surrounding region. Information contained herein has been obtained from literature studies, field investigations, and laboratory testing and is to be used as a basis for evaluations required to provide a safe design for the facility. The basic data contained in this section and in Reference 27 of Section 2.3 are referenced in several other sections of this FSAR Update.

2.5.1.1 Regional Geology

2.5.1.1.1 Regional Physiography

Diablo Canyon is in the southern Coast Range which is a part of the California Coast Ranges section of the Pacific Border physiographic province (see Figure 2.5-1). The region surrounding the power plant site consists of mountains, foothills, marine terraces, and valleys. The dominant features are the San Luis Range adjacent to the site to the

DCPP UNITS 1 & 2 FSAR UPDATE

northeast, the Santa Lucia Range farther inland, the lowlands of the Los Osos and San Luis Obispo Valleys separating the San Luis and Santa Lucia Ranges, and the marine terrace along the coastal margin of the San Luis Range.

Landforms of the San Luis Range and the adjacent marine terrace produce the physiography at the site and in the region surrounding the site. The westerly end of the San Luis Range is a mass of rugged high ground that extends from San Luis Obispo Creek and San Luis Obispo Bay on the east and is bounded by the Pacific Ocean on the south and west. Except for its narrow fringe of coastal terraces, the range is featured by west-northwesterly-trending ridge and canyon topography. Ridge crest altitudes range from about 800 to 1800 feet. Nearly all of the slopes are steep, and they are modified locally by extensive slump and earthflow landslides.

Most of the canyons have narrow-bottomed, V-shaped cross sections. Alluvial fans and talus aprons are prominent features along the bases of many slopes and at localities where ravines debouch onto relatively gentle terrace surfaces. The coastal terrace belt extends between a steep mountain-front backscarp and a near-vertical sea cliff 40 to 200 feet in height. Both the bedrock benches of the terraces and the present offshore wave-cut bench are irregular in detail, with numerous basins and rock projections.

The main terrace along the coastal margin of the San Luis Range is a gently to moderately sloping strip of land as much as 2000 feet in maximum width. The more landward parts of its surface are defined by broad aprons of alluvial deposits. This cover thins progressively in a seaward direction and is absent altogether in a few places along the present sea cliff. The main terrace represents a series of at least three wave-cut rock benches that have approximate shoreline-angle elevations of 70, 100, and 120 feet.

Owing to both the prevailing seaward slopes of the rock surfaces and the variable thickness of overlying marine and nonmarine cover, the present surface of the main terrace ranges from 70 to more than 200 feet in elevation. Remnants of higher terraces exist at scattered locations along upper slopes and ridge crests. The most extensive among these is a series of terrace surfaces at altitudes of 300+, 400+, and 700+ feet at the west end of the ridge between Coon and Islay Creeks, north of Point Buchon. A surface described by Headlee⁽¹⁹⁾ as a marine terrace at an altitude of about 700 feet forms the top of San Luis Hill. Remnants of a lower terrace at an altitude of 30 to 45 feet are preserved at the mouth of Diablo Canyon and at several places farther north.

Owing to contrasting resistance to erosion among the various bedrock units of the San Luis Range, the detailed topography of the wave-cut benches commonly is very irregular. As extreme examples, both modern and fossil sea stacks rise as much as 100 feet above the general levels of adjacent marine-eroded surfaces at several localities.

2.5.1.1.2 Regional Geologic and Tectonic Setting

2.5.1.1.2.1 Geologic Setting

The San Luis Range is underlain by a synclinal section of Tertiary sedimentary and volcanic rocks, which have been downfolded into a basement of Mesozoic rocks now exposed along its southwest and northeast sides. Two zones of faulting have been recognized within the range. The Edna fault zone trends along its northeast side, and the Miguelito fault zone extends into the range from the vicinity of Avila Bay. Minor faults and bedding-plane shears can be seen in the parts of the section that are well exposed along the sea cliff fringing the coastal terrace benches. None of these faults shows evidence of geologically recent activity, and the most recent movements along those in the rocks underlying the youngest coastal terraces can be positively dated as older than 80,000 to 120,000 years. Geologic and tectonic maps of the region surrounding the site are shown in Figures 2.5-5 (2 sheets), 2.5-6, 2.5-8, and 2.5-9.

2.5.1.1.2.2 Tectonic Features of the Central Coastal Region

DCPP site lies within the southern Coast Ranges structural province, and approximately upon the centerline axis of the northwest-trending block of crust that is bounded by the San Andreas fault on the northeast and the continental margin on the southwest. This crustal block is characterized by northwest-trending structural and geomorphic features, in contrast to the west-trending features of the Transverse Ranges to the south. A major geologic boundary within the block is associated with the Sur-Nacimiento and Rinconada faults, which separate terrains of contrasting basement rock types. The ground southwest of the Sur-Nacimiento zone and the southerly half of the Rinconada fault, referred to as the Coastal Block, is underlain by Franciscan basement rocks of dominantly oceanic types, whereas that to the northeast, referred to as the Salinia Block, is underlain by granitic and metamorphic basement rocks of continental types. Page⁽¹⁰⁾ outlined the geology of the Coast Ranges, describing it generally in terms of "core complexes" of basement rocks and surrounding sections of younger sedimentary rocks. The principal Franciscan core complex of the southern Coast Range crops out on the coastal side of the Santa Lucia Range from the vicinity of San Luis Obispo to Point Sur, a distance of 120 miles. Its complex features reflect numerous episodes of deformation that evidently included folding, faulting, and the tectonic emplacement of extensive bodies of ultrabasic rocks. Other core complexes consisting of granitic and metamorphic basement rocks are exposed in the southern Coast Ranges in the ground between the Sur-Nacimiento and Rinconada and in the San Andreas fault zones. The locations of these areas of basement rock exposure are shown in Figure 2.5-6 and in Figure 1 of Appendix 2.5D of Reference 27 in Section 2.3.

Younger structural features include thick folded basins of Tertiary strata and the large faults that form structural boundaries between and within the core complexes and basins.

DCPP UNITS 1 & 2 FSAR UPDATE

The structure of the southern Coast Ranges has evolved during a lengthy history of deformation extending from the time when the ancestral Sur-Nacimiento zone was a site for subduction (a Benioff zone) along the then-existing continental margin, through subsequent parts of Cenozoic time when the San Andreas fault system was the principal expression of the regional stress-strain system. The latest episodes of major deformation involved folding and faulting of Pliocene and older sediments during mid-Pliocene time, and renewed movements along preexisting faults during early or mid-Pliocene time. Present tectonic activity within the region is dominated by interaction between the Pacific and American crustal plates on opposite sides of the San Andreas fault and by continuing vertical uplift of the Coast Ranges. In the regional setting of DCPD site, the major structural features are the San Andreas, Rinconada-San Marcos-Jolon, Sur-Nacimiento, and Santa Lucia Bank faults. The San Simeon fault may also be included with this group. These faults are described as follows:

1. San Andreas Fault

The San Andreas fault is recognized as a major transform fault of regional dimensions that forms an active boundary between the Pacific and North American crustal plates. Cumulative slip along the San Andreas fault may have amounted to several hundred miles, and a substantial fraction of the total slip has occurred during late Cenozoic time. The fault has spectacular topographic expression, generally lying within a rift valley or along an escarpment mountain front, and having associated sag ponds, low scarps, right-laterally deflected streams, and related manifestations of recent activity.

The most recent episode of large-scale movement along the reach of the San Andreas fault that is closest to the San Luis Range occurred during the great Fort Tejon earthquake of 1857. Geologic evidence pertinent to the behavior of the fault during this and earlier seismic events was studied in great detail by Wallace^(15, 32) who reported in terms of infrequent great earthquakes accompanied by ground rupture of 10 to 30 feet, with intervening periods of near total quiescence. Allen⁽¹⁶⁾ suggested that such behavior has been typical for this reach of the San Andreas fault and has been fundamentally different from the behavior of the fault along the reach farther northwest, where creep and numerous small earthquakes have occurred. He further suggested that release of accumulating strain energy might have been facilitated by the presence of large amounts of serpentine in the fault zone to the northwest, and retarded by the locking effect of the broad bend of the fault zone where it crosses the Transverse Ranges to the southeast.

Movement is currently taking place along large segments of the San Andreas fault. The active reach of the fault between Parkfield and San Francisco is currently undergoing relative movement of at least 3 to 4 cm/yr, as determined geodetically and analyzed by Savage and Burford⁽³³⁾. When the movement that occurs during the episodes of fault displacement in the western part of the Basin and Ranges Province is added to the minimum of 3 to 4 cm/yr of continuously and intermittently released strain, the total probably amounts to at least 5 to 6 cm/yr. This may account for essentially all of the relative motion between the Pacific and North American plates at present. In the

DCPP UNITS 1 & 2 FSAR UPDATE

Transverse Ranges to the south, this strain is distributed between lateral slip along the San Andreas system and east-west striking lateral slip faulting, thrust faulting, and folding. North of the latitude of Monterey Bay and south of the Transverse Ranges, transcurrent movement is again concentrated along the San Andreas system, but in those regions, it is distributed among several major strands of the system.

2. *Sur-Nacimiento Fault Zone*

The Sur-Nacimiento fault zone has been regarded as the system of faults that extends from the vicinity of Point Sur, near the northwest end of the Santa Lucia Range, to the Big Pine fault in the western Transverse Ranges, and that separates the granitic-metamorphic basement of the Salinian Block from the Franciscan basement of the Coastal Block. The most prominent faults that are included within this zone are, from northwest to southeast, the Sur, Nacimiento, Rinconada, and (south) Nacimiento faults. The Sur fault, which extends as far northward as Point Sur on land, continues to the northwest in the offshore continental margin. At its southerly end, the zone terminates where the (south) Nacimiento fault is cut off by the Big Pine fault. The overall length of the Sur-Nacimiento fault zone between Point Sur and the Transverse Ranges is about 180 miles. The 60 mile long Nacimiento fault, between points of juncture with the Sur and Rinconada faults, forms the longest segment within this zone. Page⁽¹¹⁾ stated that:

"It is unlikely that the Nacimiento fault proper has displaced the ground surface in Late Quaternary time, as there are no indicative offsets of streams, ridges, terrace deposits, or other topographic features. The Great Valley-type rocks on the northeast side must have been down-dropped against the older Franciscan rocks on the southwest, yet they commonly stand higher in the topography. This implies relative quiescence of the Late Quaternary time, allowing differential erosion to take place. In a few localities, the northeast side is the low side, and this inconsistency favors the same conclusion. In addition to the foregoing circumstances, the fault is offset by minor cross-faults in a manner suggesting that little, if any, Late Quaternary near-surface movement had occurred along the main fracture."

Hart⁽¹⁴⁾, on the other hand, stated that: ". . . youthful topographic features (offset streams, sag ponds, possible fault scarplets, and apparently oversteepened slopes) suggest movement along both (Sur-Nacimiento and Rinconada) fault zones." The map compiled by Jennings⁽²³⁾, however, shows only the Rinconada with a symbol indicating "Quaternary fault displacement."

The results of photogeologic study of the region traversed by the Sur-Nacimiento fault zone tend to support Page's view. A pronounced zone of fault-controlled topographic lineaments can be traced from the northwest end of the Nacimiento fault southeastward to the Rinconada (south Nacimiento), East Huasna, and West Huasna faults. Only along the Rinconada, however, are there topographic features that seem to have originated through fault disturbances of the ground surface rather than through differential erosion along zones of shearing and juxtaposition of differing rocks.

DCPP UNITS 1 & 2 FSAR UPDATE

Richter⁽¹³⁾ noted that some historic seismicity, particularly the 1952 Bryson earthquake, appears to have originated along the Nacimiento fault. This view is supported by recent work of S. W. Smith⁽³⁰⁾ that indicates that the Bryson shock and the epicenters of several smaller, more recent earthquakes were located along or near the trace of the Nacimiento.

3. Rinconada (Nacimiento)-San Marcos-Jolon-San Antonio Fault System

A system of major faults extends northwestward, parallel to the San Andreas fault, from a point of junction with the Big Pine fault in the western Transverse Ranges. This system includes several faults that have been mapped as separate features and assigned individual names. Dibblee⁽²⁷⁾ however, has suggested that these faults are part of a single system, provisionally termed the Rinconada fault zone after one of its more prominent members. He also proposed abandoning the name Nacimiento for the large fault that constitutes the most southerly part of this system, as it is not continuous with the Nacimiento fault to the north, near the Nacimiento River. The newly defined Rinconada fault system comprises the old (south) Nacimiento, Rinconada, and San Marcos faults. Dibblee proposed that the system also include the Espinosa and Reliz faults, to the north, but detailed work by Durham⁽²⁸⁾ does not seem to support this interpretation. Instead, the system may extend into Lockwood Valley and die out there along the Jolon and San Antonio faults. All the faults of the Rinconada system have undergone significant movement during middle and late Cenozoic time, though the entire system did not behave as a unit. Dibblee pointed out that: "Relative vertical displacements are controversial, inconsistent, reversed from one segment to another; the major movement may be strike slip, as on the San Andreas fault."

Regarding the structural relationship of the Rinconada fault to nearby faults, Dibblee wrote as follows:

"Thrust or reverse faults of Quaternary age are associated with the Rinconada fault along much of its course on one or both sides, within 9 miles, especially in areas of intense folding. In the northern part several, including the San Antonio fault, are present along both margins of the range of hills between the Salinas and Lockwood Valleys . . . along which this range was elevated in part. Near the southern part are the major southwest-dipping South Cuyama and Ozena faults along which the Sierra Madre Range was elevated against Cuyama Valley, with vertical displacements possibly up to 8000 feet. All these thrust or reverse faults dip inward toward the Rinconada fault and presumably either splay from it at depth, or are branches of it. These faults, combined with the intense folding between them, indicated that severe compression accompanied possible transcurrent movement along the Rinconada fault."

"The La Panza fault along which the La Panza Range was elevated in Quaternary time, is a reverse fault that dips northeast under the range, and is not directly related to the Rinconada fault."

DCPP UNITS 1 & 2 FSAR UPDATE

"The Big Pine fault against which the Rinconada fault abuts . . . is a high angle left-lateral transcurrent fault active in Quaternary time⁽³⁵⁾. The Pine Mountain fault south of it . . . is a northeast-dipping reverse fault along which the Pine Mountain Range was elevated in Quaternary time. This fault may have been reactivated along an earlier fault that may have been continuous with the Rinconada fault, but displaced about 8 miles from it by left slip on the Big Pine fault⁽¹²⁾ in Quaternary time."

"The Rinconada and Reliz faults were active after deposition of the Monterey Shale and Pancho Rico Formation, which are severely deformed adjacent and near the faults. The faults were again active after deposition of the Paso Robles Formation but to a lesser degree. These faults do not affect the alluvium or terrace deposits. There are no offset stream channels along these faults. However, in two areas several canyons and streams are deviated, possibly by right-lateral movement on the (Espinosa and San Marcos segments of the) Rinconada fault. There are no indications that these faults are presently active."

4. *San Simeon Fault*

The fault here referred to as the San Simeon fault trends along the base of the peninsula that lies north of the settlement of San Simeon. This fault is on land for a distance of 12 miles between its only outcrop, north of Ragged Point, and Point San Simeon. It may extend as much as 16 miles farther to the southeast, to the vicinity of Point Estero. This possibility is suggested by the straight reach of coastline between Cambria and Point Estero, which is directly aligned with the onshore trend of the fault; its linear form may well have been controlled by a zone of structural weakness associated with the inferred southerly part of the fault. South of Port Estero, however, there is no evidence of faulting observable in the seismic reflection profiles across Estero Bay, and the trend defined by the Los Osos Valley-Estero Bay series of lower Miocene or Oligocene intrusives extends across the San Simeon trend without deviation.

North of Point Piedras Blancas, Silver⁽²⁶⁾ reports a fault with about 5 kilometers of vertical separation between the 4-kilometer-thick Tertiary section in the offshore basin and the nearby 1-kilometer-high exposure of Franciscan basement rocks in the coastline mountain front. The existence of a fault in this region is also indicated by the 30- milligal gravity anomaly between the offshore basin and the onshore ranges (Plate II of Appendix 2.5D of Reference 27 in Section 2.3). This postulated fault may well be a northward extension of the San Simeon fault. If this is the case, the San Simeon fault may have a total length of as much as 60 miles.

Between Point San Simeon and Ragged Point, the San Simeon fault lies along the base of a broad peninsula, the surface of which is characterized by elevated marine terraces and younger, steep-walled ravines and canyons. The low, terraced topography of the peninsula contrasts sharply with that of the steep mountain front that rises immediately

DCPP UNITS 1 & 2 FSAR UPDATE

behind it. Clearly, the ground west of the main fault represents a part of the sea floor that has been locally arched up.

This has resulted in exposure of the fault, which elsewhere is concealed underwater off the shoreline.

The ground between the San Simeon fault and the southwest coastline of the Piedras Blancas peninsula is underlain by faulted blocks and slivers of Franciscan rocks, serpentinites, Tertiary sedimentary breccia and volcanic rocks, and Miocene shale. The faulted contacts between these rock masses trend somewhat more westerly than the trend of the San Simeon fault. One north-dipping reverse fault, which separates serpentinite from graywacke, has broken marine terrace deposits in at least two places, one of them in the basal part of the lowest and youngest terrace. Movement along this branch fault has therefore occurred less than 130,000 years before the present, although the uppermost, youngest Pleistocene deposits are apparently not broken. Prominent topographic lineations defined by northwest-aligned ravines that incise the upper terrace surface, on the other hand, apparently have originated through headward gully erosion along faults and faulted contacts, rather than through the effects of surface faulting.

The characteristics of the San Simeon fault can be summarized as follows: The fault may be related to a fault along the coast to the north that displays some 5 kilometers of vertical displacement. Near San Simeon, it exhibits probable Pleistocene right-lateral strike-slip movement of as much as 1500 feet near San Simeon, although it apparently does not break dune sand deposits of late Pleistocene or early Holocene age. A branch reverse fault, however, breaks upper Pleistocene marine terrace deposits. The San Simeon fault may extend as far south as Point Estero, but it dies out before crossing the northern part of Estero Bay.

5. Santa Lucia Bank Fault

South of the latitude of Point Piedras Blancas, the western boundary of the main offshore Santa Maria Basin is defined by the east-facing scarp along the east side of the Santa Lucia Bank. This scarp is associated with the Santa Lucia Bank fault, the structure that separates the subsided block under the basin from the structural high of the bank. The escarpment that rises above the west side of the fault trace has a maximum height of about 450 feet, as shown on U.S. Coast and Geodetic Survey (USC&GS) Bathymetric Map 1306N-20.

The Santa Lucia Bank fault can be traced on the sea floor for a distance of about 65 miles. Extensions that are overlapped by upper Tertiary strata continue to the south for at least another 10 miles, as well as to the north. The northern extension may be related to another, largely buried fault that crosses and may intersect the trend of the Santa Lucia Bank fault. This second fault extends to the surface only at points north of the latitude of Point Piedras Blancas.

DCPP UNITS 1 & 2 FSAR UPDATE

West of the Santa Lucia Bank fault, between N latitudes 34°30' and 30°, several subparallel faults are characterized by apparent surface scarps. The longest of these faults trends along the upper continental slope for a distance of as much as 45 miles, and generally exhibits a west-facing scarp. Other faults are present in a zone about 30 miles long lying between the 45 mile fault and the Santa Lucia Bank fault. These faults range from 5 to 15 or more miles in length, and have both east-and west-facing scarps.

This zone of faulting corresponds closely in space with the cluster of earthquake epicenters around N latitude 34°45' and 121°30'W longitude, and it probably represents the source structure for those shocks (Figure 2.5-3).

2.5.1.1.2.3 Tectonic Features in the Vicinity of the DCP Site

Geologic relationships between the major fold and fault structures in the vicinity of Diablo Canyon are shown in Figures 2.5-5, 2.5-6, and 2.5-7, and are described and illustrated in Appendix 2.5D of Reference 27 of Section 2.3. The San Luis Ranges-Estero Bay area is characterized structurally by west-northwest-trending folds and faults. These include the San Luis-Pismo syncline and the bordering Los Osos Valley and Point San Luis antiformal highs, and the West Huasna, Edna, and San Miguelito faults. A few miles offshore, the structural features associated with this trend merge into a north-northwest-trending zone of folds and faults that is referred to herein as the offshore Santa Maria Basin East Boundary zone of folding and faulting. The general pattern of structural highs and lows of the onshore area is warped and stepped downward to the west across this boundary zone, to be replaced by more northerly-trending folds in the lower part of the offshore basin section. The overall relationship between the onshore Coast Ranges and the offshore continental margin is one of differential uplift and subsidence. The East Boundary zone represents the structural expression of the zone of inflection between these regions of contrasting vertical movement.

In terms of regional relationships, structural style, and history of movement, the faults in the San Luis Ranges-Estero Bay vicinity may be characterized as follows:

1. West Huasna Fault

This fault zone separates the large downwarp of the Huasna syncline on the northeast from Franciscan assemblage rocks of the Los Osos Valley antiform and the Tertiary section of the southerly part of the San Luis-Pismo syncline on the southwest. The West Huasna fault is thought to join with the Suey fault to the south. Differences in thicknesses and facies relationships between units of apparently equivalent age on opposite sides of the fault are interpreted as indicating lateral movement along the fault; however, the available evidence regarding the amount and even the relative sense of displacement is not consistent. The West Huasna shows no evidence of late Quaternary activity.

DCPP UNITS 1 & 2 FSAR UPDATE

2. *Edna Fault Zone*

The Edna fault zone lies along a west-northwesterly trend that extends obliquely from the West Huasna fault at its southeast end to the hills of the San Luis Range south of Morro Bay. Several isolated breaks that lie on a line with the trend are present in the Tertiary strata beneath the south part of Estero Bay, east of the Santa Maria Basin East Boundary fault zone across the mouth of the bay.

The Edna fault is typically a zone of two or more anastomosing branches that range in width from 1/2 mile to as much as 1-1/2 miles. Although individual strands are variously oriented and exhibit various senses of amounts of movement, the zone as a whole clearly expresses high-angle dip-slip displacement (down to the southwest). The irregular traces of major strands suggest that little, if any, strike-slip movement has occurred. Preliminary geologic sections shown by Hall and Surdam⁽²¹⁾ and Hall⁽²⁰⁾ imply that the total amount of vertical separation ranges from 1500 to a few thousand feet along the central part of the fault zone. The amount of displacement across the main fault trend evidently decreases to the northwest, where the zone is mostly overlapped by upper Tertiary strata.

It may be, however, that most of the movement in the Baywood Park vicinity has been transferred to the north-trending branch of the Edna, which juxtaposes Pliocene and Franciscan rocks where last exposed. In the northwesterly part of the San Luis Range, the Edna fault forms much of the boundary between the Tertiary and basement rock sections. Most of the measurable displacements along this zone of rupture occurred during or after folding of the Pliocene Pismo Formation but prior to deposition of the lower Pleistocene Paso Robles Formation. Some additional movement has occurred during or since early Pleistocene time, however, because Monterey strata have been faulted against Paso Robles deposits along at least one strand of the Edna near the head of Arroyo Grande valley. This involved steep reverse fault movement, with the southwest side raised, in contrast to the earlier normal displacement down to the southwest.

Search has failed to reveal dislocation of deposits younger than the Paso Robles Formation, disturbance of late Quaternary landforms, or other evidence of Holocene or late Pleistocene activity.

3. *San Miguelito Fault Zone*

Northwesterly-trending faults have been mapped in the area between Pismo Beach and Arroyo Grande, and from Avila Beach to the vicinity of the west fork of Vineyard Canyon, north of San Luis Hill. Because these faults lie on the same trend, appear to reflect similar senses of movement, and are "separated" only by an area of no exposure along the shoreline between Pismo Beach and Avila Beach, they may well be part of a more or less continuous zone about 10 miles long. As on the Edna fault, movements along the San Miguelito fault appear to have been predominantly dip-slip, but with displacement down on the northeast. Hall's preliminary cross section indicates total

DCPP UNITS 1 & 2 FSAR UPDATE

vertical separation of about 1400 feet. The fault is mapped as being overlain by unbroken deposits of the Paso Robles Formation near Arroyo Grande.

Field checking of the ground along the projected trend of the San Miguelito fault zone northwest of Vineyard Canyon in the San Luis Range has substantiated Hall's note that the fault cannot be traced west of that area.

Detailed mapping of the nearly continuous sea cliff exposures extending across this trend northeast of Point Buchon has shown there is no faulting along the San Miguelito trend at the northwesterly end of the range. Like the Edna fault zone, the San Miguelito fault zone evidently represents a zone of high-angle dip-slip rupturing along the flank of the San Luis-Pismo syncline.

4. East Boundary Zone of the Offshore Santa Maria Basin

The boundary between the offshore Santa Maria Basin and the onshore features of the southern Coast Ranges is a 4 to 5 wide zone of generally north-northwest-trending folds, faults, and onlap unconformities referred to as the "Hosgri fault zone" by Wagner⁽³¹⁾. The geology of this boundary zone has been investigated in detail by means of extensive seismic reflection profiling, high resolution surface profiling, and side scan sonar surveying.

More general information about structural relationships along the boundary zone has been obtained from the pattern of Bouguer Gravity anomaly values that exist in its vicinity. These data show the East Boundary zone to consist of a series of generally parallel north-northwest-trending faults and folds, developed chiefly in upper Pliocene strata that flank upwarped lower Pliocene and older rocks. The zone extends from south of the latitude of Point Sal to north of Point Piedras Blancas. Within the zone, individual fault breaks range in length from less than 1000 feet up to a maximum of about 30 miles. The overall length of the zone is approximately 90 miles, with about 60 miles of relatively continuous faulting.

The apparent vertical component of movement is down to the west across some faults and down to the east across others. Along the central reach of the zone, opposite the San Luis Range, a block of ground has been dropped between the two main strands of the fault to form a graben structure. Within the graben, and at other points along the East Boundary zone, bedding in the rock has been folded down toward the upthrown side of the west side down fault. This feature evidently is an expression of "reverse drag" phenomena.

The axes of folds in the ground on either side of the principal fault breaks can be traced for distances of as much as 22 miles. The fold axes typically are nearly horizontal; maximum axial plunges seem to be 5° or less. The structure and onlap relationships of the upper Pliocene, as reflected in the configuration of the unconformity at its base, are such that it consistently rises from the offshore basin and across the boundary zone via a series of upwarps, asymmetric folds, and faults. This configuration seems to

DCPP UNITS 1 & 2 FSAR UPDATE

correspond generally to a zone of warping and partial disruption along the boundary between relatively uplifting and subsiding regions.

2.5.1.1.3 Geologic History

The geologic history reflected by the rocks, structural features, and landforms of the San Luis Range is typical of that of the southern Coast Ranges of California in its length and complexity. Six general episodes for which there is direct evidence can be tabulated as follows:

| <u>Age</u> | <u>Episode</u> | <u>Evidence</u> |
|--------------------------------|--|--|
| Late Mesozoic | Development of Franciscan and Upper Cretaceous rock assemblages | Franciscan and other Mesozoic rocks |
| Late Mesozoic - Early Tertiary | Early Coast Ranges deformation | Structural features pre-served in the Mesozoic rocks |
| Mid-Tertiary | Uplift and erosion | Erosion surface at the base of the Tertiary section |
| Mid- and late-Tertiary | Accumulation of Miocene and Pliocene sedimentary and volcanic rocks | Vaqueros, Rincon, Obispo, Point Sal, Monterey, and Pismo Formation and associated volcanic intrusive, and brecciated rocks |
| Pliocene | Folding and faulting associated with the Pliocene Coast Ranges deformation | Folding and faulting of the Tertiary and basement rocks |
| Pleistocene | Uplift and erosion, development of successive tiers of wave-cut-benches alluvial fan, talus, and landslide deposition. | Pleistocene and Holocene deposits, present land-forms. |

The earliest recognizable geologic history of the southern Coast Ranges began in Mesozoic time, during the Jurassic period when eugeosynclinal deposits (graywacke sandstone, shale, chert, and basalt) accumulated in an offshore trench developed in oceanic crust.

Some time after the initiation of Franciscan sedimentation, deposition of a sequence of miogeosynclinal or shelf sandstones and shales, known as the Great Valley Sequence, began on the continental crust, at some distance to the east of the Franciscan trench. Deposition of both sequences continued into Cretaceous time, even while the crustal basement section on which the Great Valley strata were being deposited was undergoing plutonism involving emplacement of granitic rocks. Subsequently, the Franciscan assemblage, the Great Valley Sequence, and the granite-intruded basement rocks were tectonically juxtaposed. The resulting terrane consisted generally of granitic

DCPP UNITS 1 & 2 FSAR UPDATE

basement thrust over intensely deformed Franciscan, with Great Valley Sequence strata overlying the basement, but thrust over and faulted into the Franciscan.

The processes that were involved in the tectonic juxtaposition evidently were active during the Mesozoic, and continued into the early Tertiary. Page⁽²⁵⁾ has shown that they were completed by no later than Oligocene time, so that the dual core complex basement of the southern Coast Ranges was formed by then.

The Miocene and later geologic history of the southern Coast Ranges region began with deposition of the Vaqueros and Rincon Formations on a surface eroded on the Franciscan and Great Valley core complex rocks.

Following deposition and some deformation and erosion of these formations, the stratigraphic unit that includes the Point Sal and Obispo Formations as approximately contemporaneous facies was laid down. The Obispo consists of a section of tuffaceous sandstone and mudstone, with lesser amounts of shale, and lensing layers of vitric and lithic-crystal tuff. Locally, the unit is featured by masses of clastic-textured tuffaceous rock that exhibit cross-cutting intrusive relations with the bedded parts of the formation. The Obispo and Point Sal were folded and locally eroded prior to initiation of the main episode of upper Miocene and Pliocene marine sedimentation.

During late middle Miocene to late Miocene time, deposition of the thick sections of silica-rich shale of the Monterey Formation began. Deposition of this formation and equivalent strata took place throughout much of the coastal region of California, but apparently was centered in a series of offshore basins that all developed at about the same time, some 10 to 12 million years ago. Local volcanism toward the latter part of this time is shown by the presence of diabase dikes and sills in the Monterey. Near the end of the Miocene, the Monterey strata were subjected to compressional deformation resulting in folding, in part with great complexity, and in faulting. Near the old continental margin, represented by the Sur-Nacimiento fault zone, the deformation was most intense, and was accompanied by uplift. This apparently resulted in the first development of many of the large folds of the southern Coast Ranges including the Huasna and San Luis-Pismo synclines, and in the partial erosion of the folded Monterey section in areas of uplift. The pattern of regional uplift of the Coast Ranges and subsidence of the offshore basins, with local upwarping and faulting in a zone of inflection along the boundary between the two regions, apparently became well established during the episode of late Miocene and Mio-Pliocene diastrophism.

Sedimentation resumed in Pliocene time throughout much of the region of the Miocene basins, and several thousand feet of siltstone and sandstone was deposited. This was the last significant episode of marine sedimentation in the region of the present Coast Ranges. Pliocene deposits in the region of uplift were then folded, and there was renewed movement along most of the preexisting larger faults.

Differential movements between the Coast Ranges uplift and the offshore basins were again concentrated along the boundary zone of inflection, resulting in upwarping and

DCPP UNITS 1 & 2 FSAR UPDATE

faulting of the basement, Miocene, and Pliocene sections. Relative displacement across parts of this zone evidently was dominantly vertical, because the faulting in the Pliocene has definitely extensional character, and Miocene structures can be traced across the zone without apparent lateral offset. The basement and Tertiary sections step down seaward, away from the uplift, along a system of normal faults having hundreds to nearly a thousand feet of dip-slip offset. A second, more seaward system of normal faults is antithetic to the master set and exhibits only tens to a few hundreds of feet of displacement. Strata between these faults locally exhibit reverse drag downfolding toward the edge of the Pliocene basin, whereas the section is essentially undeformed farther offshore. This style of deformation indicates a passive response, through gravity tectonics, to the onshore uplift.

The Plio-Pleistocene uplift was accompanied by rapid erosion, with consequent nearby deposition of clastic sediments such as the Paso Robles Formation in valleys throughout the southern Coast Ranges. The high-angle reverse and normal faulting observed by Compton⁽³⁸⁾ in the northern Santa Lucia Range also occurred farther south, probably more or less contemporaneously with accumulation of the continental deposits. Much of the Quaternary faulting other than that related to the San Andreas right lateral stress-strain system may well have occurred at this time.

Tectonic activity during the Quaternary has involved continued general uplift of the southern Coast Ranges, with superimposed local downwarping and continued movement along faults of the San Andreas system. The uplift is shown by the general high elevation and steep youthful topography that characterizes the Coast Ranges and by the widespread uplifted marine and stream terraces. Local downwarping can be seen in valleys, such as the Santa Maria Valley, where thick sections of Plio-Pleistocene and younger deposits have accumulated. Evidence of significant late Quaternary fault movement is seen in the topography along the Rinconada-San Marcos, Espinosa, San Simeon, and Santa Lucia Bank faults, as well as along the San Andreas itself. Only along the San Andreas, however, is there evidence of Holocene or contemporary movement.

The latest stage in the evolution of the San Luis Range has extended from mid-Pleistocene time to the present, and has involved more or less continuous interaction between apparent uplift of the range and alternating periods of erosion or deposition, especially along the coast, during times of relatively rising, falling, or unchanging sea level. The development of wave-cut benches and the accumulation of marine deposits on these benches have provided a reliable guide to the minimum age of latest displacements along breaks in the underlying bedrock. Detailed exploration of the interfaces between wave-cut benches and overlying marine deposits at the site of DCP has shown that no breaks extend across these interfaces. This demonstrates that the youngest faulting or other bedrock breakage in that area antedated the time of terrace cutting, which is on the order of 80,000 to 120,000 years before the present.

The bedrock section and the surficial deposits that formerly capped this bedrock on which the power plant facilities are located have been studied in detail to determine

DCPP UNITS 1 & 2 FSAR UPDATE

whether they express any evidence of deformation or dislocation ascribable to earthquake effects.

The surficial geologic materials at the site consisted of a thin, discontinuous basal section of rubbly marine sand and silty sand, and an overlying section of nonmarine rocky sand and sandy clay alluvial and colluvial deposits. These deposits were extensively exposed by exploratory trenches, and were examined and mapped in detail. No evidence of earthquake-induced effects such as lurching, slumping, fissuring, and liquefaction was detected during this investigation.

The initial movement of some of the landslide masses now present in Diablo Canyon upstream from the switchyard area may have been triggered by earthquake shaking. It is also possible that some local talus deposits may represent earthquake-triggered rock falls from the sea cliff or other steep slopes in the vicinity.

Deformation of the rock substrata in the site area may well have been accompanied by earthquake activity at the time of its occurrence in the geologic past. There is no evidence, however, of post-terrace earthquake effects in the bedrock where the power plant is being constructed.

2.5.1.1.4 Stratigraphy of the San Luis Range and Vicinity

The geologic section exposed in the San Luis Range comprises sedimentary, igneous, and tectonically emplaced ultrabasic rocks of Mesozoic age, sedimentary, pyroclastic, and hypabyssal intrusive rocks of Tertiary age, and a variety of surficial deposits of Quaternary age. The lithology, age, and distribution of these rocks were studied by Headlee and more recently have been mapped in detail by Hall. The geology of the San Luis Range is shown in Figure 2.5-6 with a geologic cross section constructed using exploratory oil wells shown in Figure 2.5-7. The geologic events that resulted in the stratigraphic units described in this section are discussed in Section 2.5.1.1.3, Geologic History.

2.5.1.1.4.1 Basement Rocks

An assemblage of rocks typical of the Coast Ranges basement terrane west of the Nacimiento fault zone is exposed along the south and northeast sides of the San Luis Range. As described by Headlee, this assemblage includes quartzose and greywacke sandstone, shale, radiolarian chert, intrusive serpentine and diabase, and pillow basalt. Some of these rocks have been dated as Upper Cretaceous from contained microfossils, including pollen and spores, and Headlee suggested that they may represent dislocated parts of the Great Valley Sequence. There is contrasting evidence, however, that at least the pillow basalt and associated cherty rocks may be more typically Franciscan. Certainly, such rocks are characteristic of the Franciscan terrane. Further, a potassium-argon age of 156 million years, equivalent to Upper Jurassic, has been determined for a core of similar rocks obtained from the bottom of the Montodoro Well No. 1 near Point Buchon.

2.5.1.1.4.2 Tertiary Rocks

Five formational units are represented in the Tertiary section of the San Luis Range. The lower part of this section comprises rocks of the Vaqueros, Rincon, and Obispo Formations, which range in age from lower Miocene through middle Miocene. These strata crop out in the vicinity of Hazard Canyon, at the northwest end of the range, and in a broad band along the south coastal margin of the range. In both areas the Vaqueros rests directly on Mesozoic basement rocks. The core of the western San Luis Range is underlain by the Upper Miocene Monterey Formation, which constitutes the bulk of the Tertiary section. The Upper Miocene to Lower Pliocene Pismo Formation crops out in a discontinuous band along the southwest flank and across the west end of the range, resting with some discordance on the Monterey section and elsewhere directly on older Tertiary or basement rocks.

The coastal area in the vicinity of Diablo Canyon is underlain by strata that have been variously correlated with the Obispo, Point Sal, and Monterey Formations. Headlee, for example, has shown the Point Sal as overlying the Obispo, whereas Hall has considered these two units as different facies of a single time-stratigraphic unit. Whatever the exact stratigraphic relationships of these rocks might prove to be, it is clear that they lie above the main body of tuffaceous sedimentary rocks of the Obispo Formation and below the main part of the Monterey Formation. The existence of intrusive bodies of both tuff breccia and diabase in this part of the section indicates either that local volcanic activity continued beyond the time of deposition of the Obispo Formation, or that the section represents a predominantly sedimentary facies of the upper part of the Obispo Formation. In either case, the strata underlying the power plant site range downward through the Obispo Formation and presumably include a few hundred feet of the Rincon and Vaqueros Formations resting upon a basement of Mesozoic rocks.

A generalized description of the major units in the Tertiary section follows, and a more detailed description of the rocks exposed at the power plant site is included in a later section.

The Vaqueros Formation has been described by Headlee as consisting of 100 to 400 feet of resistant, massive, coarse-grained, calcareously cemented bioclastic sandstone. The overlying Rincon Formation consists of 200 to 300 feet of dark gray to chocolate brown calcareous shale and mudstone.

The Obispo Formation (or Obispo Tuff) is 800 to 2000 feet thick and comprises alternating massive to thick-bedded, medium to fine grained vitric-lithic tuffs, finely laminated black and brown marine siltstone and shale, and medium grained light tan marine sandstone. Headlee assigned to the Point Sal Formation a section described as consisting chiefly of medium to fine grained silty sandstone, with several thin silty and fossiliferous limestone lenses; it is gradational upward into siliceous shale characteristic of the Monterey Formation. The Monterey Formation itself is composed predominantly of porcelaneous and finely laminated siliceous and cherty shales.

DCPP UNITS 1 & 2 FSAR UPDATE

The Pismo Formation consists of massive, medium to fine grained arkosic sandstone, with subordinate amounts of siltstone, sandy shale, mudstone, hard siliceous shale, and chert.

2.5.1.1.4.3 Quaternary Deposits

Deposits of Pleistocene and Holocene age are widespread on the coastal terrace benches along the southwest margin of the San Luis Range, and they exist farther onshore as local alluvial and stream-terrace deposits, landslide debris, and various colluvial accumulations. The coastal terrace deposits include discontinuous thin basal sections of marine silt, sand, gravel, and rubble, some of which are highly fossiliferous, and generally much thicker overlying sections of talus, alluvial-fan debris, and other deposits of landward origin. All of the marine deposits and most of the overlying nonmarine accumulations are of Pleistocene age, but some of the uppermost talus and alluvial deposits are Holocene. Most of the alluvial and colluvial materials consist of silty clayey sand with irregularly distributed fragments and blocks of locally exposed rock types. The landslide deposits include chaotic mixtures of rock fragments and fine-grained matrix debris, as well as some large masses of nearly intact to thoroughly disrupted bedrock.

A more detailed description of surficial deposits that are present in the vicinity of the power plant site is included in a later section.

2.5.1.1.5 Structure of the San Luis Range and Vicinity

2.5.1.1.5.1 General Features

The geologic structure of the San Luis Range-Estero Bay and adjacent offshore area is characterized by a complex set of folds and faults (Figures 2.5-5, 2.5-6, and 2.5-7). Tectonic events that produced these folds and faults are discussed in Section 2.5.1.1.3, Geologic History. The San Luis Range-Estero Bay and adjacent offshore area lies within the zone of transition from the west-trending Transverse Range structural province to the northwest-trending Coast Ranges province. Major structural features are the long narrow downfold of the San Luis-Pismo syncline and the bordering antiformal structural highs of Los Osos Valley on the northeast, and of Point San Luis and the adjacent offshore area on the southwest. This set of folds trends obliquely into a north-northwest aligned zone of basement upwarping, folding, and high-angle normal faulting that lies a few miles off the coast. The main onshore folds can be recognized, by seismic reflection and gravity techniques, in the structure of the buried, downfaulted Miocene section that lies across (west of) this zone.

Lesser, but yet important structural features in this area include smaller zones of faulting and trends of volcanic intrusives. The Edna and San Miguelito fault zones disrupt parts of the northeast and southwest flanks of the San Luis-Pismo syncline. A southward extension of the San Simeon fault, the existence of which is inferred on the basis of the linearity of the coastline between Cambria and Point Estero, and of the gravity gradient

DCPP UNITS 1 & 2 FSAR UPDATE

in that area, may extend into, and die out within, the northern part of Estero Bay. An aligned series of plugs and lensoid masses of Tertiary volcanic rocks that intrude the Franciscan Formation along the axis of the Los Osos Valley antiform extends from the outer part of Estero Bay southeastward for 22 miles (Figure 2.5-6).

These features define the major elements of geologic structure in the San Luis Range-Estero Bay area. Other structural elements include the complex fold and fault structures within the Franciscan core complex rocks and the numerous smaller folds within the Tertiary section.

2.5.1.1.5.2 San Luis-Pismo Syncline

The main synclinal fold of the San Luis Range, referred to here as the San Luis-Pismo syncline, trends about N60°W and forms a structural trend more than 15 miles in length. The fold system comprises several parallel anticlines and synclines across its maximum onshore width of about 5 miles. Individual folds of the system typically range in length from hundreds of feet to as much as 10,000 feet. The folds range from zero to more than 30° in plunge, and have flank dips as steep as 90°. Various kinds of smaller folds exist locally, especially flexures and drag folds associated with tuff intrusions and with zones of shear deformation.

Near Estero Bay, the major fold extends to a depth of more than 6000 feet. Farther south, in the central part of the San Luis Range, it is more than 11,000 feet deep. Parts of the northeast flank of the fold are disrupted by faults associated with the Edna fault zone. Local breaks along the central part of the southwest flank have been referred to as the San Miguelito fault zone.

2.5.1.1.5.3 Los Osos Valley Antiform

The body of Franciscan and Great Valley Sequence rocks that crops out between the San Luis-Pismo and Huasna synclines is here referred to as the Los Osos Valley antiform. This composite structure extends southward from the Santa Lucia Range, across the central and northern part of Estero Bay, and thence southeastward to the point where it is faulted out at the juncture of the Edna and the West Huasna fault zones.

Notable structural features within this core complex include northwest- and west-northwest- trending-faults that separate Franciscan melange, graywacke, metavolcanic, and serpentinite units. The serpentinites have been intruded or dragged within faults, apparently over a wide range of scales. One of the more persistent zones of serpentinite bodies occurs along a trend which extends west-northwestward from the West Huasna fault. It has been suggested that movement from this fault may have taken place within this serpentine belt. The range of hills that lies between the coast and Highway 1 between Estero Bay and Cambria is underlain by sandstone and minor shale of the Great Valley Sequence, referred to as the Cambria slab, which has been underthrust by Franciscan rocks. The thrust contact extends southeastward under

Estero Bay near Cayucos. This contact is probably related to the fault contact between Great Valley and Franciscan rocks located just north of San Luis Obispo, which Page has shown to be overlain by unbroken lower Miocene strata.

A prominent feature of the Los Osos Valley antiform is the line of plugs and lensoid masses of intrusive Tertiary volcanic rocks. These distinctive bodies are present at isolated points along the approximate axis of the antiform over a distance of 22 miles, extending from the center of outer Estero Bay to the upper part of Los Osos Valley (Figure 2.5-6). The consistent trend of the intrusives provides a useful reference for assessing the possibility of northwest-trending lateral slip faulting within Estero Bay. It shows that such faulting has not extended across the trend from either the inferred San Simeon fault offshore south extension, or from faults in the ground east of the San Simeon trend.

2.5.1.1.5.4 Edna and San Miguelito Fault Zones

These fault zones are described in Section 2.5.1.1.2.3.

2.5.1.1.5.5 Adjacent Offshore Area and East Boundary of the Offshore Santa Maria Basin

The stratigraphy and west-northwest-trending structure that characterize the onshore region from Point Sal to north of Point Estero have been shown by extensive marine geophysical surveying to extend into the adjacent offshore area as far as the north-northwest trending structural zone that forms a boundary with the main offshore Santa Maria Basin. Owing to the irregular outline of the coast, the width of the offshore shelf east of this boundary zone ranges from 2-1/2 to as much as 12 miles. The shelf area is narrowest opposite the reach of coast between Point San Luis and Point Buchon, and widest in Estero Bay and south of San Luis Bay.

The major geologic features that underlie the near-shore shelf include, from south to north, the Casmalia Hills anticline, the broad Santa Maria Valley downwarp, the anticlinal structural high off Point San Luis, the San Luis-Pismo syncline, and the Los Osos Valley antiform.

The form of these features is defined by the outcrop pattern and structure of the older Pliocene, Miocene, and basement core complex rocks. The younger Pliocene strata that constitute the upper 1000 to 2000 feet of section in the adjacent offshore Santa Maria Basin are partly buttressed and partly faulted against the rocks that underlie the near-shore shelf, and they unconformably overlap the boundary zone and parts of the shelf in several areas.

The boundaries between the San Luis-Pismo syncline and the adjacent Los Osos Valley and Point San Luis antiforms can be seen in the offshore area to be expressed chiefly as zones of inflection between synclinal and anticlinal folds, rather than as zones of fault rupture such as occurs farther south along the Edna and San Miguelito faults.

DCPP UNITS 1 & 2 FSAR UPDATE

Isolated west-northwest- trending faults of no more than a few hundred feet displacement are located along the northeast flank of the syncline in Estero Bay. These faults evidently are the northwesternmost expressions of breakage along the Edna fault trend.

The main San Luis-Pismo synclinal structure opens to the northwest, attaining a maximum width of 8 or 9 miles in the southerly part of Estero Bay. The Point San Luis high, on the other hand, is a domal structure, the exposed basement rock core of which is about 10 miles long and 5 miles wide.

The general characteristics of the Santa Maria Basin East Boundary zone have been described in Section 2.5.1.1.2.3. As was noted there, the zone is essentially an expression of the boundary between the synclinal downwarp of the offshore basin and the regional uplift of the southern Coast Ranges. In the vicinity of the San Luis Range, the zone is characterized by pronounced upwarping and normal faulting of the basement and overlying Tertiary rock sections. Both modes of deformation have contributed to the structural relief of about 500 feet in the Pliocene section, and of 1500 feet or more in the basement rocks, across this boundary. Successively younger strata are banked unconformably against the slopes that have formed from time to time in response to the relative uplifting of the ground east of the boundary zone.

A series of near-surface structural troughs forms prominent features within the segment of the boundary zone structure that extends between the approximate latitudes of Arroyo Grande and Estero Bay. This trough structure apparently has formed through the extension and subsidence of a block of ground in the zone where the downwarp of the offshore basin has pulled away from the Santa Lucia uplift. Continued subsidence of this block has resulted in deformation and partial disruption of the buttress unconformity between the offshore Pliocene section and the near-shore Miocene and older rocks. This deformation is expressed by normal faulting and reverse drag type downfolding of the Pliocene strata adjacent to the contact, along the east side of the trough.

On the opposite, seaward side of the trough, a series of antithetic down-to-the-east normal faults of small displacement has formed in the Pliocene strata west of the contact zone. These faults exhibit only a few tens of feet displacement, and they seem to exhibit constant or even decreasing displacement downward.

The structural evolution of the offshore area near Estero Bay and the San Luis Range involved episodes of compressional deformation that affected the upper Tertiary section similarly on opposite sides of the boundary zone. The section on either side exhibits about the same intensity and style of folding. Major folds, such as the San Luis-Pismo syncline and the Piedras Blancas anticline, can be traced into the ground across the boundary zone.

The internal structure of the zone, including the presence of several on-lap unconformities in the adjacent Pliocene section, shows that, at least during Pliocene

DCPP UNITS 1 & 2 FSAR UPDATE

and early Pleistocene time, the boundary zone has been the inflection line between the Coast Ranges uplift and the offshore Santa Maria Basin downwarp.

Evidence that uplift has continued through late Pleistocene time, at least in the vicinity of the San Luis Range, is given by the presence of successive tiers of marine terraces along the seaward flank of the range. The wave-cut benches and back scarps of these terraces now exist at elevations ranging from about -300 feet (below sea level) to more than 300 feet above sea level.

The ground within which the East Boundary zone lies has been beveled by the post-Wisconsin marine transgression, and so the zone generally is not expressed topographically. Small topographic features, such as a seaward topographic step-up of the sea floor surface across the east-down fault at the BBN⁽³⁷⁾ (offshore) survey line 27 crossing, in Estero Bay, and several possible fault-line notch back scarps, however, may represent minor topographic expressions of deformation within the zone.

2.5.1.1.6 Structural Stability

The potential for surface or subsurface subsidence, uplift, or collapse at the site or in the region surrounding the site, is discussed in Section 2.5.4, Stability of Subsurface Materials.

2.5.1.1.7 Regional Groundwater

Groundwater in the region surrounding the site is used as a backup source due to its poor quality and the lack of a significant groundwater reservoir. Section 2.4.13 states that most of the groundwater at the site or in the area around the site is either in the alluvial deposits of Diablo Creek or seeps from springs encountered in excavations at the site.

2.5.1.2 Site Geology

2.5.1.2.1 Site Physiography

The site consists of approximately 750 acres near the mouth of Diablo Creek and is located on a sloping coastal terrace, ranging from 60 to 150 feet above sea level. The terrace terminates at the Pacific Ocean on the southwest and extends toward the San Luis Mountains on the northeast. The terrace consists of bedrock overlain by surficial deposits of marine and nonmarine origin.

The remainder of this section presents a detailed description of site geology.

2.5.1.2.2 General Features

The area of the DCPP site is a coastal tract in San Luis Obispo County approximately 6.5 miles northwest of Point San Luis. It lies immediately southeast of the mouth of

DCPP UNITS 1 & 2 FSAR UPDATE

Diablo Canyon, a major westward-draining feature of the San Luis Range, and about a mile southeast of Lion Rock, a prominent offshore element of the highly irregular coastline.

The ground being developed as a power plant site occupies an extensive topographic terrace about 1000 feet in average width. In its pregrading, natural state, the gently undulating surface of this terrace sloped gradually southwestward to an abrupt termination along a cliff fronting the ocean; in a landward, or northeasterly, direction, it rose with progressively increasing slope to merge with the much steeper front of a foothill ridge of the San Luis Range. The surface ranged in altitude from 65 to 80 feet along the coastline to a maximum of nearly 300 feet along the base of the hillslope to the northeast, but nowhere was its local relief greater than 10 feet. Its only major interruption was the steep-walled canyon of lower Diablo Creek, a gash about 75 feet in average depth.

The entire subject area is underlain by a complex sequence of stratified marine sedimentary rocks and tuffaceous volcanic rocks, all of Tertiary (Miocene) age. Diabasic intrusive rocks are locally exposed high on the walls of Diablo Canyon at the edge of the area. Both the sedimentary and volcanic rocks have been folded and otherwise disturbed over a considerable range of scales.

Surficial deposits of Quaternary age are widespread. In a few places, they are as thick as 50 feet, but their average thickness probably is on the order of 20 feet over the terrace areas and 10 feet or less over the entire mapped ground. The most extensive deposits underlie the main topographic terrace.

Like many other parts of the California coast, the Diablo Canyon area is characterized by several wave-cut benches of Pleistocene age. These surfaces of irregular but generally low relief were developed across bedrock by marine erosion, and they are ancient analogues of the benches now being cut approximately at sea level along the present coast. They were formed during periods when the sea level was higher, relative to the adjacent land, than it is now. Each is thinly and discontinuously mantled with marine sand, gravel, and rubble similar to the beach and offshore deposits that are accumulating along the present coastline. Along its landward margin each bears thicker and more localized coarse deposits similar to the modern talus along the base of the present sea cliff.

Both the ancient wave-cut benches and their overlying marine and shoreline deposits have been buried beneath silty to gravelly detritus derived from landward sources after the benches were, in effect, abandoned by the ocean. This nonmarine cover is essentially an apron of coalescing fan deposits and other alluvial debris that is thickest adjacent to the mouths of major canyons.

Where they have been deeply trenched by subsequent erosion, as along Diablo Canyon in the map areas, these deposits can be seen to have buried some of the benches so deeply that their individual identities are not reflected by the present (pregrading) rather

DCPP UNITS 1 & 2 FSAR UPDATE

smooth terrace topography. Thus, the surface of the main terrace is defined mainly by nonmarine deposits that conceal both the older benches of marine erosion and some of the abruptly rising ground that separates them (see Figures 2.5-8 and 2.5-10).

The observed and inferred relationships among the terrace surfaces and the wave-cut benches buried beneath them can be summarized as follows:

| <u>Wave-cut Bench</u> | | <u>Terrace Surface</u> | |
|-----------------------|---|------------------------|---|
| <u>Altitude, feet</u> | <u>Location</u> | <u>Altitude, feet</u> | <u>Location</u> |
| 170-175 | Small remnants on side of Diablo Canyon | Mainly 170-190 | Sides of Diablo Canyon upper parts of main terrace; in places separated from lower |
| 145-155 | Very small remnants on sides of Diablo Canyon | Mainly 150-170 | parts of terrace by scarps |
| 120-130 | Subparallel benches elongate in a northwest-southeast direction but with considerable aggregate width wholly beneath main terrace surface | Mainly 70-160 | Most of main terrace, a widespread surface on a composite section of nonmarine deposits; no well-defined scarps |
| 90-100 | | | |
| 30-45 | | | |
| Approx. 0 | Small to moderately large area along present coastline | | No depositional terrace |

Within the subject area the wave-cut benches increase progressively in age with increasing elevation above present sea level; hence, their order in the above list is one of decreasing age. By far, the most extensive of these benches slopes gently seaward from a shoreline angle that lies at an elevation of 100 feet above present sea level.

The geology of the power plant site is shown in the site geologic maps, Figures 2.5-8 and 2.5-9, and geologic section, Figure 2.5-10.

2.5.1.2.3 Stratigraphy

2.5.1.2.3.1 Obispo Tuff

The Obispo Tuff, which has been classified either as a separate formation or as a member of the Miocene Monterey Formation, is the oldest bedrock unit exposed in the site area. Its constituent rocks generally are well exposed, appear extensively in the coastward parts of the area, and form nearly all of the offshore prominences and shoals. They are dense to highly porous, and thinly layered to almost massive. Their color

DCPP UNITS 1 & 2 FSAR UPDATE

ranges from white to buff in fresh exposures, and from yellowish to reddish brown on weathered surfaces, many of which are variegated in shades of brown. Outcrop surfaces have a characteristic "punky" to crusty appearance, but the rocks in general are tough, cohesive, and relatively resistant to erosion.

Several pyroclastic rock types constitute the Obispo Tuff ("To" on map, Figure 2.5-8) in and near the subject area. By far, the most widespread is fine-grained vitric tuff with rare to moderately abundant tabular crystals of sodic plagioclase. The constituent glass commonly appears as fresh shards, but in many places it has been partly or completely devitrified. Crystal tuffs are locally prominent, and some of these are so crowded with 1/8 to 3/8 inch crystals of plagioclase that they superficially resemble granitoid plutonic rocks. Other observed rock types include pumiceous tuffs, pumice-pellet tuff breccias, perlitic vitreous tuffs, tuffaceous siltstones and mudstones, and fine-grained tuff breccias with fragments of glass and various Monterey rocks. No massive flow rocks were recognized anywhere in the exposed volcanic section.

In terms of bulk composition, the pyroclastic rocks appear to be chiefly soda rhyolites and soda quartz latites. Their plagioclase, which ranges from calcic albite to sodic oligoclase, commonly is accompanied by lesser amounts of quartz as small rounded crystals and irregular crystal fragments. Biotite, zircon, and apatite also are present in many of the specimens that were examined under the microscope. Most of the tuffaceous rocks, and especially the more vitreous ones, have been locally to pervasively altered. Products of silicification, zeolitization, and pyritization are readily recognizable in many exposures, where the rocks generally are traversed by numerous thin, irregular veinlets and layers of cherty to opaline material. Veinlets and thin, pod-like concentrations of gypsum also are widespread. Where pyrite is present, the rocks weather yellowish to brownish and are marked by gossan-like crusts.

The various contrasting rock types are simply interlayered in only a few places; much more typical are abutting, intertonguing, and irregularly interpenetrating relationships over a wide range of scales. Septa and inclusions of Monterey rocks are abundant, and a few of them are large enough to be shown separately on the accompanying geologic map (Figure 2.5-8). Highly irregular inclusions, a few inches to several feet in maximum dimension, are so densely packed together in some places that they form breccias with volcanic matrices.

The Obispo Tuff is underlain by mudstones of early Miocene (pre-Monterey) age, on which it rests with a highly irregular contact that appears to be in part intrusive. This contact lies offshore in the vicinity of the power plant site, but it is exposed along the seacoast to the southeast.

In a gross way, the Obispo underlies the basal part of the Monterey formation, but many of its contacts with these sedimentary strata are plainly intrusive. Moreover, individual sills and dikes of slightly to thoroughly altered tuffaceous rocks appear here and there in the Monterey section, not uncommonly at stratigraphic levels well above its base (see Figures 2.5-8 and 2.5-13). The observed physical relationships, together with the local

DCPP UNITS 1 & 2 FSAR UPDATE

occurrence of diatoms and foraminifera within the principal masses of volcanic rocks, indicate that much of the Obispo Tuff in this area probably was emplaced at shallow depths beneath the Miocene sea floor during accumulation of the Monterey strata. The tuff unit does not appear to represent a single, well-defined eruptive event, nor is it likely to have been derived from a single source conduit.

2.5.1.2.3.2 Monterey Formation

Stratified marine rocks variously correlated with the Monterey Formation, Point Sal Formation, and Obispo Tuff underlie most of the subject area, including all of that portion intended for power plant location. They are almost continuously exposed along the crescentic sea cliff that borders Diablo Cove, and elsewhere they appear in much more localized outcrops. For convenience, they are here assigned to the Monterey Formation ("Tm" on map, Figure 2.5-8) in order to delineate them from the adjacent more tuffaceous rocks so typical of the Obispo Tuff.

The observed rock types, listed in general order of decreasing abundance, are silty and tuffaceous sandstone, siliceous shale, shaly siltstone and mudstone, diatomaceous shale, sandy to highly tuffaceous shale, calcareous shale and impure limestone, bituminous shale, fine- to coarse-grained sandstone, impure vitric tuff, silicified limestone and shale, and tuff-pellet sandstone. Dark colored and relatively fine-grained strata are most abundant in the lowest part of the section, as exposed along the east side of Diablo Cove, whereas lighter colored sandstones and siliceous shales are dominant at stratigraphically higher levels farther north. In detail, however, the different rock types are interbedded in various combinations, and intervals of uniform lithology rarely are thicker than 30 feet. Indeed, the closely-spaced alternations of contrasting strata yield a prominent rib-like pattern of outcrop along much of the sea cliff and shoreline bench forming the margin of Diablo Cove.

The sandstones are mainly fine- to medium-grained, and most are distinctly tuffaceous. Shards of volcanic glass generally are recognizable under the microscope, and the very fine-grained siliceous matrix may well have been derived largely through alteration of original glassy material. Some of the sandstone contains small but megascopically visible fragments of pumice, perlite glass, and tuff, and a few beds grade along strike into submarine tuff breccia. The sandstones are thinly to very thickly layered; individual beds 6 inches to 4 feet thick are fairly common, and a few appear to be as thick as 15 feet. Some of them are hard and very resistant to erosion, and they typically form subdued but nearly continuous elongated projections on major hillslopes (Figure 2.5-8).

The siliceous shales are buff to light gray platy rocks that are moderately hard to extremely hard according to their silica content, but they tend to break readily along bedding and fracture surfaces. The bituminous rocks and the siltstones and mudstones are darker colored, softer, and grossly more compact. Some of them are very thinly bedded or laminated, others appear almost massive or form matrices for irregularly ellipsoidal masses of somewhat sandier material. The diatomaceous, tuffaceous, and sandy rocks are lighter colored. The more tuffaceous types are softer, and the

DCPP UNITS 1 & 2 FSAR UPDATE

diatomaceous ones are soft to the degree of punkiness; both kinds of rocks are easily eroded, but are markedly cohesive and tend to retain their gross positions on even the steepest of slopes.

The siliceous shale and most of the hardest, highly silicified rocks weather to very light gray, and the dark colored, fine-grained rocks tend to bleach when weathered. The other types, including the sandstones, weather to various shades of buff and light brown. Stains of iron oxides are widespread on exposures of nearly all the Monterey rocks, and are especially well developed on some of the finest-grained shales that contain disseminated pyrite. All but the hardest and most thick-bedded rocks are considerably broken to depths of as much as 6 feet in the zone of weathering on slopes other than the present sea cliff, and the broken fragments have been separated and displaced by surface creep to somewhat lesser depths.

2.5.1.2.3.3 Diabasic Intrusive Rocks

Small, irregular bodies of diabasic rocks are poorly exposed high on the walls of Diablo Canyon at and beyond the northeasterly edge of the map area. Contact relationships are readily determined at only a few places where these rocks evidently are intrusive into the Monterey Formation. They are considerably weathered, but an ophitic texture is recognizable. They consist chiefly of calcic plagioclase and augite, with some olivine, opaque minerals, and zeolitic alteration products.

2.5.1.2.3.4 Masses of Brecciated Rocks

Highly irregular masses of coarsely brecciated rocks, a few feet to many tens of feet in maximum dimension, are present in some of the relatively siliceous parts of the Monterey section that adjoin the principal bodies of Obispo Tuff. The fracturing and dislocation is not genetically related to any recognizable faults, but instead seems to have been associated with emplacement of the volcanic rocks; it evidently was accompanied by, or soon followed by, extensive silicification. Many adjacent fragments in the breccias are closely juxtaposed and have matching opposed surfaces, so that they plainly represent no more than coarse crackling of the brittle rocks. Other fragments, though angular or subangular, are not readily matched with adjacent fragments and hence may represent significant translation within the entire rock masses.

The ratio of matrix materials to coarse fragments is very low in most of the breccias and nowhere was it observed to exceed about 1:3. The matrices generally comprise smaller angular fragments of the same Monterey rocks that are elsewhere dominant in the breccias, and they characteristically are set in a siliceous cement. Tuffaceous matrices, with or without Monterey fragments, also are widespread and commonly show the effects of pervasive silicification. All the exposed breccias are firmly cemented, and they rank among the hardest and most resistant units in the entire bedrock section.

A few 3 to 18 inch beds of sandstone have been pulled apart to form separate tabular masses along specific stratigraphic horizons in higher parts of the Monterey sequence. Such individual tablets, which are boudins rather than ordinary breccia fragments, are especially well exposed in the sea cliff at the northern corner of Diablo Cove. They are flanked by much finer-grained strata that converge around their ends and continue essentially unbroken beyond them. This boudinage or separation and stringing out of sandstone beds that lie within intervals of much softer and more shaly rocks has resulted from compression during folding of the Monterey section. Its distribution is stratigraphically controlled and is not systematically related to recognizable faults in the area.

2.5.1.2.3.5 Surficial Deposits

1. Coastal Terrace Deposits

The coastal wave-cut benches of Pleistocene age, as described in a foregoing section, are almost continuously blanketed by terrace deposits (Qter in Figure 2.5-8) of several contrasting types and modes of origin. The oldest of these deposits are relatively thin and patchy in their occurrence, and were laid down along and adjacent to ancient beaches during Pleistocene time. They are covered by considerably thicker and more extensive nonmarine accumulations of detrital materials derived from various landward sources.

The marine deposits consist of silt, sand, gravel, and cobbly to bouldery rubble. They are approximately 2 feet in average thickness over the entire terrace area and reach a maximum observed thickness of about 8 feet. They rest directly upon bedrock, some of which is marked by numerous holes attributable to the action of boring marine mollusks, and they commonly contain large rounded cobbles and boulders of Monterey and Obispo rocks that have been similarly bored. Lenses and pockets of highly fossiliferous sand and gravel are present locally.

The marine sediments are poorly to very well sorted and loose to moderately well consolidated. All of them have been naturally compacted; the degree of compaction varies according to the material, but it is consistently greater than that observed in any of the associated surficial deposits of other types. Near the inner margins of individual wave-cut benches the marine deposits merge landward into coarser and less well-sorted debris that evidently accumulated along the bases of ancient sea cliffs or other shoreline slopes. This debris is locally as much as 12 feet thick; it forms broad but very short aprons, now buried beneath younger deposits, that are ancient analogues of the talus accumulations along the inner margin of the present beach in Diablo Cove. One of these occurrences, identified as "fossil Qtb" in the geologic map of Figure 2.5-8, is well exposed high on the northerly wall of Diablo Canyon.

A younger, thicker, and much more continuous nonmarine cover is present over most of the coastal terrace area. It consistently overlies the marine deposits noted above, and, where these are absent, it rests directly upon bedrock. It is composed in part of alluvial

DCPP UNITS 1 & 2 FSAR UPDATE

detritus contributed during Pleistocene time from Diablo Canyon and several smaller drainage courses, and it thickens markedly as traced sourceward toward these canyons. The detritus represents a series of alluvial fans, some of which appear to have partly coalesced with adjacent ones. It is chiefly fine- to moderately-coarse-grained gravel and rubble characterized by tabular fragments of Monterey rocks in a rather abundant silty to clayey matrix. Most of it is thinly and regularly stratified, but the distinctness of this layering varies greatly from place to place.

Slump, creep, and slope-wash deposits, derived from adjacent hillsides by relatively slow downhill movement over long periods of time, also form major parts of the nonmarine terrace cover. All are loose and uncompacted. They comprise fragments of Monterey rocks in dark colored clayey matrices, and their internal structure is essentially chaotic. In some places they are crudely interlayered with the alluvial fan deposits, and elsewhere they overlie these bedded sediments. On parts of the main terrace area not reached by any of the alluvial fans, a cover of slump, creep, and slope-wash deposits, a few inches to nearly 10 feet thick, rests directly upon either marine terrace deposits or bedrock.

Thus, the entire section of terrace deposits that caps the coastal benches of Pleistocene marine erosion is heterogeneous and internally complex; it includes contributions of detritus from contrasting sources, from different directions at different times, and via several basically different modes of transport and deposition.

2. Stream-terrace Deposits

Several narrow, irregular benches along the walls of Diablo Canyon are veneered by a few inches to 6 feet of silty gravels that are somewhat coarser but otherwise similar to the alluvial fan deposits described above. These stream-terrace deposits (Qst) originally occupied the bottom of the canyon at a time when the lower course of Diablo Creek had been cut downward through the alluvial fan sediments of the main terrace and well into the underlying bedrock. Subsequent deepening of the canyon left remnants of the deposits as cappings on scattered small terraces.

3. Landslide Deposits

The walls of Diablo Canyon also are marked by tongue- and bench-like accumulations of loose, rubbly landslide debris (Qls), consisting mainly of highly broken and jumbled masses of Monterey rocks with abundant silty and soily matrix materials. These landslide bodies represent localized failure on naturally oversteepened slopes, generally confined to fractured bedrock in and immediately beneath the zone of weathering. Individual bodies within the mapped area are small, with probable maximum thicknesses no greater than 20 feet. All of them lie outside the area intended for power plant construction.

Landslide deposits along the sea cliff have been recognized at only one locality, on the north side of Diablo Cove about 400 feet northwest of the mouth of Diablo Canyon.

DCPP UNITS 1 & 2 FSAR UPDATE

Here slippage has occurred along bedding and fracture surfaces in siliceous Monterey rocks, and it has been confined essentially to the axial region of a well-defined syncline (see Figure 2.5-8). Several episodes of sliding are attested by thin, elongate masses of highly broken ground separated from one another by well-defined zones of dislocation. Some of these masses are still capped by terrace deposits. The entire composite accumulation of debris is not more than 35 feet in maximum thickness, and ground failure at this locality does not appear to have resulted in major recession of the cliff. Elsewhere within the mapped area, landsliding along the sea cliff evidently has not been a significant process.

Large landslides, some of them involving substantial thickness of bedrock, are present on both sides of Diablo Canyon not far northeast of the power plant area. These occurrences need not be considered in connection with the plant site, but they have been regarded as significant factors in establishing a satisfactory grading design for the switchyard and other up-canyon installations. They are not dealt with in this section.

4. Slump, Creep, and Slope-wash Deposits

As noted earlier, slump, creep, and slope-wash deposits (Qsw) form parts of the nonmarine sedimentary blanket on the main terrace. These materials are shown separately on the geologic map only in those limited areas where they have been considerably concentrated along well-defined swales and are readily distinguished from other surficial deposits. Their actual distribution is much wider, and they undoubtedly are present over a large fraction of the areas designated as Qter; their average thickness in such areas, however, is probably less than 5 feet.

Angular fragments of Monterey rocks are sparsely to very abundantly scattered through the slump, creep, and slope-wash deposits, whose most characteristic feature is a fine-grained matrix that is dark colored, moderately rich in clay minerals, and extremely soft when wet. Internal layering is rarely observable and nowhere is sharply expressed. The debris seems to have been rather thoroughly intermixed during its slow migration down hillslopes in response to gravity. That it was derived mainly from broken materials in the zone of weathering is shown by several exposures in which it grades downward through soily debris into highly disturbed and partly weathered bedrock, and thence into progressively fresher and less broken bedrock.

5. Talus and Beach Deposits

Much of the present coastline in the subject area is marked by bare rock, but Diablo Cove and a few other large indentations are fringed by narrow, discontinuous beaches and irregular concentrations of sea cliff talus. These deposits (Qtb) are very coarse grained. Their total volume is small, and they are of interest mainly as modern analogues of much older deposits at higher levels beneath the main terrace surface.

The beach deposits consist chiefly of well-rounded cobbles. They form thin veneers over bedrock, and in Diablo Cove they grade seaward into patches of coarse pebbly

DCPP UNITS 1 & 2 FSAR UPDATE

sand. The floors of both Diablo Cove and South Cove probably are irregular in detail and are featured by rather hard, fresh bedrock that is discontinuously overlain by irregular thin bodies of sand and gravel. The distribution and abundance of kelp suggest that bedrock crops out over large parts of these cove areas where the sea bottom cannot be observed from onshore points.

6. *Stream-laid Alluvium*

Stream-laid alluvium (Qal) occurs as a strip along the present narrow floor of Diablo Canyon, where it is only a few feet in average thickness. It is composed of irregularly intertongued silt, sand, gravel, and rubble. It is crudely to sharply stratified, poorly to well sorted, and, in general, somewhat compacted. Most of it is at least moderately porous.

7. *Other Deposits*

Earlier inhabitation of the area by Indians is indicated by several midden deposits that are rich in charcoal and fragments of shells and bones. The most extensive of these occurrences marks the site of a long-abandoned village along the edge of the main terrace immediately northwest of Diablo Canyon. Others have been noted on the main terrace just east of the mouth of Diablo Canyon, on the shoreward end of South Point, and at several places in and near the plant site.

2.5.1.2.4 Structure

2.5.1.2.4.1 Tectonic Structures Underlying the Region Surrounding the Site

The dominant tectonic structure in the region of the power plant site is the San Luis-Pismo downwarp system of west-northwest-trending folds. This structure is bounded on the northeast by the antiformal basement rock structure of the Los Osos and San Luis Valley trend. The west-northwest-trending Edna fault zone lies along the northeast flank of the range, and the parallel Miguelito fault extends into the southeasterly end of the range. A north-northwest-trending structural discontinuity that may be a fault has been inferred or interpolated from widely spaced traverses in the offshore, extending within about 5 miles of the site at its point of closest approach. To the west of this discontinuity, the structure is dominated by north to north-northwest-trending folds in Tertiary rocks. These features are illustrated in Figure 2.5-3 and described in this section.

Tectonic structures underlying the site and region surrounding the site are identified in the above and following sections, and they are shown in Figures 2.5-3, 2.5-5, 2.5-8, 2.5-10, 2.5-15, and 2.5-16. They are listed as follows:

2.5.1.2.4.2 Tectonic Structures Underlying the Site

DCPP UNITS 1 & 2 FSAR UPDATE

The rocks underlying the DCP site have been subjected to intrusive volcanic activity and to later compressional deformation that has given rise to folding, jointing and fracturing, minor faulting, and local brecciation. The site is situated in a section of moderately to steeply north-dipping strata, about 300 feet south of an east-west-trending synclinal fold axis (Figures 2.5-8 and 2.5-10). The rocks are jointed throughout, and they contain local zones of closely spaced high-angle fractures (Figure 2.5-16).

A minor fault zone extends into the site from the west, but dies out in the vicinity of the Unit 1 turbine building. Two other minor faults were mapped for distances of 35 to more than 200 feet in the bedrock section exposed in the excavation for the Unit 1 containment structure. In addition to these features, cross-cutting bodies of tuff and tuff breccia, and cemented "crackle breccia" could be considered as tectonic structures.

Exact ages of the various tectonic structures at the site are not known. It has been clearly demonstrated, however, that all of them are truncated by, and therefore antedate, the principal marine erosion surface that underlies the coastal terrace bench. This terrace can be correlated with coastal terraces to the north and south that have been dated as 80,000 to 120,000 years old. The tectonic structures probably are related to the Pliocene-lower Pleistocene episode of Coast Ranges deformation, which occurred more than 1 million years ago.

The bedrock units within the entire subject area form part of the southerly flank of a very large syncline that is a major feature of the San Luis Range. The northerly-dipping sequence of strata is marked by several smaller folds with subparallel trends and flank-to-flank dimensions measured in hundreds of feet. One of these, a syncline with gentle to moderate westerly plunge, is the largest flexure recognized in the vicinity of the power plant site. Its axis lies a short distance north of the site and about 450 feet northeast of the mouth of Diablo Canyon (Figures 2.5-8 and 2.5-10). East of the canyon this fold appears to be rather open and simple in form, but farther west it probably is complicated by several large wrinkles and may well lose its identity as a single feature. Some of this complexity is clearly revealed along the northerly margin of Diablo Cove, where the beds exposed in the sea cliff have been closely folded along east to northeast trends. Here a tight syncline (shown in Figure 2.5-8) and several smaller folds can be recognized, and steep to near-vertical dips are dominant in several parts of the section.

The southerly flank of the main syncline within the map area steepens markedly as traced southward away from the fold axis. Most of this steepening is concentrated within an across-strike distance of about 300 feet as revealed by the strata exposed in the sea cliff southeastward from the mouth of Diablo Canyon; farther southward the beds of sandstone and finer-grained rocks dip rather uniformly at angles of 70° or more. A slight overturning through the vertical characterizes the several hundred feet of section exposed immediately north of the Obispo Tuff that underlies South Point and the north shore of South Cove (see Figure 2.5-8). Thus the main syncline, though simple in gross form, is distinctly asymmetric. The steepness of its southerly flank may well have

DCPP UNITS 1 & 2 FSAR UPDATE

resulted from buttressing, during the folding, by the relatively massive and competent unit of tuffaceous rocks that adjoins the Monterey strata at this general level of exposure.

Smaller folds, corrugations, and highly irregular convolutions are widespread among the Monterey rocks, especially the finest-grained and most shaley types. Some of these flexures trend east to southeast and appear to be drag features systematically related to the larger-scale folding in the area. Most, however, reflect no consistent form or trend, range in scale from inches to only a few feet, and evidently are confined to relatively soft rocks that are flanked by intervals of harder and more massive strata. They constitute crudely tabular zones of contortion within which individual rock layers can be traced for short distances but rarely are continuous throughout the deformed ground.

Some of this contortion appears to have derived from slumping and sliding of unconsolidated sediments on the Miocene sea floor during accumulation of the Monterey section. Most of it, in contrast, plainly occurred at much later times, presumably after conversion of the sediments to sedimentary rocks, and it can be most readily attributed to highly localized deformation during the ancient folding of a section that comprises rocks with contrasting degrees of structural competence.

2.5.1.2.4.3 Faults

Numerous faults with total displacements ranging from a few inches to several feet cut the exposed Monterey rocks. Most of these occur within, or along the margins of, the zones of contortion noted above. They are sharp, tight breaks with highly diverse attitudes, and they typically are marked by 1/16-inch or less of gouge or microbreccia. Nearly all of them are curving or otherwise somewhat irregular surfaces, and many can be seen to terminate abruptly or to die out gradually within masses of tightly folded rocks. These small faults appear to have been developed as end products of localized intense deformation caused by folding of the bedrock section. Their unsystematic attitudes, small displacements, and limited effects upon the host rocks identify them as second-order features, i.e., as results rather than causes of the localized folding and convolution with which they are associated.

Three distinctly larger and more continuous faults also were recognized within the mapped area. They are well exposed on the sea cliff that fringes Diablo Cove (see Figure 2.5-8), and each lies within a zone of moderately to severely contorted fine-grained Monterey strata. Each is actually a zone, 6 inches to several feet wide, within which two or more subparallel tight breaks are marked by slickensides, 1/4-inch or less of gouge, and local stringers of gypsum. None of these breaks appears to be systematically related to individual folds within the adjoining rocks. None of them extends upward into the overlying blanket of Quaternary terrace deposits.

One of these faults, exposed on the north side of the cove, trends north-northwest essentially parallel to the flanking Monterey beds, but it dips more steeply than these beds. Another, exposed on the east side of the cove, trends east-southeast and is essentially vertical; thus, it is essentially parallel to the structure of the host Monterey

DCPP UNITS 1 & 2 FSAR UPDATE

section. Neither of these faults projects toward the ground intended for power plant construction. The third fault, which appears on the sea cliff at the mouth of Diablo Canyon, trends northeast and projects toward the ground in the northernmost part of the power plant site. It dips northward somewhat more steeply than the adjacent strata.

Total displacement is not known for any of these three faults on the basis of natural exposures, but it could amount to as much as tens of feet. That these breaks are not major features, however, is strongly suggested by their sharpness, by the thinness of gouge along individual surfaces of slippage, and by the essential lack of correlation between the highly irregular geometry of deformation in the enclosing strata and any directions of movement along the slip surfaces.

The possibility that these surfaces are late-stage expressions of much larger-scale faulting at this general locality was tested by careful examination of the deformed rocks that they transect. On megascopic scales, the rocks appear to have been deformed much more by flexing than by rupture and slippage, as evidenced by local continuity of numerous thin beds that denies the existence of pervasive faulting within much of the ground in question. That the finer-grained rocks are not themselves fault gouged was confirmed by examination of 34 samples under the microscope.

Sedimentary layering, recognized in 27 of these samples, was observed to be grossly continuous even though dislocated here and there by tiny fractures. Moreover, nearly all the samples were found to contain shards of volcanic glass and/or the tests of foraminifera; some of these delicate components showed effects of microfracturing and a few had been offset a millimeter or less along tiny shear surfaces, but none appeared to have been smeared out or partially obliterated by intense shearing or grinding. Thus, the three larger faults in the area evidently were superimposed upon ground that already had been deformed primarily by small-scale and locally very intense folding rather than by pervasive grinding and milling.

It is not known whether these faults were late-stage results of major folding in the region or were products of independent tectonic activity. In either case, they are relatively ancient features, as they are capped without break by the Quaternary terrace deposits exposed along the upper part of the sea cliff. They probably are not large-scale elements of regional structure, as examination of the nearest areas of exposed bedrock along their respective landward projections revealed no evidence of substantial offsets among recognizable stratigraphic units.

Seaward projection of one or more of these faults might be taken to explain a possible large offset of the Obispo Tuff units exposed on North Point and South Point. The notion of such an offset, however, would rest upon the assumption that these two units are displaced parts of an originally continuous body, for which there is no real evidence. Indeed, the two tuff units are bounded on their northerly sides by lithologically different parts of the Monterey Formation; hence, they were clearly originally emplaced at different stratigraphic levels and are not directly correlative.

2.5.1.2.5 Geological Relationships at the Units 1 and 2 Power Plant Site

2.5.1.2.5.1 Geologic Investigations at the Site

The geologic relationships at DCP site have been studied in terms of both local and regional stratigraphy and structure, with an emphasis on relationships that could aid in dating the youngest tectonic activity in the area. Geologic conditions that could affect the design, construction, and performance of various components of the plant installation also were identified and evaluated. The investigations were carried out in three main phases, which spanned the time between initial site selection and completion of foundation construction.

2.5.1.2.5.2 Feasibility Investigation Phase

Work directed toward determining the pertinent general geologic conditions at the plant site comprised detailed mapping of available exposures, limited hand trenching in areas with critical relationships, and petrographic study of the principal rock types. The results of this feasibility program were presented in a report that also included recommendations for determining suitability of the site in terms of geologic conditions. Information from this early phase of studies is included in the preceding four sections and illustrated in Figures 2.5-8, 2.5-9, and 2.5-10.

2.5.1.2.5.3 Suitability Investigation Phase

The record phase of investigations was directed toward testing and confirming the favorable judgments concerning site feasibility. Inasmuch as the principal remaining uncertainties involved structural features in the local bedrock, additional effort was made to expose and map these features and their relationships. This was accomplished through excavation of large trenches on a grid pattern that extended throughout the plant area, followed by photographing the trench walls and logging the exposed geologic features. Large-scale photographs were used as a mapping base, and the recorded data were then transferred to controlled vertical sections at a scale of 1 inch = 20 feet. The results of this work were reported in three supplements to the original geologic report⁽¹⁾. Supplementary Reports I and III presented data and interpretation based on trench exposures in the areas of the Unit 1 and Unit 2 installations, respectively. Supplementary Report II described the relationships of small bedrock faults exposed in the exploratory trenches and in the nearby sea cliff. During these suitability investigations, special attention was given to the contact between bedrock and overlying terrace deposits in the plant site area. It was determined that none of the discontinuities present in the bedrock section displaces either the erosional surface developed across the bedrock or the terrace deposits that rest upon this surface. The pertinent data are presented farther on in this section and illustrated in Figures 2.5-11, 2.5-12, 2.5-13, and 2.5-14.

2.5.1.2.5.4 Construction Geology Investigation Phase

Geologic work done during the course of construction at the plant site spanned an interval of 5 years, which encompassed the period of large-scale excavation. It included detailed mapping of all significant excavations, as well as special studies in some areas of rock bolting and other work involving rock reinforcement and temporary instrumentation. The mapping covered essentially all parts of the area to be occupied by structures for Units 1 and 2, including the excavations for the circulating water intake and outlet, the turbine-generator building, the auxiliary building, and the containment structures. The results of this mapping are described farther on and illustrated in Figures 2.5-15 and 2.5-16.

2.5.1.2.5.5 Exploratory Trenching Program, Unit 1 Site

Four exploratory trenches were cut beneath the main terrace surface at the power plant site, as shown in Figures 2.5-8, 2.5-11, 2.5-12, and 2.5-13. Trench AF (Trench A), about 1080 feet long, extended in a north-northwesterly direction and thus was roughly parallel to the nearby margin of Diablo Cove. Trench BE (Trench B), 380 feet long, was parallel to Trench A and lay about 150 feet east of the northerly one-third of the longer trench. Trenches C and D, 450 and 490 feet long, respectively were nearly parallel to each other, 130 to 150 feet apart, and lay essentially normal to Trenches A and B. The two pairs of trenches crossed each other to form a "#" pattern that would have been symmetrical were it not for the long southerly extension of Trench A. They covered the area intended for Unit 1 power plant construction, and the intersection of Trenches B and C coincided in position with the center of the Unit 1 nuclear reactor structure.

All four trenches, throughout their aggregate length of approximately 2400 feet, revealed a section of surficial deposits and underlying bedrock that corresponds to the two-ply sequence of surficial deposits and Monterey strata exposed along the sea cliff in nearby Diablo Cove. The trenches ranged in depth from 10 feet to nearly 40 feet, and all had sloping sides that gave way downward to essentially vertical walls in the bedrock encountered 3 to 8 feet above their floors.

To facilitate detailed geologic mapping, the easterly walls of Trenches A and B and the southerly walls of Trenches C and D were trimmed to near-vertical slopes extending upward from the trench floors to levels well above the top of bedrock. These walls subsequently were scaled back by means of hand tools in order to provide fresh, clean exposures prior to mapping of the contact between bedrock and overlying unconsolidated materials.

1. *Bedrock*

The bedrock that was continuously exposed in the lowest parts of all the exploratory trenches lies within a portion of the Monterey Formation characterized by a preponderance of sandstone. It corresponds to the part of the section that crops out in lower Diablo Canyon and along the sea cliff southeastward from the canyon mouth. The

DCPP UNITS 1 & 2 FSAR UPDATE

sandstone ranges from light gray through buff to light reddish brown, from silty to markedly tuffaceous, and from thin-bedded and platy to massive. The distribution and thickness of beds can be readily appraised from sections along Trenches A and B (Figure 2.5-12) that show nearly all individual bedding surfaces that could be recognized on the ground.

The sandstone ranges from very hard to moderately soft, and some of it feels slightly punky when struck with a pick. All of it is, however, firm and very compact. In general, the most platy parts of the sequence are also the hardest, but the soundest rock in the area is almost massive sandstone of the kind that underlies the site of the intended reactor structure. This rock is well exposed on the nearby hillslope adjoining the main terrace area, where it has been markedly resistant to erosion and stands out as distinct low ridges.

Tuff, consisting chiefly of altered volcanic glass, forms irregular sills and dikes in several parts of the bedrock section. This material, generally light gray to buff, is compact but distinctly softer than the enclosing sandstone. Individual bodies are 1/2 inch to 4 feet thick. They are locally abundant in Trench C west of Trench A, and in Trench A southward beyond the end of the section in Figure 2.5-12. They are very rare or absent in Trenches B and D, and in the easterly parts of Trench C and the northerly parts of Trench A. These volcanic rocks probably are related to the Obispo Tuff as described earlier, but all known masses of typical Obispo rocks in this area lie at considerable distances west and south of the ground occupied by the trenches.

2. Bedrock Structure

The stratification of the Monterey rocks dips northward wherever it was observable in the trenches, in general, at angles of 35 to 55°. Thus, the bedrock beneath the power plant site evidently lies on the southerly flank of the major syncline noted and described earlier. Zones of convolution and other expressions of locally intense folding were not recognized, and probably are much less common in this general part of the section than in other, previously described parts that include intervals of softer and more shaley rocks.

Much of the sandstone is traversed by fractures. Planar, curving, and irregular surfaces are well represented, and, in places, they are abundant and closely spaced. All prominent fractures and many of the minor and discontinuous ones are shown in the sections of Figure 2.5-12. Also shown in these sections are all recognized slip joints, shear surfaces, and faults, i.e., all surfaces along which the bedrock has been displaced. Such features are most abundant in Trenches A and C near their intersection, in Trench D west of the intersection with Trench A, and near the northerly end of Trench B.

Most of the surfaces of movement are hairline features with or without thin films of clay and/or gypsum. Displacements range from a small fraction of an inch to several inches. The other surfaces are more prominent, with well-defined zones of gouge and fine-

DCPP UNITS 1 & 2 FSAR UPDATE

grained breccia ordinarily 1/8 inch or less in thickness. Such zones were observed to reach a maximum thickness of nearly 1/2 inch along two small faults, but only as local lenses or pockets. Exposures were not sufficiently extensive in three dimensions for definitely determining the magnitude of slip along the more prominent faults, but all of these breaks appeared to be minor features. Indeed, no expressions of major faulting were recognized in any of the trenches despite careful search, and the continuous bedrock exposures precluded the possibility that such features could have been readily overlooked.

A northeast-trending fault that appears on the sea cliff at the mouth of Diablo Canyon projects toward the ground in the northernmost part of the power plant site, as noted in a foregoing section. No zone of breaks as prominent as this one was identified in the trench exposures, and any distinct northeastward continuation of the fault would necessarily lie north of the trenched ground. Alternatively, this fault might well separate northeastward into several smaller faults; some or all of these could correspond to some or all of the breaks mapped in the northerly parts of Trenches A and B.

3. *Terrace Deposits*

Marine terrace deposits of Pleistocene age form a cover, generally 2 to 5 feet thick, over the bedrock that lies beneath the power plant site. This cover was observed to be continuous in Trench C and the northerly part of Trench A, and to be nearly continuous in the other two trenches. Its lithology is highly variable, and includes bouldery rubble, loose beach sand, pebbly silt, silty to clayey sand with abundant shell fragments, and soft clay derived from underlying tuffaceous rocks. Nearly all of these deposits are at least sparsely fossiliferous, and, in a few places, they consist mainly of shells and shell fragments. Vertebrate fossils, chiefly vertebral and rib materials representing large marine mammals, are present locally; recognized occurrences are designated by the symbol X in the sections of Figure 2.5-12.

At the easterly ends of Trenches C and D, the marine deposits intergrade and intertongue in a landward direction with thicker and coarser accumulations of poorly sorted debris. This material evidently is talus that was formed along the base of an ancient sea cliff or other shoreline slope. In some places, the marine deposits are overlain by nonmarine terrace sediments with a sharp break, but elsewhere the contact between these two kinds of deposits is a dark colored zone, a few inches to as much as 2 feet thick, that appears to represent a soil developed on the marine section. Fragments of these soily materials appear here and there in the basal parts of the nonmarine section.

The nonmarine sediments that were exposed in Trenches B, C, and D and in the northerly part of Trench A are mainly alluvial deposits derived in ancient times from Diablo Canyon. They consist of numerous tabular fragments of Monterey rocks in a relatively dark colored silty to clayey matrix, and, in general, they are distinctly bedded and moderately to highly compact. As indicated in the sections of Figure 2.5-12, they

DCPP UNITS 1 & 2 FSAR UPDATE

thicken progressively in a north-northeastward direction, i.e., toward their principal source, the ancient mouth of Diablo Canyon.

Slump, creep, and slope-wash deposits, which constitute the youngest major element of the terrace section, overlie the alluvial fan gravels and locally are interlayered with them. Where the gravels are absent, as in the southerly part of Trench A, this younger cover rests directly upon bedrock. It is loose and uncompacted, internally chaotic, and is composed of fragments of Monterey rocks in an abundant dark colored clayey matrix.

All the terrace deposits are soft and unconsolidated, and hence are much less resistant to erosion than is the underlying bedrock. Those appearing along the walls of exploratory trenches were exposed to heavy rainfall during two storms, and showed some tendency to wash and locally to rill. Little slumping and no gross failure were noted in the trenches, however, and it was not anticipated that these materials would cause special problems during construction of a power plant.

4. Interface Between Bedrock and Surficial Deposits

As once exposed continuously in the exploratory trenches, the contact between bedrock and overlying terrace deposits represents a broad wave-cut platform of Pleistocene age. This buried surface of ancient marine erosion ranges in altitude between extremes of 82 and 100 feet, and more than three-fourths of it lies within the more limited range of 90 to 100 feet. It terminates eastward against a moderately steep shoreline slope, the lowest parts of which were encountered at the extreme easterly ends of Trenches C and D, and beyond this slope is an older buried bench at an altitude of 120 to 130 feet.

Available exposures indicate that the configuration of the erosional platform is markedly similar, over a wide range of scales, to that of the platform now being cut approximately at sea level along the present coast. Grossly viewed, it slopes very gently in a seaward (westerly) direction and is marked by broad, shallow channels and by upward projections that must have appeared as low spines and reefs when the bench was being formed (Figures 2.5-12 and 2.5-13). The most prominent reef, formerly exposed in Trenches B and D at and near their intersection, is a wide, westerly-trending projection that rises 5 to 15 feet above neighboring parts of the bench surface. It is composed of massive sandstone that was relatively resistant to the ancient wave erosion.

As shown in the sections and sketches of Figure 2.5-12, the surface of the platform is nearly planar in some places but elsewhere is highly irregular in detail. The small-scale irregularities, generally 3 feet or less in vertical extent, including knob, spine, and rib like projections and various wave-scoured pits, crevices, notches, and channels. The upward projections clearly correspond to relatively hard, resistant beds or parts of beds in the sandstone section. The depressions consistently mark the positions of relatively soft silty or shaley sandstone, of very soft tuffaceous rocks, or of extensively jointed rocks. The surface traces of most faults and some of the most prominent joints are in sharp depressions, some of them with overhanging walls. All these irregularities of

DCPP UNITS 1 & 2 FSAR UPDATE

detail have modern analogues that can be recognized on the bedrock bench now being cut along the margins of Diablo Cove.

The interface between bedrock and overlying surficial deposits is of particular interest in the trenched area because it provides information concerning the age of youngest fault movements within the bedrock section. This interface is nowhere offset by faults revealed in the trenches, but instead has been developed irregularly across these faults after their latest movements. The consistency of this general relationship was established by highly detailed tracing and inspection of the contact as freshly exhumed by scaling of the trench walls. Gaps in exposure of the interface necessarily were developed at the four intersections of trenches; at these localities, the bedrock was carefully laid bare so that all joints and faults could be recognized and traced along the trench floors to points where their relationships with the exposed interface could be determined.

Corroborative evidence concerning the age of the most recent fault displacements stems from the marine deposits that overlie the bedrock bench and form the basal part of the terrace section. That these deposits rest without break across the traces of faults in the underlying bedrock was shown by the continuity of individual sedimentary beds and lenses that could be clearly recognized and traced.

Further, some of the faults are directly capped by individual boulders, cobbles, pebbles, shells, and fossil bones, none of which have been affected by fault movements. Thus, the most recent fault displacements in the plant site area occurred prior to marine planation of the bedrock and deposition of the overlying terrace sediments. As pointed out earlier, the age of the most recent faulting in this area is therefore at least 80,000 years and more probably at least 120,000 years. It might be millions of years.

2.5.1.2.5.6 Exploratory Trenching Program, Unit 2 Site

Eight additional trenches were cut beneath the main terrace surface south of Diablo Canyon (Figure 2.5-13) in order to extend the scope of subsurface exploration to include all ground in the Unit 2 plant site. As in the area of the Unit 1 plant site, the trenches formed two groups; those in each group were parallel with one another and were oriented nearly normal to those of the other group. The excavations pertinent to the Unit 2 plant site can be briefly identified as follows:

1. North-northwest Alignment

- a. Trench EJ, 240 feet long, was a southerly extension of older Trench BE (originally designated as Trench B).
- b. Trench WU, 1300 feet long, extended southward from Trench DG (originally designated as Trench D), and its northerly part lay about 65 feet east of Trench EJ. The northernmost 485 feet of this trench was mapped in connection with the Unit 2 trenching program.

DCPP UNITS 1 & 2 FSAR UPDATE

- c. Trench MV, 700 feet long, lay about 190 feet east of Trench WU. The northernmost 250 feet of this trench was mapped in connection with the Unit 2 trenching program.
- d. Trench AF (originally designated as Trench A) was mapped earlier in connection with the detailed study of the Unit 1 plant site. A section for this trench, which lay about 140 feet west of Trench EJ, was included with others in the report on the Unit 1 trenching program.

2. *East-northeast Alignment*

- a. Trench KL, about 750 feet long, lay 180 feet south of Trench DG (originally designated as Trench D) and crossed Trenches AF, EJ, and WU.
- b. Trench NO, about 730 feet long, lay 250 feet south of Trench KL and crossed Trenches AF, WU, and MV.

These trenches, or parts thereof, covered the area intended for the Unit 2 power plant construction, and the intersection of Trenches WU and KL coincided in position with the center of the Unit 2 nuclear reactor structure.

All five additional trenches, throughout their aggregate length of nearly half a mile, revealed a section of surficial deposits and underlying Monterey bedrock that corresponded to the two-ply sequence of surficial deposits and Monterey strata exposed in the older trenches and along the sea cliff in nearby Diablo Cove. The trenches ranged in depth from 10 feet (or less along their approach ramps) to nearly 35 feet, and all had sloping sides that gave way downward to essentially vertical walls in the bedrock encountered 3 to 22 feet above their floors. To facilitate detailed geologic mapping, the easterly walls of Trenches EJ, WU, and MV and the southerly walls of Trenches KL and NO were trimmed to near-vertical slopes extending upward from the trench floors to levels well above the top of bedrock. These walls subsequently were scaled back by means of hand tools in order to provide fresh, clean exposures prior to mapping of the contact between bedrock and overlying unconsolidated materials.

The geologic sections shown in Figures 2.5-12 and 2.5-13 correspond in position to the vertical portions of the mapped trench walls. Relationships exposed at higher levels on sloping portions of the trench walls have been projected to the vertical planes of the sections. Centerlines of intersecting trenches are shown for convenience, but the planes of the geologic sections do not contain the centerlines of the respective trenches.

3. *Bedrock*

The bedrock that was continuously exposed in the lowest parts of all the exploratory trenches lies within a part of the Monterey Formation characterized by a preponderance

DCPP UNITS 1 & 2 FSAR UPDATE

of sandstone. It corresponds to the portion of the section that crops out along the sea cliff southward from the mouth of Diablo Canyon. The sandstone is light to medium gray where fresh, and light gray to buff and reddish brown where weathered. It ranges from silty to markedly tuffaceous, with tuffaceous units tending to dominate southward and southwestward from the central parts of the trenched area (see geologic section in Figure 2.5-13). Much of the sandstone is thin-bedded and platy, but the most siliceous parts of the section are characterized by a strata a foot or more in thickness. Individual beds commonly are well defined by adjacent thin layers of more silty material.

Bedding is less distinct in the more tuffaceous parts of the section, some of which seem to be almost massive. These rocks typically are broken by numerous tight fractures disposed at high angles to one another so that, where weathered, their appearance is coarsely blocky rather than layered.

As broadly indicated in the geologic sections, the sandstone ranges from very hard to moderately soft, and some of it feels slightly punky when struck with a pick. All of it, however, is firm and very compact. In general, the most platy parts of the sequence are relatively hard, but the hardest and soundest rock in the area is thick-bedded to almost massive sandstone of the kind at and immediately north of the site for the intended reactor structure. This resistant rock is well exposed as distinct low ridges on the nearby hillslope adjoining the main terrace area.

Tuff, consisting chiefly of altered volcanic glass, is abundant within the bedrock section. Also widely scattered, but much less abundant, is tuff breccia, consisting typically of small fragments of older tuff, pumice, or Monterey rocks in a matrix of fresh to altered volcanic glass. These materials, which form sills, dikes, and highly irregular intrusive masses, are generally light gray to buff, gritty, and compact but distinctly softer than much of the enclosing sandstone. Individual bodies range from stringers less than a quarter of an inch thick to bulbous or mushroom-shaped masses with maximum exposed dimensions measured in tens of feet. As shown on the geologic sections, they are abundant in all the trenches.

These volcanic rocks probably are related to the Obispo Tuff, large masses of which are well exposed west and south of the trenched ground. The bodies exposed in the trenches doubtless represent a rather lengthy period of Miocene volcanism, during which the Monterey strata were repeatedly invaded by both tuff and tuff breccia. Indeed, several of the mapped tuff units were themselves intruded by dikes of younger tuff, as shown, for example, in Sections KL and NO.

4. Bedrock Structure

The stratification of the Monterey rocks dips northward wherever it was observable in the trenches, in general, at angles of 45 to 85°. The steepness of dip increases progressively from north to south in the trenched ground, a relationship also noted along the sea cliff southward from the mouth of Diablo Canyon. Thus, the bedrock beneath the power plant site evidently lies on the southerly flank of the major syncline that was

DCPP UNITS 1 & 2 FSAR UPDATE

described previously. Zones of convolution and other expressions of locally intense folding were not recognized, and they probably are much less common in this general part of the section than in other (previously described) parts that include intervals of softer and more shaley rocks.

Much of the sandstone is traversed by fractures. Planar, curving, and irregular surfaces are well represented, and in places they are abundant and closely spaced. All prominent fractures and nearly all of the minor and discontinuous ones are shown on the geologic sections (Figure 2.5-13). Also shown in these sections are all recognized shear surfaces, faults, and other discontinuities along which the bedrock has been displaced. Such features are nowhere abundant in the trench exposures.

Most of the surfaces of movement are hairline breaks with or without thin films of clay, calcite, and/or gypsum. Displacements range from a small fraction of an inch to several inches. A few other surfaces are more prominent, with well-defined zones of fine-grained breccia and/or infilling mineral material ordinarily 1/8 inch or less in thickness. Such zones were observed to reach maximum thicknesses of 3/8 to 1/2 inch along three small faults, but only as local lenses or pockets.

Exposures are not sufficiently extensive in three dimensions for definitely determining the magnitude of slip along all the faults, but for most of them it is plainly a few inches or less. None of them appears to be more than a minor break in a bedrock section that has been folded on a large scale. Indeed, no expressions of major faulting were recognized in any of the trenches despite careful search, and the continuous bedrock exposures preclude the possibility that such features could be readily overlooked.

Most surfaces of past movement probably were active during times when the Monterey rocks were being deformed by folding, when rupture and some differential movements would be expected in a section comprising such markedly differing rock types. Some of the fault displacements may well have been older, as attested in two places by relationships involving small faults, the Monterey rocks, and tuff.

In Trench WU south of Trench KL, for example, sandstone beds were seen to have been offset about a foot along a small fault. A thin sill of tuff occupies the same stratigraphic horizon on opposite sides of this fault, but the sill has not been displaced by the fault. Instead, the tuff occupies a short segment of the fault to effect the slight jog between its positions in the strata on either side. Intrusion of the tuff plainly postdated all movements along this fault.

5. Terrace Deposits

Marine terrace deposits of Pleistocene age form covers, generally 2 to 5 feet thick, but locally as much as 12 feet thick, over the bedrock that lies beneath the Unit 2 plant site. These covers were observed to be continuous in some parts of all the trenches, and thin and discontinuous in a few other parts. Elsewhere, the marine sediments were

DCPP UNITS 1 & 2 FSAR UPDATE

absent altogether, as in the lower and more southerly parts of Trenches EJ and WU and in the lower and more westerly parts of Trenches KL and NO.

The range in lithology of these deposits is considerable, and includes bouldery rubble, gravel composed of well-rounded fragments of shells and/or Monterey rocks, beach sand, loose accumulations of shells, pebbly silt, silty to clayey sand with abundant shell fragments, and soft clay derived from underlying tuffaceous rocks. Nearly all of the deposits are at least sparsely fossiliferous, and many of them contain little other than shell material. Vertebrate fossils, chiefly vertebral and rib materials representing large marine mammals, are present locally.

The trenches in and near the site of the reactor structure exposed a buried narrow ridge of hard bedrock that once projected westward as a bold promontory along an ancient sea coast, probably at a time when sea level corresponded approximately to the present 100 foot contour (see Figure 2.5-11). Along the flanks of this promontory and the face of an adjoining buried sea cliff that extends southeastward through the area in which Trenches MV and NO intersected, the marine deposits intergrade and intertongue with thicker and coarser accumulations of poorly sorted debris. This rubbly material evidently is talus that was formed and deposited along the margins of the ancient shoreline cliff.

Similar gradations of older marine deposits into older talus deposits were observable at higher levels in the easternmost parts of Trenches KL and NO, where the rubbly materials doubtless lie against a more ancient sea cliff that was formed when sea level corresponded to the present 140 foot contour. The cliff itself was not exposed, however, as it lies slightly beyond the limits of trenching.

In many places, the marine covers are overlain by younger nonmarine terrace sediments with a sharp break, but elsewhere the contact between these two kinds of deposits is a zone of dark colored material, a few inches to as much as 6 feet thick, that represents weathering and development of soils on the marine sections. Fragments of these soily materials are present here and there in the basal parts of the nonmarine section. Over large areas, the porous marine deposits have been discolored through infiltration by fine-grained materials derived from the overlying ancient soils.

The nonmarine accumulations, which form the predominant fraction of the entire terrace cover, consist mainly of slump, creep, and slope-wash debris that is characteristically loose, uncompacted, and internally chaotic. These relatively dark colored deposits are fine grained and clayey, but they contain sparse to very abundant fragments of Monterey rocks generally ranging from less than an inch to about 2 feet in maximum dimension. Toward Diablo Canyon they overlie and, in places, intertongue with silty to clayey gravels that are ancient contributions from Diablo Creek when it flowed at levels much higher than its present one. These "dirty" alluvial deposits appeared only in the most northerly parts of the more recently trenched terrace area, and they are not distinguished from other parts of the nonmarine cover on the geologic sections (Figure 2.5-13).

DCPP UNITS 1 & 2 FSAR UPDATE

All the terrace deposits are soft and unconsolidated, and hence are much less resistant to erosion than is the underlying bedrock. Those appearing along the walls of the exploratory trenches showed some tendency to wash and locally to rill when exposed to heavy rainfall, but little slumping and no gross failure were noted in the trenches.

6. Interface Between Bedrock and Surficial Deposits

As exposed continuously in the exploratory trenches, the contact between bedrock and overlying terrace deposits represents two wave-cut platforms and intervening slopes, all of Pleistocene age. The broadest surface of ancient marine erosion ranges in altitude from 80 to 105 feet, and its shoreward margin, at the base of an ancient sea cliff, lies uniformly within 5 feet of the 100 foot contour. A higher, older, and less extensive marine platform ranges in altitude from 130 to 145 feet, and most of it lies within the ranges of 135 to 140 feet. As noted previously, these are two of several wave-cut benches in this coastal area, each of which terminates eastward against a cliff or steep shoreline slope and westward at the upper rim of a similar but younger slope.

Available exposures indicate that the configurations of the erosional platforms are markedly similar, over a wide range of scales, to that of the platform now being cut approximately at sea level along the present coast. Grossly viewed, they slope very gently in a seaward (westerly) direction and are marked by broad, shallow channels and by upward projections that must have appeared as low spines and reefs when the benches were being formed. The most prominent reefs, which rise from a few inches to about 5 feet above neighboring parts of the bench surfaces, are composed of hard, thick-bedded sandstone that was relatively resistant to ancient wave erosion.

As shown in the geologic sections (Figure 2.5-13), the surfaces of the platforms are nearly planar in some places but elsewhere are highly irregular in detail. The small scale irregularities, generally 3 feet or less in vertical extent, include knob-, spine-, and rib-like projections and various wave-scoured pits, notches, crevices, and channels. Most of the upward projections closely correspond to relatively hard, resistant beds or parts of beds in the sandstone section. The depressions consistently mark the positions of relatively soft silty or shaley sandstone, of very soft tuffaceous rocks, or of extensively jointed rocks. The surface traces of most faults and some of the most prominent joints are in sharp depressions, some of them with overhanging walls. All these irregularities of detail have modern analogues that can be recognized on the bedrock bench now being cut along the margins of Diablo Cove.

The interface between bedrock and overlying surficial deposits provides information concerning the age of youngest fault movements within the bedrock section. This interface is nowhere offset by faults that were exposed in the trenches, but instead has been developed irregularly across the faults after their latest movements. The consistency of this general relationship was established by highly detailed tracing and inspection of the contact as freshly exhumed by scaling of the trench walls. Gaps in exposure of the interface necessarily were developed at the intersections of trenches as in the exploration at the Unit 1 site. At such localities, the bedrock was carefully laid

DCPP UNITS 1 & 2 FSAR UPDATE

bare so that all joints and faults could be recognized and traced along the trench floors to points where their relationships with the exposed interface could be determined.

Corroborative evidence concerning the age of the most recent fault displacements stems from the marine deposits that overlie the bedrock bench and form a basal part of the terrace section. That these deposits rest without break across the traces of faults in the underlying bedrock was shown by the continuity of individual sedimentary beds and lenses that could be clearly recognized and traced. As in other parts of the site area, some of the faults are directly capped by individual boulders, cobbles, pebbles, shells, and fossil bones, none of which have been affected by fault movements. Thus, the most recent fault displacements in the plant site area occurred before marine planation of the bedrock and deposition of the overlying terrace sediments.

The age of the most recent faulting in this area is therefore at least 80,000 years. More probably, it is at least 120,000 years, the age most generally assigned to these terrace deposits along other parts of the California coastline. Evidence from the higher bench in the plant site area indicates a much older age, as the unfaulted marine deposits there are considerably older than those that occupy the lower bench corresponding to the 100 foot terrace. Moreover, it can be noted that ages thus determined for most recent fault displacements are minimal rather than absolute, as the latest faulting actually could have occurred millions of years ago.

During the Unit 2 exploratory trenching program, special attention was directed to those exposed parts of the wave-cut benches where no marine deposits are present, and hence where there are no overlying reference materials nearly as old as the benches themselves. At such places, the bedrock beneath each bench has been weathered to depths ranging from less than 1 inch to at least 10 feet, a feature that evidently corresponds to a lengthy period of surface exposure from the time when the bench was abandoned by the sea to the time when it was covered beneath encroaching nonmarine deposits derived from hillslopes to the east.

Stratification and other structural features are clearly recognizable in the weathered bedrock, and they obviously have exercised some degree of control over localization of the weathering. Moreover, in places where upward projections of bedrock have been gradually bent or rotationally draped in response to weathering and creep, their contained fractures and surfaces of movement have been correspondingly bent. Nowhere in such a section that has been disturbed by weathering have the materials been cut by younger fractures that would represent straight upward projections of breaks in the underlying fresh rocks. Nor have such fractures been observed in any of the overlying nonmarine terrace cover.

Thus, the minimum age of any fault movement in the plant site area is based on compatible evidence from undisplaced reference features of four kinds: (a) Pleistocene wave-cut benches developed on bedrock, (b) immediately overlying marine deposits that are very slightly younger, (c) zones of weathering that represent a considerable span of subsequent time, and (d) younger terrace deposits of nonmarine origin.

2.5.1.2.5.7 Bedrock Geology of the Plant Foundation Excavations

Bedrock was continuously exposed in the foundation excavations for major structural components of Units 1 and 2. Outlines and invert elevations of these large openings, which ranged in depth from about 5 to nearly 90 feet below the original ground surface, are shown in Figures 2.5-15 and 2.5-16. The complex pattern of straight and curved walls with various positions and orientations provided an excellent three-dimensional representation of bedrock structure. These walls were photographed at large scales as construction progressed, and the photographs were used directly as a geologic mapping base. The largest excavations also were mapped in detail on a surveyed planimetric base.

Geologic mapping of the plant excavations confirmed the conclusions based on earlier investigations at the site. The exposed section of Monterey strata was found to correspond in lithology and structure to what had been predicted from exposures at the mouth of Diablo Canyon, along the sea cliffs in nearby Diablo Cove, and in the test trenches. Thus, the plant foundation is underlain by a moderately to steeply north-dipping sequence of thin to thick bedded sandy mudstone and fine-grained sandstone. The rocks at these levels are generally fresh and competent, as they lie below the zone of intense near-surface weathering.

Several thin interbeds of claystone were exposed in the southwestern part of the plant site in the excavations for the Unit 2 turbine-generator building, intake conduits, and outlet structure. These beds, which generally are less than 6 inches thick, are distinctly softer than the flanking sandstone. Some of them show evidence of internal shearing.

Layers of tuffaceous sandstone and sills, dikes, and irregular masses of tuff and tuff breccia are present in most parts of the foundation area. They tend to increase in abundance and thickness toward the south, where they are relatively near the large masses of Obispo Tuff exposed along the coast south of the plant site.

Some of the tuff bodies are conformable with the enclosing sandstone, but others are markedly discordant. Most are clearly intrusive. Individual masses, as exposed in the excavations, range in thickness from less than 1 inch to about 40 feet. The tuff breccia, which is less abundant than the tuff, consists typically of small fragments of older tuff, pumice, or Monterey rocks in a matrix of fresh to highly altered volcanic glass. At the levels of exposure in the excavations, both the tuff and tuff breccia are somewhat softer than the enclosing sandstone.

The stratification of the Monterey rocks dips generally northward throughout the plant foundation area. Steepness of dips increases progressively and, in places, sharply from north to south, ranging from 10 to 15° on the north side of Unit 1 to 75 to 80° in the area of Unit 2. A local reversal in direction of dip reflects a small open fold or warp in the Unit 1 area. The axis of this fold is parallel to the overall strike of the bedding, and strata on the north limb dip southward at angles of 10 to 15°. The more general

steepening of dips from north to south may reflect buttressing by the large masses of Obispo Tuff south of the plant site.

The bedrock of the plant area is traversed throughout by fractures, including various planar, broadly curving, and irregular breaks. A dominant set of steeply dipping to vertical joints trends northerly, nearly normal to the strike of bedding. Other joints are diversely oriented with strikes in various directions and dips ranging from 10° to vertical. Many fractures curve abruptly, terminate against other breaks, or die out within single beds or groups of beds.

Most of the joints are widely spaced, ranging from about 1 to 10 feet apart, but within several northerly trending zones, ranging in width from 10 to 20 feet, closely spaced near vertical fractures give the rocks a blocky or platy appearance. The fracture and joint surfaces are predominantly clean and tight, although some irregular ones are thinly coated with clay or gypsum. Others could be traced into thin zones of breccia with calcite cement.

Several small faults were mapped in the foundation excavations for Unit 1 and the outlet structure. A detailed discussion of these breaks and their relationship to faults that were mapped earlier along the sea cliff and in the exploratory trenches is included in the following section.

2.5.1.2.5.8 Relationships of Faults and Shear Surfaces

Several subparallel breaks are recognizable on the sea cliff immediately south of Diablo Canyon, where they transect moderately thick-bedded sandstone of the kind exposed in the exploratory trenches to the east. These breaks are nearly concordant with the bedrock stratification but, in general, they dip more steeply (see detailed structure section, Figure 2.5-14) and trend more northerly than the stratification. Their trend differs significantly from much of their mapped trace, as the trace of each inclined surface is markedly affected by the local steep topography. The indicated trend, which projects eastward toward ground north of the Unit 1 reactor site, has been summed from numerous individual measurements of strike on the sea cliff exposures, and it also corresponds to the trace of the main break as observed in nearly horizontal outcrop within the tidal zone west of the cliff.

The structure section shows all recognizable surfaces of faulting and shearing in the sea cliff that are continuous for distances of 10 feet or more. Taken together, they represent a zone of dislocation along which rocks on the north have moved upward with respect to those on the south as indicated by the attitude and roughness sense of slickensides. The total amount of movement cannot be determined by any direct means, but it probably is not more than a few tens of feet and could well be less than 10 feet. This is suggested by the following observed features:

- (1) All individual breaks are sharp and narrow, and the strata between them are essentially undeformed except for their gross inclination.

DCPP UNITS 1 & 2 FSAR UPDATE

- (2) Some breaks plainly die out as traced upward along the cliff surface, and others merge with adjoining breaks. At least one well-defined break butts downward against a cross-break, which in turn butts upward against a break that branches and dies out approximately 20 feet away (see structure section, Figure 2.5-14, for details).
- (3) Nearly all the breaks curve moderately to abruptly in the general direction of movement along them.
- (4) Most of the breaks are little more than knife-edge features along which rock is in direct contact with rock, and others are marked by thin films of gouge. Maximum thickness of gouge anywhere observed is about 1/2 inch, and such exceptional occurrences are confined to short curving segments of the main break at the southerly margin of the zone.
- (5) No fault breccia is present; instead, the zone represents transection of otherwise undeformed rocks by sharply-defined breaks. No bedrock unit is cut off and juxtaposed against a unit of different lithology along any of the breaks.
- (6) Local prominence of the exposed breaks, and especially the main one, is due to slickensides, surface coatings of gypsum, and iron-oxide stains rather than to any features reflecting large-scale movements.

This zone of faulting cannot be regarded as a major tectonic element, nor is it the kind of feature normally associated with the generation of earthquakes. It appears instead to reflect second-order rupturing related to a marked change in dip of strata to the south, and its general sense of movement is what one would expect if the breaks were developed during folding of the Monterey section against what amounts to a broad buttress of Obispo Tuff farther south (see geologic map, Figure 2.5-8). That the fault and shear movements were ancient is positively indicated by upward truncation of the zone at the bench of marine erosion along the base of the overlying terrace deposits.

As indicated earlier, bedrock was continuously exposed along several exploratory trenches. This bedrock is traversed by numerous fractures, most of which represent no more than rupture and very small amounts of simple separation. The others additionally represent displacement of the bedrock, and the map in Figure 2.5-14 shows every exposed break in the initial set of trenches along which any amount of displacement could be recognized or inferred.

That the surfaces of movement constitute no more than minor elements of the bedrock structure was verified by detailed mapping of the large excavations for the plant structures. Detailed examination of the excavation walls indicated that the faults exposed in the sea cliff south of Diablo Canyon continue through the rock under the Unit 1 turbine-generator building, where they are expressed as three subparallel breaks with easterly trend and moderately steep northerly dips (Figure 2.5-15).

DCPP UNITS 1 & 2 FSAR UPDATE

Stratigraphic separation along these breaks ranges from a few inches to nearly 5 feet, and, in general, decreases eastward on each of them. They evidently die out in the ground immediately west of the containment excavation, and their eastward projections are represented by several joints along which no offsets have occurred. Such joints, with eastward trend and northward dip, also are abundant in some of the ground adjacent to the faults on the south (Figure 2.5-15).

The easterly reach of the Diablo Canyon sea cliff faults apparently corresponds to the two most northerly of the north-dipping faults mapped in Trench A (Figure 2.5-14). Dying out of these breaks, as established from subsequent large excavations in the ground east of where Trench A was located, explains and verifies the absence of faults in the exposed rocks of Trenches B and C. Other minor faults and shear surfaces mapped in the trench exposures could not be identified in the more extensive exposures of fresher rocks in the Unit 1 containment and turbine-generator building excavations. The few other minor faults that were mapped in these large excavations evidently are not sufficiently continuous to have been present in the exploratory trenches.

2.5.1.2.6 Site Engineering Properties

2.5.1.2.6.1 Field and Laboratory Investigations

In order to determine anticipated ground accelerations at the site, it was necessary to conduct field surveys and laboratory testing to evaluate the engineering properties of the materials underlying the site.

Bore holes were drilled into the rock upon which Category I structures are founded. The borings were located at or near the intersection of the then existing Unit 1 exploration trenches. (See Figures 2.5-11, 2.5-12, and 2.5-13 for exploratory trenching programs and boring locations.) These holes were cored continuously and representative samples were taken from the cores and submitted for laboratory testing.

The field work also included a reconnaissance to evaluate physical condition of the rocks that were exposed in trenches, and samples were collected from the ground surface in the trenches for laboratory testing. These investigations included seismic refraction measurements across the ground surface and uphole seismic measurements in the various drill holes to determine shear and compressional velocities of vertically propagated waves.

Laboratory testing, performed by Woodward-Clyde-Sherard & Associates, included unconfined compression tests, dynamic elastic moduli tests under controlled stress conditions, density and water content determinations, and Poisson's ratio tests. Tests were also carried out by Geo-Recon, Incorporated, to determine seismic velocities on selected rock samples in the laboratory. The results of seismic measurements in the field were used to construct a three-dimensional model of the subsurface materials beneath the plant site showing variations of shear wave velocity and compressional wave velocity both laterally and vertically. The seismic velocity data and elastic moduli

DCPP UNITS 1 & 2 FSAR UPDATE

determined from laboratory testing were correlated to determine representative values of elastic moduli necessary for use in dynamic analyses of structures.

Details of field investigations and results of laboratory testing and correlation of data are contained in Appendices 2.5A and 2.5B of Reference 27 in Section 2.3.

2.5.1.2.6.2 Summary and Correlation of Data

The foundation material at the site can be categorized as a stratified sequence of fine to very fine grained sandstone deeply weathered to an average elevation of 75 to 80 feet, mean sea level (MSL). The rock is closely fractured, with tightly closed or healed fractures generally present below elevation 75 feet. Compressional and shear wave velocity interfaces generally are at an average elevation of 75 feet, correlating with fracture conditions.

Time-distance plots and seismic velocity profiles presenting results of each seismic refraction line and time depth plots with results for each uphole seismic survey are included in Appendices 2.5A and 2.5B of Reference 27 in Section 2.3. Compressional wave velocities range from 2350 to 5700 feet per second and shear wave velocities from 1400 to 3600 feet per second as determined by the refraction survey. These same parameters range from 2450 to 9800 and 1060 to 6050 feet per second as determined by the uphole survey. An isometric diagram summarizing results of the refraction survey for Unit 1 is also included in Appendix 2.5A of Reference 27 in Section 2.3.

Table 1 of Appendix 2.5A of Reference 27 of Section 2.3 shows calculations of Poisson's ratio and Young's Modulus based on representative compressional and shear wave velocities from the field geophysical investigations and laboratory measurements of compressional wave velocities. Table 2 of Appendix 2.5A of the same reference presents laboratory test results including density, unconfined compressive strength, Poisson's ratio and calculated values for compressional and shear wave velocities, shear modulus, and constrained modulus. Secant modulus values in Table 2 were determined from cyclic stress-controlled laboratory tests.

Compressional wave velocity measurements were made in the laboratory of four selected core samples and three hand specimens from exposures in the trench excavations. Measured values ranged from 5700 to 9500 feet per second. A complete tabulation of these results can be found in Appendix 2.5A of Reference 27 of Section 2.3.

2.5.1.2.6.3 Dynamic Elastic Moduli and Poisson's Ratio

Laboratory test results are considered to be indicative of intact specimens of foundation materials. Field test results are considered to be indicative of the gross assemblage of foundation materials, including fractures and other defects. Load stress conditions are obtained by evaluating cyclic load tests. In-place load stress conditions and confinement of the material at depth are also influential in determining elastic behavior.

DCPP UNITS 1 & 2 FSAR UPDATE

Because of these considerations, originally recommended representative values for Young's Modulus of Elasticity and Poisson's ratio for the site were:

| <u>Depth Below Bottom of Trench</u> | <u>E</u> | <u>δ</u> |
|-------------------------------------|-----------------------------------|----------------------------|
| 0 to approximately 15 feet | $44 \times 10^6 \text{ lb/ft}^2$ | 0.20 |
| Below 15 feet | $148 \times 10^6 \text{ lb/ft}^2$ | 0.18 |

A single value was selected for Young's Modulus below 15 feet because the initial analyses of the seismic response of the structures utilized a single value that was considered representative of the foundation earth materials as a whole.

More detailed seismic analyses were performed subsequent to the initial analyses. These analyses, discussed in Section 3.7.2, incorporated the finite element method and made it possible to model the rock beneath the plant site in a more refined manner by accounting for changes in properties with increasing depth. To determine the refined properties of the founding materials for these analyses, the test data were reviewed and consideration was given to: (a) strain range of the materials at the site, (b) overburden pressure and confinement, (c) load imposed by the structure, (d) observation of fracture condition and geometry of the founding rock in the open excavation, (e) decreases in Poisson's ratio with depth, and (f) significant advances in state-of-the-art techniques of testing and analysis in rock mechanics that had been made and which resulted in considerably more being known about the behavior of rock under seismic strains in 1970 than in 1968 or 1969.

For the purposes of developing the mathematical models that represented the rock mass, the foundation was divided into horizontal layers based on: (a) the estimated depth of disturbance of the foundation rock below the base of the excavation, (b) changes in rock type and physical condition as determined from bore hole logs, (c) velocity interfaces as determined by refraction geophysical surveys, and (d) estimated depth limit of fractures across which movement cannot take place because of confinement and combined overburden and structural load. Based on these considerations, the founding material properties as shown in Figure 2.5-19 were selected as being representative of the physical conditions in the founding rock.

2.5.1.2.6.4 Engineered Backfill

Backfill operations were carefully controlled to ensure stability and safety. All engineered backfill was placed in lifts not exceeding 8 inches in loose depth. Yard areas and roads were compacted to 95 percent relative compaction as determined by the method specified in ASTM D1557. Rock larger than 8 inches in its largest dimension that would not break down under the compactors was not permitted. Figures 2.5-17 and 2.5-18 show the plan and profile view of excavation and backfill for major plant structures.

2.5.1.2.6.5 Foundation Bearing Pressures

Seismic Category I structures were analyzed to determine the foundation pressures resulting from the combination of dead load, live load, and the double design earthquake (DDE). The maximum pressure was found to be 158 ksf and occurs under the containment structure foundation slab. This analysis assumed that the lateral seismic shear force will be transferred to the rock at the base of the slab which is embedded 11 feet into rock. This computed bearing pressure is considered conservative in that no passive lateral pressure was assumed to act on the sides of the slab. Based on the results of the laboratory tests of unconfined compressive strength of representative samples of rock at the site, which ranged from 800 to 1300 ksf, the calculated foundation pressure is well below the ultimate in situ rock bearing capacity.

Adverse hydrologic effects on the foundations of Seismic Category I structures (there are no Seismic Category I embankments) can be safely neglected at this site, since Seismic Category I structures are founded on a substantial layer of bedrock, and the groundwater level lies well below grade, at a level corresponding to that of Diablo Creek. Additionally, the computed factors of safety (minimum of 5 under DDE) of foundation pressures versus unconfined compressive strength of rock are sufficiently high to ensure foundation integrity in the unlikely event groundwater levels temporarily rose to foundation grade.

Soil properties such as grain size, Atterberg limits, and water content need not be considered since Seismic Category I structures and non-Seismic Category I structures housing Design Class I equipment are founded on rock.

2.5.2 VIBRATORY GROUND MOTION

2.5.2.1 Geologic Conditions of the Site and Vicinity

DCPP is situated at the coastline on the southwest flank of the San Luis Range, in the southern Coast Ranges of California. The San Luis Range branches from the main coastal mountain chain, the Santa Lucia Range, in the area north of the Santa Maria Valley and southeast of the plant site, and thence follows an alignment that curves toward the west. Owing to this divergence in structural grain, the range juts out from the regional coastline as a broad peninsula and is separated from the Santa Lucia Range by an elongated lowland that extends southeasterly from Morro Bay and includes Los Osos and San Luis Obispo Valleys. It is characterized by rugged west-northwesterly trending ridges and canyons, and by a narrow fringe of coastal terraces along its southwesterly flank.

Diablo Canyon follows a generally west-southwesterly course from the central part of the range to the north-central part of the terraced coastal strip. Detailed discussions of the lithology, stratigraphy, structure, and geologic history of the plant site and surrounding region are presented in Section 2.5.1.

2.5.2.2 Underlying Tectonic Structures

Evidence pertaining to tectonic and seismic conditions in the region of the DCPD site is summarized later in the section, and is illustrated in Figures 2.5-2, 2.5-3, 2.5-4, and 2.5-5. Table 2.5-1 includes a summary listing of the nature and effects of all significant historic earthquakes within 75 miles of the site that have been reported. Table 2.5-2 shows locations of 19 selected earthquakes that have been investigated by S. W. Smith. Table 2.5-3 lists the principal faults in the region and indicates major elements of their histories of displacement, in geological time units.

Benioff and Smith⁽⁵⁾ have assessed the maximum earthquakes to be expected at the site, and John A. Blume and Associates^(6,7) have derived the site vibratory motions that could result from these maximum earthquakes. An extensive discussion of the geology of the southern Coast Ranges, the western Transverse Ranges, and the adjoining offshore region is presented in Appendix 2.5D of Reference 27 of Section 2.3. Tectonic features of the central coastal region are discussed in Section 2.5.1.1.2, Regional Geologic and Tectonic Setting.

2.5.2.3 Behavior During Prior Earthquakes

Physical evidence that indicates the behavior of subsurface materials, strata, and structure during prior earthquakes is presented in Section 2.5.1.2.5. The section presents the findings of the exploratory trenching programs conducted at the site.

2.5.2.4 Engineering Properties of Materials Underlying the Site

A description of the static and dynamic engineering properties of the materials underlying the site is presented in Section 2.5.1.2.6, Site Engineering Properties.

2.5.2.5 Earthquake History

The seismicity of the southern Coast Ranges region is known from scattered records extending back to the beginning of the 19th century, and from instrumental records dating from about 1900. Detailed records of earthquake locations and magnitudes became available following installation of the California Institute of Technology and University of California (Berkeley) seismograph arrays in 1932.

A plot of the epicenters for all large historical earthquakes and for all instrumentally recorded earthquakes of Magnitude 4 or larger that have occurred within 200 miles of DCPD site is given in Figure 2.5-2. Plots of all historically and instrumentally recorded epicenters and all mapped faults within about 75 miles of the site are shown in Figures 2.5-3 and 2.5-4.

A tabulated list of seismic events, representing the computer printout from the Berkeley Seismograph Station records, supplemented with records of individual shocks of greater than Magnitude 4 that appear only in the Caltech records, is included as Table 2.5-1.

DCPP UNITS 1 & 2 FSAR UPDATE

Table 2.5-2 gives a summary of revised epicenters of a representative sample of earthquakes off the coast of California near San Luis Obispo, as determined by S. W. Smith.

2.5.2.6 Correlation of Epicenters With Geologic Structures

Studies of particular aspects of the seismicity of the southern Coast Ranges region have been made by Benioff and Smith, Richter, and Allen. From results of these studies, together with data pertaining to the broader aspects of the geology and seismicity of central and eastern California, it can be concluded that, although the southern Coast Ranges region may be subjected to vibratory ground motion from earthquakes originating along faults as distant as 200 miles or more, the region itself is traversed by faults capable of producing large earthquakes, and that the strongest shaking possible for sites within the region probably would be caused by earthquakes no more than a few tens of miles away. Therefore, only the seismicity of the southern Coast Ranges, the adjacent offshore area, and the western Transverse Ranges is reviewed in detail.

Figure 2.5-3 shows three principal concentrations of earthquake epicenters, three smaller or more diffuse areas of activity, and a scattering of other epicenters. The most active areas, in terms of numbers of shocks, are the reach of the San Andreas fault north of about 35°7' latitude, the offshore area near Santa Barbara, and the offshore Santa Lucia Bank area. Notable concentrations of epicenters also are located as occurring in Salinas Valley, at Point San Simeon, and near Point Conception. The scattered epicenters are most numerous in the general vicinities of the most active areas, but they also occur at isolated points throughout the region.

The reliability of the position of instrumentally located epicenters of small shocks in the central California region has been relatively poor in the past, owing to its position between the areas covered by the Berkeley and Caltech seismograph networks. A recent study by Smith, however, resulted in relocation of nineteen epicenters in the coastal and offshore region between the latitudes of Point Arguello and Point Sur. Studies by Gawthrop⁽²⁹⁾ and reported in Wagner have led to results that seem to accord generally with those achieved by Smith.

The epicenters relocated by Smith and those recorded by Gawthrop are plotted in Figure 2.5-3. This plot shows that most of the epicenters recorded in the offshore region seem to be spatially associated with faults in the Santa Lucia Bank region, the East Boundary zone, and the San Simeon fault. Other epicenters, including ones for the 1952 Bryson shock, and several smaller shocks originally located in the offshore area, were determined to be centered on or near the Sur-Nacimiento fault north of the latitude of San Simeon.

2.5.2.7 Identification of Active Faults

Faults that have evidence of recent activity and have portions passing within 200 miles of the site are identified in Section 2.5.1.1.2.

2.5.2.8 Description of Active Faults

Active faults that have any part passing within 200 miles of the site are described in Section 2.5.1.1.2.

2.5.2.9 Maximum Earthquake

Benioff and Smith, in reviewing the seismicity of the region around DCP site, determined the maximum earthquakes that could reasonably be expected to affect the site. Their conclusions regarding the maximum size earthquakes that can be expected to occur during the life of the reactor are listed below:

- (1) Earthquake A: A great earthquake may occur on the San Andreas fault at a distance from the site of more than 48 miles. It would be likely to produce surface rupture along the San Andreas fault over a distance of 200 miles with a horizontal slip of about 20 feet and a vertical slip of 3 feet. The duration of strong shaking from such an event would be about 40 seconds, and the equivalent magnitude would be 8.5.
- (2) Earthquake B: A large earthquake on the Nacimiento (Rinconada) fault at a distance from the site of more than 20 miles would be likely to produce a 60 mile surface rupture along the Nacimiento fault, a slip of 6 feet in the horizontal direction, and have a duration of 10 seconds. The equivalent magnitude would be 7.5.
- (3) Earthquake C: Possible large earthquakes occurring on offshore fault systems that may need to be considered for the generation of seismic sea waves are listed below:

| <u>Location</u> | <u>Length of Fault Break</u> | <u>Slip, feet</u> | <u>Magnitude</u> | <u>Distance to Site</u> |
|---|------------------------------|----------------------------|------------------|-------------------------|
| Santa Ynez Extension | 80 miles | 10 horizontal | 7.5 | 50 miles |
| Cape Mendocino, NW Extension of San Andreas fault | 100 miles | 10 horizontal | 7.5 | 420 miles |
| Gorda Escarpment | 40 miles | 5 vertical or 7 horizontal | | 420 miles |

DCPP UNITS 1 & 2 FSAR UPDATE

- (4) Earthquake D: Should a great earthquake occur on the San Andreas fault, as described in "A" above, large aftershocks may occur out to distances of about 50 miles from the San Andreas fault, but those aftershocks which are not located on existing faults would not be expected to produce new surface faulting, and would be restricted to depths of about 6 miles or more and magnitudes of about 6.75 or less. The distance from the site to such aftershocks would thus be more than 6 miles.

A further assessment of the seismic potential of faults mapped in the region of DCP site has been made following the extensive additional studies of on- and offshore geology of the last few years that are reported in Appendix 2.5D of Reference 27 of Section 2.3. This was done in terms of observed Holocene activity, to achieve assessment of what seismic activity is reasonably probable, in terms of observed late Pleistocene activity, fault dimensions, and style of deformation.

PG&E was requested by the NRC to evaluate the plant's capability to withstand a postulated Richter Magnitude 7.5 earthquake centered along an offshore zone of geologic faulting, generally referred to as the "Hosgri fault." The detailed methods, results, and plant modifications performed based on this evaluation are dealt with in Section 3.7.

The available information suggests that the faults in this region can be associated with contrasting general levels of seismic potential. These are as follows:

- (1) Level I: Potential for great earthquakes involving surface faulting over distances on the order of 100 miles: seismic activity at this level should occur only on the reach of the San Andreas fault that extends between the locales of Cajon Pass and Parkfield. This was the source of the 1857 Fort Tejon earthquake, estimated to have been of Magnitude 8.
- (2) Level II: Potential for large earthquakes involving faulting over distances on the order of tens of miles: seismic activity at this level can occur along offshore faults in the Santa Lucia Bank region (the likely source of the Magnitude 7.3 earthquake of 1927), and possibly along the Big Pine and Santa Ynez faults in the Transverse Ranges.

Although the Rinconada-San Marcos-Jolon, Espinosa, Sur-Nacimiento, and San Simeon faults do not exhibit historical or even Holocene activity indicating this level of seismic potential, the fault dimensions, together with evidence of late Pleistocene movements along these faults, suggest that they may be regarded as capable of generating similarly large earthquakes.

- (3) Level III: Potential for earthquakes resulting chiefly from movement at depth with no surface faulting, but at least with some possibility of surface faulting of as much as a few miles strike length and a few feet of slip:

DCPP UNITS 1 & 2 FSAR UPDATE

Seismic activity at this level probably could occur on almost any major fault in the southern Coast Ranges and adjacent regions.

From the observed geologic record of limited fault activity extending into Quaternary time, and from the historical record of apparently associated seismicity, it can be inferred that both the greater frequency of earthquake activity and larger shocks from earthquake source structures having this level of seismic potential probably will be associated with one of the relatively extensive faults. Faults in the vicinity of the San Luis Range that may be considered to have such seismic potential include the West Huasna, Edna, and offshore Santa Maria Basin East Boundary zone.

- (4) Level IV: Potential for earthquakes and aftershocks resulting from crustal movements that cannot be associated with any near-surface fault structures: such earthquakes apparently can occur almost anywhere in the region.

2.5.2.10 Ground Accelerations and Response Spectra

The maximum ground acceleration that would occur at DCPD site has been estimated for each of the postulated earthquakes listed in Section 2.5.2.9, using the methods set forth in References 12 and 24. The plant site acceleration is primarily dependent on the following parameters: Gutenberg-Richter magnitude and released energy, distance from the earthquake focus to the plant site, shear and compressional velocities of the rock media, and density of the rock. Rock properties are discussed under Section 2.5.1.2.6, Site Engineering Properties.

The maximum rock accelerations that would occur at the DCPD site are estimated as:

| | | | |
|----------------------|--------|----------------------|--------|
| Earthquake A | 0.10 g | Earthquake C | 0.05 g |
| Earthquake B | 0.12 g | Earthquake D | 0.20 g |

In addition to the maximum acceleration, the frequency distribution of earthquake motions is important for comparison of the effects on plant structures and equipment. In general, the parameters affecting the frequency distribution are distance, properties of the transmitting media, length of faulting, focus depth, and total energy release. Earthquakes that might reach the site after traveling over great distances would tend to have their high frequency waves filtered out. Earthquakes that might be centered close to the site would tend to produce wave forms at the site having minor low frequency characteristics.

In order to evaluate the frequency distribution of earthquakes, the concept of the response spectrum is used.

For nearby earthquakes, the resulting response spectra accelerations would peak sharply at short periods and would decay rapidly at longer periods. Earthquake D would

DCPP UNITS 1 & 2 FSAR UPDATE

produce such response spectra. The March 1957 San Francisco earthquake as recorded in Golden Gate Park (S80°E component) was the same type. It produced a maximum recorded ground acceleration of 0.13 g (on rock) at a distance of about 8 miles from the epicenter. Since Earthquake D has an assigned hypocentral distance of 12 miles, it would be expected to produce response spectra similar in shape to those of the 1957 event.

Large earthquakes centered at some distance from the plant site would tend to produce response spectra accelerations that peak at longer periods than those for nearby smaller shocks. Such spectra maintain a higher spectral acceleration throughout the period range beyond the peak period. Earthquakes A and C are events that would tend to produce this type of spectra. The intensity of shaking as indicated by the maximum predicted ground acceleration shows that Earthquake C would always have lower spectral accelerations than Earthquake A.

Since the two shocks would have approximately the same shape spectra, Earthquake C would always have lower spectral accelerations than Earthquake A, and it is therefore eliminated from further consideration. The north-south component of the 1940 El Centro earthquake produced response spectra that emphasized the long period characteristics described above. Earthquake A, because of its distance from the plant site, would be expected to produce response spectra similar in shape to those produced by the El Centro event. Smoothed response spectra for Earthquake A were constructed by normalizing the El Centro spectra to 0.10 g. These spectra, however, show smaller accelerations than the corresponding spectra for Earthquake B (discussed in the next paragraph) for all building periods, and thus Earthquake A is also eliminated from further consideration.

Earthquake B would tend to produce response spectra that emphasize the intermediate period range inasmuch as the epicenter is not close enough to the plant site to produce large high frequency (short-period) effects, and it is too close to the site and too small in magnitude to produce large low frequency (long-period) effects. The N69°W component to the 1952 Taft earthquake produced response spectra having such characteristics. That shock was therefore used as a guide in establishing the shape of the response spectra that would be expected for Earthquake B.

Following several meetings with the AEC staff and their consultants, the following two modifications were made in order to make the criteria more conservative:

- (1) The Earthquake D time-history was modified in order to obtain better continuity of frequency distribution between Earthquakes D and B.
- (2) The accelerations of Earthquake B were increased by 25 percent in order to provide the required margin of safety to compensate for possible uncertainties in the basic earthquake data.

DCPP UNITS 1 & 2 FSAR UPDATE

Accordingly, Earthquake D-modified was derived by modifying the S80°E component of the 1957 Golden Gate Park, San Francisco earthquake, and then normalizing to a maximum ground acceleration of 0.20 g. Smoothed response spectra for this earthquake are shown in Figure 2.5-21. Likewise, Earthquake B was derived by normalizing the N69°W component of the 1952 Taft earthquake to a maximum ground acceleration of 0.15 g. Smoothed response spectra for Earthquake B are shown in Figure 2.5-20. The maximum vibratory motion at the plant site would be produced by either Earthquake D-modified or Earthquake B, depending on the natural period of the vibrating body.

As mentioned earlier, based on a review of the studies presented in Appendices 2.5D and 2.5E (of Reference 27 in Section 2.3) by the NRC and the USGS (acting as the NRC's geological consultant), Supplement No. 4 to the NRC Safety Evaluation Report (SER) was issued in May 1976. This supplement included the USGS conclusion that a magnitude 7.5 earthquake could occur on the Hosgri fault at a point nearest to the Diablo Canyon site. The USGS further concluded that such an earthquake should be described in terms of near fault horizontal ground motion using techniques and conditions presented in Geological Survey Circular 672. The USGS also recommended that an effective, rather than instrumental, acceleration be derived for seismic analysis.

The NRC adopted the USGS recommendation of the seismic potential of the Hosgri fault. In addition, based on the recommendation of Dr. N. M. Newmark, the NRC prescribed that an effective horizontal ground acceleration of 0.75g be used for the development of response spectra to be employed in a seismic evaluation of the plant. The NRC outlined procedures considered appropriate for the evaluation including an adjustment of the response spectra to account for the filtering effect of the large building foundations. An appropriate allowance for torsion and tilting was to be included in the analysis. A guideline for the consideration of inelastic behavior, with an associated ductility ratio, was also established.

The NRC issued Supplement No. 5 to the SER in September 1976. This supplement included independently-derived response spectra and the rationale for their development. Parameters to be used in the foundation filtering calculation were delineated for each major structure. The supplement prescribed that either the spectra developed by Blume or Newmark would be acceptable for use in the evaluation with the following conditions:

- (1) In the case of the Newmark spectra no reduction for nonlinear effects would be taken except in certain specific areas on an individual case basis.
- (2) In the case of the Blume spectra a reduction for nonlinear behavior using a ductility ratio of up to 1.3 may be employed.
- (3) The Blume spectra would be adjusted so as not to fall below the Newmark spectra at any frequency.

DCPP UNITS 1 & 2 FSAR UPDATE

The development of the Blume ground response spectra, including the effect of foundation filtering, is briefly discussed below. The rationale and derivation of the Newmark ground response spectra is discussed in Appendix C to Supplement No. 5 of the SER.

The time-histories of strong motion for selected earthquakes recorded on rock close to the epicenters were normalized to a 0.75g peak acceleration. Such records provide the best available models for the Diablo Canyon conditions relative to the Hosgri fault zone. The eight earthquake records used are listed in the table below.

| <u>Earthquake</u> | <u>M</u> | <u>Depth, km</u> | <u>Recorded at</u> | <u>Epicentral Distance, km</u> | <u>Component</u> | <u>Peak Acceleration g</u> |
|-------------------|----------|----------------------|--------------------|--|------------------|------------------------------------|
| Helena 1935 | 6 | 5 | Helena | 3 to 8 | EW | 0.16 |
| Helena 1935 | 6 | 5 | Helena | 3 to 8 | NS | 0.13 |
| Daly City 1957 | 5.3 | 9 | Golden Gate Park | 8 | N80W | 0.13 |
| Daly City 1957 | 5.3 | 9 | Golden Gate Park | 8 | N10E | 0.11 |
| Parkfield 1966 | 5.6 | 7 | Temblor 2 | 7 | S25W | 0.33 |
| Parkfield 1966 | 5.6 | 7 | Temblor 2 | 7 | N65W | 0.28 |
| San Fernando 1971 | 6.6 | 13 | Pacoima Dam | 3 | S14W | 1.17 |
| San Fernando 1971 | 6.6 | 13 | Pacoima | 3 | N76W | 1.08 |

The magnitudes are the greatest recorded thus far (September 1985) close in on rock stations and range from 5.3 to 6.6. Adjustments were made subsequently in the period range of the response spectrum above 0.40 sec for the greater long period energy expected in a 7.5M shock as compared to the model magnitudes.

The procedure followed was to develop 7 percent damped response spectra for each of the eight records normalized to 0.75g and then to treat the results statistically according to period bands to obtain the mean, the median, and the standard deviations of spectral response. At this stage, no adjustments for the size of the foundation or for ductility were made. The 7 percent damped response spectra were used as the basis for calculating spectra at other damping values.

Figures 2.5-29 and 2.5-30 show free-field horizontal ground response spectra as determined by Blume and Newmark, respectively, at damping levels from two to seven percent.

Figures 2.5-31 and 2.5-32 show vertical ground response spectra as determined by Blume and Newmark, respectively, for two to seven percent damping. The ordinates of vertical spectra are taken as two-thirds of the corresponding ordinates of the horizontal spectra.

2.5.3 SURFACE FAULTING

2.5.3.1 Geologic Conditions of the Site

The geologic history and lithologic, stratigraphic, and structural conditions of the site and the surrounding area are described in Section 2.5.1 and are illustrated in the various figures included in Section 2.5.

2.5.3.2 Evidence for Fault Offset

Substantive geologic evidence, described under Section 2.5.1.2, Geology of DCP Site, indicates that the ground at and near the site has not been displaced by faulting for at least 80,000 to 120,000 years. It can be inferred, on the basis of regional geologic history, that minor faults in the site bedrock date from the mid-Pliocene or, at the latest, from mid-Pleistocene episodes of tectonic activity.

2.5.3.3 Identification of Active Faults

Three zones that include faults greater than 1000 feet in length have been mapped within about 5 miles of the site. Two of these, the Edna and San Miguelito fault zones, were mapped on land in the San Luis Range. The third, consisting of several breaks associated with the offshore Santa Maria Basin East Boundary zone of folding and faulting, is described in Sections 2.5.1.1.2.3 and 2.5.1.1.5.5 under Regional Geologic and Tectonic Setting. The mapped trace of each of these structures is shown in Figures 2.5-3 and 2.5-4.

2.5.3.4 Earthquakes Associated With Active Faults

The Edna fault or fault zone has been active at some time since the deposition of the Plio-Pleistocene Paso Robles Formation, which it displaces. It has no morphologic expression suggestive of late Pleistocene activity, nor is it known to displace late Pleistocene or younger deposits. Four epicenters of small (3.9 to 3M) shocks and 42 other epicenters for shocks of "small" or "unknown" intensity have been reported as occurring in the approximate vicinity of the Edna fault (Figures 2.5-3 and 2.5-4). Owing to the small size of the earthquakes that they represent, however, all of these epicenters are only approximately located. Further, they fall in the energy range of shocks that can be generated by fairly large construction blasts. At present, no conclusive evidence is available to determine whether the Edna fault could be classified as seismically active, or as geologically active in the sense of having undergone multiple movements within the last 500,000 years.

The San Miguelito fault has been mapped as not displacing the Plio-Pleistocene Paso Robles Formation. No instrumental epicenter has been reliably recorded from its vicinity, but the Berkeley Seismological Laboratory indicates Avila Bay as the presumed epicentral location for a moderately damaging (Intensity VII at Avila) earthquake that

DCPP UNITS 1 & 2 FSAR UPDATE

occurred on December 1, 1916. It seems likely, however, that this shock occurred along the offshore East Boundary zone rather than on the San Miguelito fault zone.

The East Boundary zone has an overall length of about 70 miles. Individual breaks within the zone are as much as 30 miles long, though the varying amount of displacement that occurs along specific breaks indicates that movement along them is not uniform, and it suggests that breakage may have occurred on separate, limited segments of the faults. The reach of the zone that is opposite DCP site contains four fault breaks. These breaks range from 1 to 15 miles in length, and they have minimum distances of 2.1 to 4.5 miles from the site. The East Boundary zone is considered to be seismically active, since at least five instrumentally well located epicenters and as many as ten less reliably located other epicenters are centered along or near the zone. One of the breaks (located 3-1/2 miles offshore from the site) exhibits topographic expression that may represent a tectonic offset of the sea floor surface at a point along its trace 6 miles north of the site. Other faults in the East Boundary zone have associated erosion features, a few of which could possibly be partly of faultline origin.

The earthquake of December 1, 1916, though listed as having an epicentral location at Avila Bay, is considered more probably to have originated along either the East Boundary zone or, possibly, the Santa Lucia Bank fault. Effects of this shock at Avila included landsliding in Dairy Canyon, 2 miles north of town, and "...disturbance of waters in the Bay of San Luis Obispo." "...plaster in several cottages...was jarred loose...while some of the smokestacks on the (Union Oil Company) refinery were toppled over." It is apparently on this basis that the Berkeley listing of earthquakes assigns this shock a "large" intensity and places its approximate epicentral location at Port San Luis.

A small (Magnitude 2.9) shock that apparently originated near the East Boundary zone a short distance south of DCP site was lightly felt at the site on September 24, 1974. This shock, like most of those recorded along the East Boundary zone, was not damaging.

The minor fault zone that was mapped in the sea cliff at the mouth of Diablo Creek and in the excavation for the Unit 1 turbine building has an onshore length of about 550 feet, and it probably continues for some distance offshore. It has been definitely determined to be not active.

2.5.3.5 Correlation of Epicenters With Active Faults

Earthquake epicenters located within 50 miles of DCP site have been approximately located in the vicinity of each of the faults. The reported earthquakes are listed in Table 2.5-1 and as follows, and their indicated epicentral locations are shown in Figures 2.5-3 and 2.5-4:

DCPP UNITS 1 & 2 FSAR UPDATE

Earthquake Epicenters Reported as Being Located Approximately in the Vicinity of San Luis Obispo, Avila, and Arroyo Grande

| <u>Date</u> | <u>Geographic N Latitude</u> | <u>Coordinates W Longitude</u> | <u>Magni- tude</u> | <u>Inten- sity</u> | <u>Notes and Greenwich Mean Time (GMT)</u> |
|----------------------|----------------------------------|------------------------------------|------------------------|------------------------|--|
| 7.10.1889 | 35.17° | 120.58° | | | Arroyo Grande. Shocks for several days. |
| 12.1.1916 | 35.17° | 120.75° | | VII | VII at Avila. Considerable glass broken and goods in stores thrown from shelves at San Luis Obispo. Water in bay disturbed, plaster in cottages jarred loose, smoke stacks of Union Oil refinery toppled over at Avila. Severe at Port San Luis. III at Santa Maria: 22:53:00 |
| 4.26.1950 | 35.20° | 120.60° | 3.5 | V | V at Santa Maria. Also felt at Orcutt: 7:23:29 |
| 1.26.1971 | 35.20° | 120.70° | 3 | | Near San Luis Obispo: 21:53:53 |
| 1830 to 7.21.1931 | 35.25° | 120.67° | | | 42 epicenters |

DCPP UNITS 1 & 2 FSAR UPDATE

Earthquake Epicenters Reported as Being Located Approximately in the Vicinity of the Offshore Santa Maria Basin East Boundary Zone

| <u>Date</u> | <u>Geographic Coordinates</u> | | <u>Magni- tude</u> | <u>Inten- sity</u> | <u>Notes and Greenwich Mean Time (GMT)</u> |
|-------------------------------|-------------------------------|---------|------------------------|------------------------|---|
| 5.27.1935 ⁽³⁰⁻¹⁾ | 35.62° | 121.64° | 3 | III | Felt at Templeton: 16:08:00 |
| 9.7.1939 ⁽³⁰⁻⁶⁾ | 34.46° | 121.50° | 3 | | Off San Luis Obispo County; felt at Cambria: 2:50:30 |
| 1.27.1945 | 34.75° | 120.67° | 3.9 | | 17:50:31 |
| 12.31.1948 ⁽³⁰⁻¹⁰⁾ | 35.60° | 121.23° | 4.6 | | Felt along coast from Lompoc to Moss Landing. VI at San Simeon. V at Cayucos, Creston, Moss Landing, Piedras Blancas Light Station: 14:35:46 |
| 11.17.1949 | 34.80° | 120.70° | 2.8 | | IV at Santa Maria. Near Priest: 5:06:60 |
| 2.5.1955 ⁽³⁰⁻²³⁾ | 35.86° | 121.15° | 3.3 | | West of San Simeon: 7:10:19 |
| 6.21.1957 ^(30-25A) | 35.23° | 120.95° | 3.7 | | Off Coast. Felt in San Luis Obispo, Morro Bay: 20:46:42 |
| 8.18.1958 | 35.60° | 121.30 | 3.4 | | Near San Simeon: 5:30:42 |
| 10.25.1967 | 35.73° | 121.45° | 2.6 | | Near San Simeon: 23:05:39.5 |

(Figures in parentheses refer to events relocated by S. W. Smith, see Table 2.5-2).

2.5.3.6 Description of Active Faults

Data pertaining to faults with lengths greater than 1000 feet and reaches within 50 miles of the site are included in Section 2.5.1.1.5, Structure of the San Luis Range and Vicinity, and in Figures 2.5-3 and 2.5-4. These data indicate the fault lengths, relationship of the faults to regional tectonic structures, known history of displacements, outer limits, and whether the faults can be considered as active.

2.5.3.7 Results of Faulting Investigation

The site for Units 1 and 2 of DCPD was investigated in detail for faulting and other possibly detrimental geologic conditions. From studies made prior to design of the plant, it was determined that there was need to take into account the possibility of surface faulting in such design. The data on which this determination was based are presented in Section 2.5.1.2, Site Geology.

2.5.4 Stability of Subsurface Materials

The possibility of past or potential surface or subsurface ground subsidence, uplift, or collapse in the vicinity of DCPD was considered during the course of the geologic investigations for Units 1 and 2.

2.5.4.1 Geologic Features

The site is underlain by folded bedrock strata consisting predominantly of sandy mudstone and fine-grained sandstone. The existence of an unbroken and otherwise undeformed section of upper Pleistocene terrace deposits overlying a wave-cut bedrock bench at the site provides positive evidence that all folding and faulting in the bedrock antedated formation of the terrace. Local depressions and other irregularities on the bedrock surface plainly reflect erosion in an ancient surf zone.

The rocks that constitute the bedrock section are not subject to significant solution effects (i.e., development of cavities or channels that could affect the engineering or fluid conducting character of the rock) because the bedrock section does not contain thick or continuous bodies of soluble rock types such as limestone or gypsum. Voids encountered during excavation at the site were limited to thin zones of vuggy breccia and isolated vugs in some beds of calcareous mudstone. Areas where such minor vuggy conditions were present were noted at a few locations in the excavation for the Unit 2 containment and fuel handling structures (at plant grid coordinates N59, N597, E10, E005 and N59, N700, E10, E120).

The maximum size of any individual opening was 3 inches or less, and most were less than 1 inch in maximum dimension. Because of the limited extent and isolated nature of these small voids, they were not considered significant in foundation engineering or slope stability analyses.

DCPP UNITS 1 & 2 FSAR UPDATE

It has been determined by field examination that no sea caves exist in the immediate vicinity of the site. The only cave like natural features in the area are shallow pits and hollows in some of the sea cliff outcrops of resistant tuff. These features generally have dimensions of a few inches to about 10 feet. They are superficial, and have originated through differential weathering of variably cemented rock.

Several exploratory wells have been drilled for petroleum within the San Luis Range, but no production was achieved and the wells were abandoned. The area is not now active in terms of either production or exploration. The location of the abandoned wells is shown in Figure 2.5-6, and the geologic relationships in the Range are illustrated in Section A-A' of Figure 2.5-6 and in Figure 2.5-7, Section D-D'. The nearest oil-producing area is the Arroyo Grande field, about 15 miles to the southeast.

The potential for future problems of ground instability at the site, because of nearby petroleum production, can be assessed in terms of the geologic potential for the occurrence of oil within, or offshore from, the San Luis Range. In addition, assessment can be made in terms of the geologic relationships in the site as contrasted with geologic conditions in places where oil field exploitation has resulted in deformation of the ground surface.

As shown in Figures 2.5-6 and 2.5-7, the San Luis Range has the structural form of a broad synclinal fold, which in turn is made up of several tightly compressed anticlines and synclines of lesser order. The configuration is not conducive to entrapment of hydrocarbon fluids, as such fluids tend to migrate upward through bedding and fracture-controlled zones of higher primary and secondary permeability until they reach a local trap or escape into the near surface or surface environment.

Within the San Luis Range, the only recognizable structural traps are in local zones where plunge reversals exist along the crests of the second-order anticlines. Such structures evidently were the actual or hoped-for targets for most of the exploratory wells that have been drilled in the San Luis Range, but none of these wells has produced enough oil or gas to record; thus, the traps have not been effective, or perhaps the strata are essentially lacking in hydrocarbon fluids. Other conditions that indicate poor petroleum prospects for the Range include the general absence of good reservoir rocks within the section and the relatively shallow basement of non-petroliferous Franciscan rocks.

In the offshore, adjacent to the southerly flank of the San Luis Range, subsurface conditions are not well known, but are probably generally similar. Scattered data suggest that a structural high, perhaps defined by a west-northwest plunging anticline, may exist a few miles offshore from DCP site. Such a feature could conceivably serve as a structural trap, if local closure were present along its axis; however, it seems unlikely that it would contain significant amounts of petroleum.

Available data pertaining to exploratory oil wells drilled in the region of the site are given here:

DCPP UNITS 1 & 2 FSAR UPDATE

Exploratory Oil Wells in the Vicinity of DCPD Site

Data from exploratory wells drilled outside of oil and gas fields in California to December 31, 1963: Division of Oil and Gas, San Francisco.

| Mount Diablo B. & M. | | | <u>Well No.</u> | <u>Elev, ft</u> | <u>Date Started</u> | <u>Total Depth, ft</u> | <u>Stratigraphy (depth in ft) Age at Bottom of Hole</u> |
|-------------------------|----------|------------|-------------------------------|--|-------------------------|--------------------------------|--|
| <u>T</u> | <u>R</u> | <u>Sec</u> | | | | | |
| 31S | 10E | 3 | Tidewater Oil Co. | "Montadoro" 1 | 365 April 1954 | 6,146 | Monterey 0-3800; Obispo Tuff 3800; Franciscan; U. Jurassic |
| 30S | 10E | 24 | Gretna Corp. | "Maino- Gonzales" 1 | 275 March 1937 | 1,575 | Franciscan; Jurassic |
| | | 24 | Wm. H. Provost | "Spooner" 1 | 325 July 1952 | 1,749 | Jurassic |
| | | 24 | Shell Oil Co. | "Buchon" | - - - | - | - |
| | | 34 | A. O. Lewis | "Pecho" 1 | 177 May 1937 | 2,745 | Monterey 0-2612; U. Miocene |
| 30S | 11E | 9 | Van Stone and Dallaston | "Souza" 1 | 42 Oct 1951 | 1,233 | Franciscan; Jurassic |
| 31S | 11E | 15 | Tidewater Oil Co. | "Honolulu- Tidewater- U.S.L.- Heller Lease " 1 | 1,614 Jan 1958 | 10,788 | Monterey 0-4363; Pt. Sal 4363; Obispo Tuff 4722; Rincon Shale 5370; 2nd Tuff 5546; 2nd Rincon Shale 6354; 3rd Tuff 10,174; L. Miocene |

For the purpose of assessing the potential for the occurrence of adverse oil field related ground deformation effects at DCPD site, in the unlikely event that petroleum should be discovered and produced at a nearby location, it is useful to review the nature and causes of such ground deformation, and the types of geologic conditions at places where it has been observed.

DCPP UNITS 1 & 2 FSAR UPDATE

The general subject of surface deformation associated with oil and gas field operations has been reviewed by Yerkes and Castle⁽²²⁾, among others. Such deformation includes differential subsidence, development of horizontally compressive strain effects within the central parts of subsidence bowls and horizontally extensive strain effects around their margins, and development or activation of cracks and faults. Pull-apart cracks and normal faults may develop in the marginal zone of extensive strain, while reverse and thrust faults sometimes occur in the central, compressive part of subsidence bowls. These effects all can develop when extraction of petroleum, water, and sand, plus lowering of fluid pressures, result in compression within and adjacent to producing zones, and attendant subsidence of the overlying ground. Other effects, including rebound of the ground surface, fault activation, and earthquake generation, have resulted from injection of fluid into the ground for purposes of secondary recovery, subsidence control, and disposal of fluid waste.

In virtually all instances of ground-surface deformation associated with petroleum production, the producing field has been centered on an anticlinal structure, in general relatively broad and internally faulted. The strata in the producing and overlying parts of the section typically are poorly consolidated sandstone, siltstone, claystone, and shale of low structural competence. The field generally is one with relatively large production, with significant decline of fluid pressure in the producing zones.

The conditions just cited can be contrasted with those obtained in the vicinity of DCPD site, where the rocks lie along the flank of a major syncline. They consist of tight sandstone, tuffaceous sandstone, mudstone, and shale, together with large resistant masses of tuff and diabase. Bedding dips range from near horizontal to vertical and steeply overturned, as shown in Section D-D' of Figure 2.5-7 and Section A-B of Figure 2.5-10. This structural setting is unlike any reported from areas where oil-field-associated surface deformation has occurred.

The foregoing discussion leads to the following conclusions: (a) future development of a producing oil field in the vicinity of DCPD site is highly unlikely because of unfavorable geologic conditions, and (b) geologic conditions in the site vicinity are not conducive to the occurrence of surface deformation, even if nearby petroleum production could be achieved.

As was noted in Section 2.4, the rocks underlying the site do not constitute a significant groundwater reservoir, so that future development of deep rock water wells in the vicinity is not a reasonable possibility. The considerations pertaining to surface deformation resulting from water extraction are about the same as for petroleum extraction, so there is no likelihood that DCPD site could experience artificially induced and potentially damaging subsidence, uplift, collapse, or changes in subsurface effective stress related to pore pressure phenomena.

There are no mineral deposits of economic significance in the ground underlying the site.

DCPP UNITS 1 & 2 FSAR UPDATE

Although some regional warping and uplift may well be taking place in the southern Coast Ranges, such deformation cannot be sufficiently rapid and local to impose significant effects on coastal installations. Apparent elevation of the San Luis Range has increased about 100 feet relative to sea level since the cutting of the main terrace bench at least 80,000 years ago.

Expressions of deformation preserved in the bedrock at the site include minor faults, folds, and zones of blocky fracturing in sandstone and intra-bed shearing in claystone. Zones of cemented breccia also are present, as is widespread evidence of disturbance adjacent to intrusive bodies of tuff. Local weakening of the rocks in some of these zones led to some problems during construction, but these were handled by conventional techniques such as overexcavation and rock bolting. No observed features of deformation are large or continuous enough to impose significant effects on the overall performance of the site foundation.

The foundation excavations for Units 1 and 2 were extended below the zone of intense near surface weathering so that the exposed bedrock was found to be relatively fresh and firm. The principal zones of structural weakness are associated with small bodies of altered tuff and with internally sheared beds of claystone. The claystone intra-bed shear was expressed by the development of numerous slickensided shear surfaces within parts of the beds, especially in places where the claystone had locally been squeezed into pod like masses. The shearing and local squeezing clearly are expressions of the preferential occurrence of differential adjustments in the relatively weaker claystone beds during folding of the section.

The claystone beds are localized in a part of the rock section that underlies the discharge structure and extends across the southerly part of the Unit 2 turbine-generator building, thence continuing easterly, along a strike through the ground south of the Unit 2 containment. The bedding dips 48 to 75° north within this zone. Individual claystone beds range from 1/2 inch to about 6 inches in thickness, and they occur as interbeds in the sandstone-mudstone rock section.

The relationship of the claystone layers to the foundation excavation is such that they crop out in several narrow bands across the floor and walls (see Figures 2.5-15 and 2.5-16). Thus, the claystone bed remains confined within the rock section, except in a narrow strip at the face of the excavation. Because of the small amount of claystone mass and the geometric relationship of the steeply dipping claystone interbeds to the foundation structures, it was determined that the finished structure would not be affected by any tendency of the claystone to undergo further changes in volume.

The only area in which claystone swelling was monitored was along the north wall of the lower part of the large slot cut for the cooling water discharge structure. There are several thin (6 inches or less) claystone interbeds in the sandstone-mudstone section. Because the orientation of the bedding and the plane of the cut face differ by only about 30°, and the bedding dips steeply into the face, opening of the cut served both to remove lateral support from the rock behind the face, and also to expose the clay beds

DCPP UNITS 1 & 2 FSAR UPDATE

to rainfall and runoff. This apparently resulted in both load relief and hydration swelling of the newly exposed claystone, which in turn caused some outward movement of the cut face. The movement then continued as gravity creep of the locally destabilized mass of rock between the claystone beds and the free face. The movement was finally controlled by installation of drilled-in lateral tie-backs, prior to placement of the reinforced concrete wall of the discharge structure.

No evidence of unrelieved residual stresses in the bedrock was noted during the excavation or subsequent construction of the plant foundation. Isolated occurrences of temporary slope instability clearly were related to locally weathered and fractured rock, hydration swelling of claystone interbeds, and local saturation by surface runoff. The Units 1 and 2 power plant facilities are founded on physically and chemically stable bedrock.

2.5.4.2 Properties of Underlying Materials

Static and dynamic engineering properties of materials in the subsurface at the site are presented in Section 2.5.1.2.6, Site Engineering Properties.

2.5.4.3 Plot Plan

Plan views of the site indicating exploratory boring and trenching locations are presented in Figures 2.5-8 and 2.5-11 through 2.5-15. Profiles illustrating the subsurface conditions relative to the Seismic Category I structures are furnished in Figures 2.5-12 through 2.5-16. Discussions of engineering properties of materials and groundwater conditions are included in Section 2.5.1.2.6, Site Engineering Properties.

2.5.4.4 Soil and Rock Characteristics

Information on compressional and shear wave velocity surveys performed at the site are included in Appendices 2.5A and 2.5B of Reference 27 of Section 2.3. Values of soil modulus of elasticity and Poisson's ratio calculated from seismic measurements are presented in Table 1 of Appendix 2.5A of Reference 27 of Section 2.3, and in Figure 2.5-19. Boring and trench logs are presented in Figures 2.5-23 through 2.5-28.

2.5.4.5 Excavations and Backfill

Plan and profile drawings of excavations and backfill at the site are presented in Figures 2.5-17 and 2.5-18. The engineered backfill placement operations are discussed in Section 2.5.1.2.6.4, Engineered Backfill.

2.5.4.6 Groundwater Conditions

Groundwater conditions at the site are discussed in Section 2.4.13. The effect on foundations of Seismic Category I structures is discussed in Section 2.5.1.2.6, Site Engineering Properties.

2.5.4.7 Response of Soil and Rock to Dynamic Loading

Details of dynamic testing on site materials are contained in Appendices 2.5A and 2.5B of Reference 27 in Section 2.3.

2.5.4.8 Liquefaction Potential

As stated in Section 2.5.1.2.6.5, adverse hydrologic effects on foundations of Seismic Category I structures can be neglected due to the structures being founded on bedrock and the groundwater level lying well below final grade.

There is a small local zone of medium dense sand located northeast of the intake structure and beneath a portion of buried ASW piping that is not attached to the circulating water tunnels. This zone is susceptible to liquefaction during design basis seismic events (References 45 and 46). The associated liquefaction-induced settlements from seismic events are considered in the design of the buried ASW piping. (References 48 and 49)

2.5.4.9 Earthquake Design Basis

The earthquakes postulated for DCP site are discussed in Section 2.5.2.9, and a discussion of the design response spectra is in Section 3.7. Response acceleration curves for the site resulting from Earthquake B and Earthquake D-modified are shown in Figures 2.5-20 and 2.5-21, respectively. Response spectrum curves for the 7.5M Hosgri earthquake are shown in Figures 2.5-29 through 2.5-32.

2.5.4.10 Static Analysis

A discussion of the analyses performed on materials at the site is presented in Section 2.5.1.2.6, Site Engineering Properties.

2.5.4.11 Criteria and Design Methods

The criteria and methods used in evaluating subsurface material stability are presented in Section 2.5.1.2.6, Site Engineering Properties.

2.5.4.12 Techniques to Improve Subsurface Conditions

Due to the bearing of in situ rock being well in excess of the foundation pressure, no treatment of the in situ rock is necessary. Compaction specifications for backfill are presented in Section 2.5.1.2.6.4, Engineered Backfill.

2.5.5 SLOPE STABILITY

2.5.5.1 Slope Characteristics

The only slope whose failure during a DDE could adversely affect the nuclear power plant is the slope east of the building complex (see Figures 2.5-17, 2.5-18, and 2.5-22). To evaluate the stability of this slope, the soil and rock conditions were investigated by exploratory borings, test pits, and a thorough geological reconnaissance by the soil consultant, Harding-Lawson Associates, and was in addition to the overall geologic investigation performed by other consultants.

The slope configuration and representative locations of the subsurface conditions determined from the exploration are shown on Plates 2, 3, and 4 of Appendix 2.5C of Reference 27 of Section 2.3. Reference 44 provides further information compiled in 1997 in response to NRC questions on landslide potential.

Bedrock is exposed along the lower portions of the cut slope up to about the lower bench at elevation 115 feet. It consists of tuffaceous siltstone and fine-grained sandstone of the Monterey Formation. Terrace gravel overlies bedrock and extends to an approximate elevation of 145 feet. Stiff clays and silty soils with gravel and rock fragments constitute the upper material on the site. The upper few feet of fine-grained soils are dark brown and expansive.

No free groundwater was observed in any of the borings which were drilled in April 1971, nor was any evidence of groundwater observed in this slope during the previous years of investigation and construction of the project.

2.5.5.2 Design Criteria and Analyses

Undisturbed samples of the materials encountered in pits and borings were examined by the soil consultant in the laboratory and were subsequently tested to determine the shear strength, moisture content, and dry density. Strain controlled, unconsolidated, undrained triaxial tests at field moisture were performed on the clay to evaluate the shear strength of the materials penetrated. (The samples were maintained at field moisture since adverse moisture or seepage conditions were not encountered during this investigation nor previous investigations.) The confining stress was varied in relation to depth at which the undisturbed sample was taken. The test results are presented on the boring logs and are explained by the Key to Test Data, Figure 2.5-28.

The results of strength tests were correlated with the results developed during earlier investigations of DCP site. Mohr circles of stresses at failure (6 to 7 percent strain) were drawn for each strength test result, and failure lines were developed through points representing one-half the deviator stresses. An average $C-\theta$ strength equal to a cohesion (C) value of 1000 psf and an angle of internal friction (θ) of 29° was selected for the slope stability analysis. The analysis was checked by maintaining the angle of

DCPP UNITS 1 & 2 FSAR UPDATE

internal friction (θ) constant at 19° and varying the cohesion (C) from 950 psf (weakest layer) to 3400 psf (deepest and strongest layer).

Because of the presence of large gravel sizes, it was not possible to accurately determine the strength of the sand and gravel lense. However, based on tests on sand samples from other parts of the site, an angle of internal friction of 35° was selected as being the minimum available. An assumed rock strength of 5000 psf was used. This value is consistent with strength tests performed on remold rock samples from other areas of the site.

The stability of the slope was analyzed for the forces of gravity using a static method that is, the conventional method of slices. This analysis was checked using Bishop's modified method. The static method of analysis was chosen because, for the soil conditions at the site, it was judged to be more conservative than a dynamic analysis.

Because the overall strength of the rock would preclude a stability failure except along a plane of weakness which was not encountered in the borings or during the many geologic mappings of the slope, only the stability of the soil over the rock was analyzed. The strength parameters were varied as previously discussed to determine the minimum factor of safety under the most critical strength condition. For the static analysis excluding horizontal forces, the factor of safety was computed to be 3. When the additional unbalanced horizontal force of 0.4 times the weight of the soil within the critical surface combined with a vertical force of 0.26 times the weight was included, the minimum computed factor of safety was 1.1.

On the basis of the investigation and analysis, it was concluded that the slope adjacent to DCP site would not experience instability of sufficient magnitude to damage adjacent safety-related structures.

The above conclusion is substantiated by additional field exploration, laboratory tests, and dynamic analyses using finite element techniques. See Appendix 2.5C of Reference 27 in Section 2.3, Harding-Lawson Associates' report on this work.

In response to an NRC request in early 1997, PG&E conducted further investigations of slope stability at the site⁽⁴⁴⁾. The results of the investigations showed that earthquake loading following periods of prolonged precipitation will not produce any significant slope failure that can impact Design Class I structures and equipment. In addition, potential slope failures under such conditions will not adversely impact other important facilities, including the raw water reservoirs, the 230 kV and 500 kV switchyards, and the intake and discharge structures. Potential landslides may temporarily block the access road at several locations. However, there is considerable room adjacent to and north of the road to reroute emergency traffic.

2.5.5.3 Field Exploration

The investigation of the cut slope included geologic mapping of the soil and rock conditions exposed on the surface of slope and existing benches. Subsurface conditions were investigated by drilling test borings and by excavating test pits in the natural slope above the plant site (see Figure 2.5-22). The test borings were drilled with a truck mounted, 24 inch flight auger drill rig, and the test pits were excavated with a track-mounted backhoe. Boring and Log of Test Pits 1, 2, and 3 were logged by the soil consultant; borings 2 and 3 were logged by PG&E engineering personnel. The logs of all borings were verified by the soil consultant, who examined all samples obtained from each boring. Undisturbed samples were obtained from boring 2 and each of the test pits. Because of the stiffness of the soil, hardness of the rock, and type of drilling equipment used, the undisturbed samples were obtained by pushing an 18-inch steel tube that measured 2.5 inches in outside diameter. A Sprague & Henwood split-barrel sampler containing brass liners was used to obtain undisturbed soil samples from the test pits. The brass liners measured 2.5 inches in outside diameter and 6 inches in height. Logs of the borings and pits are shown in Figures 2.5-23 through 2.5-27. The soils were classified in accordance with the Unified Soil Classification System presented in Figure 2.5-28.

2.5.5.4 Slope Stability for Buried Auxiliary Saltwater System Piping

A portion of the buried ASW piping for Unit 1 ascends an approximate 2:1 (horizontal/vertical) slope to the parking area near the meteorology tower (Plates 1 and 2 of Reference 47). To ensure the stability of this slope in which the ASW piping is buried, a geotechnical evaluation, considering various design basis seismic events, was performed by Harding Lawson Associates. This evaluation is described in Reference 47. Based on this evaluation, it was concluded that this slope will be stable during seismic events and that additional loads resulting from permanent deformation of the slope will not impact the buried ASW piping.

2.5.6 REFERENCES

1. R. H. Jahns, "Geology of the Diablo Canyon Power Plant Site, San Luis Obispo County, California," 1967-Supplementary Reports I and II, 1968-Supplementary Report III, Diablo Canyon PSAR, Docket No. 50-275, (Main Report and Supplementary Report I). Diablo Canyon PSAR, Docket No. 50-323, (All reports, 1966 and 1967).
2. R. H. Jahns, "Guide to the Geology of the Diablo Canyon Nuclear Power Plant Site, San Luis Obispo County, California," Geol. Soc. Amer., Guidebook for 66th Annual Meeting, Cordilleran Section, 1970.
3. Deleted in Revision 1
4. Deleted in Revision 1

DCPP UNITS 1 & 2 FSAR UPDATE

5. H. Benioff and S. W. Smith, "Seismic Evaluation of the Diablo Canyon Site," Diablo Canyon Unit 1 PSAR, Docket No. 50-275. Also, Diablo Canyon Unit 2 PSAR Docket No. 50-323, 1967.
6. John A. Blume & Associates, Engineers, "Earthquake Design Criteria for the Nuclear Power Plant - Diablo Canyon Site," Diablo Canyon Unit 1 PSAR, Docket No. 50-275., January 12, 1967. Also, Diablo Canyon Unit 2 PSAR Docket No. 50-323.
7. John A. Blume & Associates, Engineers, "Recommended Earthquake Design Criteria for the Nuclear Power Plant - Unit No. 2, Diablo Canyon Site," Diablo Canyon Unit 2 PSAR, Docket No. 50-323, June 24, 1968.
8. Deleted in Revision 1
9. Deleted in Revision 1
10. B. M. Page, "Geology of the Coast Ranges of California," E. H. Bailey (editor), Geology of Northern California, California Division, Mines and Geology, Bull. 190, 1966, pp 255-276.
11. B. M. Page, "San Jacinto Fault Zone of California: Continental Margin Tectonics," Geol. Soc. Amer., Bull., Vol. 81, 1970, pp 667-690.
12. J. G. Vedder and R. D. Brown, "Structural and Stratigraphic Relations Along the San Jacinto Fault in the Santa Lucia Range and San Rafael Mountains, California," W. R. Dickinson and Arthur Grantz (editors), Proceedings of Conference on Geologic Problems of the San Andreas Fault System, Stanford University Publs. in the Geol. Sciences, Vol. XI, 1968, pp 242-258.
13. C. F. Richter, "Possible Seismicity of the San Jacinto Fault, California," Geol. Soc. Amer., Bull., Vol. 80, 1969, pp 1363-1366.
14. E. W. Hart, "Possible Active Fault Movement Along the San Jacinto Fault Zone, Southern Coast Ranges, California," (abs.), Geol. Soc. Amer., Abstracts with Programs for 1969, pt. 3, 1969, pp 22-23.
15. R. E. Wallace, "Notes on Stream Channels Offset by the San Andreas Fault, Southern Coast Ranges, California," W. R. Dickinson and Arthur Grantz (editors), Proceedings of Conference on Geologic Problems of the San Andreas Fault System, Stanford University Publs. in the Geol. Sciences, Vol. XI, 1968, pp 242-258.

DCPP UNITS 1 & 2 FSAR UPDATE

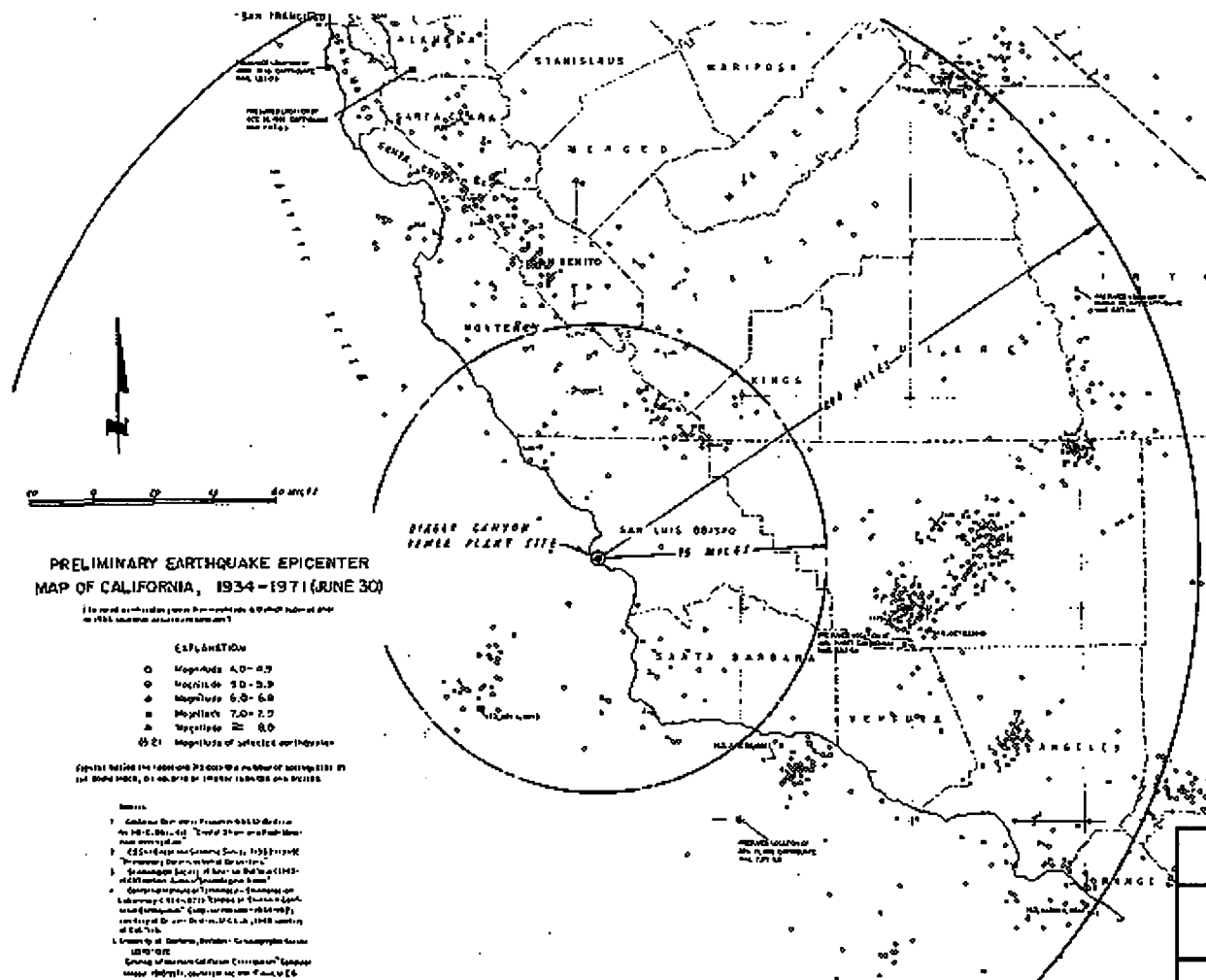
16. C. R. Allen, "The Tectonic Environments of Seismically Active and Inactive Areas Along the San Andreas Fault System," W. R. Dickinson and Arthur Grantz (editors), Proceedings of Conference on Geologic Problems of the San Andreas Fault System, Stanford University Publs. in the Geol. Sciences, Volume XI, 1968, pp 70-82.
17. Deleted in Revision 1
18. Deleted in Revision 1
19. L. A. Headlee, Geology of the Coastal Portion of the San Luis Range, San Luis Obispo County, California, Unpublished MS thesis, University of Southern California, 1965.
20. C. A. Hall, "Geologic Map of the Morro Bay South and Port San Luis Quadrangles, San Luis County, California," U.S. Geological Survey Miscellaneous Field Studies Map MF-511, 1973.
21. C. A. Hall and R. C. Surdam, "Geology of the San Luis Obispo-Nipomo Area, San Luis Obispo County, California," Geol. Soc. Amer., Guidebook for 63rd Ann. Meeting, Cordilleran Section, 1967.
22. R. F. Yerkes and R. O. Castle, "Surface Deformation Associated with Oil and Gas Field Operations in the United States in Land Subsidence," Proceedings of the Tokyo Symposium, Vol. 1, 1ASH/A1HS Unesco, 1969, pp 55-65.
23. C. W. Jennings, et al., Geologic Map of California, South Half, scale 1:750,000, California Div. Mines and Geology, 1972.
24. John H. Wiggins, Jr., "Effect of Site Conditions on Earthquake Intensity," ASCE Proceedings, Vol. 90, ST2, Part 1, 1964.
25. B. M. Page, "Time of Completion of Underthrusting of Franciscan Beneath Great Valley Rocks West of Salinian Block, California," Geol. Soc. Amer., Bull., Vol. 81, 1970, pp 2825-2834.
26. Eli A. Silver, "Basin Development Along Translational Continental Margins," W. R. Dickinson (editor), Geologic Interpretations from Global Tectonics with Applications for California Geology and Petroleum Exploration, San Joaquin Geological Society, Short Course, 1974.
27. T. W. Dibblee, The Riconada Fault in the Southern Coast Ranges, California, and Its Significance, Unpublished abstract of talk given to the AAPG, Pacific Section, 1972.

DCPP UNITS 1 & 2 FSAR UPDATE

28. D. L. Durham, "Geology of the Southern Salinas Valley Area, California," U.S. Geol. Survey Prof. Paper 819, 1974, p 111.
29. William Gawthrop, Preliminary Report on a Short-term Seismic Study of the San Luis Obispo Region, in May 1973 (Unpublished research paper), 1973.
30. S. W. Smith, Analysis of Offshore Seismicity in the Vicinity of the Diablo Canyon Nuclear Power Plant, report to Pacific Gas and Electric Company, 1974.
31. H. C. Wagner, "Marine Geology between Cape San Martin and Pt. Sal, South-Central California Offshore; a Preliminary Report, August 1974," USGS Open File Report 74-252, 1974.
32. R. E. Wallace, "Earthquake Recurrence Intervals on the San Andreas Fault", Geol. Soc. Amer., Bull., Vol. 81, 1970, pp 1875-2890.
33. J. C. Savage and R. O. Burford, "Geodetic Determination of Relative Plate Motion in Central California", Jour. Geophys. Res., Vol. 78, No. 5, 1973, pp 832-845.
34. Deleted in Revision 1
35. Hill, et al., "San Andreas, Garlock, and Big Pine faults, California" - A Study of the character, history, and significance of their displacements, Geol. Soc. Amer., Bull., Vol. 64, No. 4, 1953, pp 443-458.
36. C.A. Hall and C.E. Corbato, "Stratigraphy and Structure of Mesozoic and Cenozoic Rocks, Nipomo Quadrangle, Southern Coast Ranges, California," Geol. Soc. Amer., Bull., Vol. 78, No. 5, 1969, pp 559-582. (Table 2.5-3, Sheet 1 of 2).
37. Bolt, Beranek, and Newman, Inc., Sparker Survey Line, Plates III and IV, 1973/1974. (Appendix 2.5D, to Diablo Canyon Power Plant Final Safety Analysis Report as amended through August 1980). (See also Reference 27 of Section 2.3.)
38. R. R. Compton, "Quaternary of the California Coast Ranges," E. H. Bailey (editor), Geology of Northern California, California Division Mines and Geology, Bull. 190, 1966, pp 277-287.
39. Regulatory Guide 1.70, Revision 1, Standard Format and Content of Safety Analysis Reports for Nuclear Power Plants, USNRC, October 1972.
40. Pacific Gas and Electric Company, Final Report of the Diablo Canyon Long Term Seismic Program, July 1988.

DCPP UNITS 1 & 2 FSAR UPDATE

41. Pacific Gas and Electric Company, Addendum to the 1988 Final Report of the Diablo Canyon Long Term Seismic Program, February 1991.
42. NUREG-0675, Supplement No. 34, Safety Evaluation Report Related to the Operation of Diablo Canyon Nuclear Power Plant, Units 1 and 2, USNRC, June 1991.
43. NRC letter to PG&E, Transmittal of Safety Evaluation Closing Out Diablo Canyon Long-Term Seismic Program, (TAC Nos. M80670 and M80671), April 17, 1992.
44. Pacific Gas and Electric Company, Assessment of Slope Stability Near the Diablo Canyon Power Plant, April 1997.
45. Harding Lawson Associates, Liquefaction Evaluation - Proposed ASW Bypass - Diablo Canyon Power Plant, August 23, 1996.
46. Harding Lawson Associates Letter, "Geotechnical Consultation - Liquefaction Evaluation - Proposed ASW Bypass - Diablo Canyon Power Plant," October 1, 1996.
47. Harding Lawson Associates Report, Geotechnical Slope Stability Evaluation - ASW System Bypass, Unit 1 - Diablo Canyon Power Plant, July 3, 1996.
48. License Amendment Request 97-11, Submitted to the NRC by PG&E Letters DCL-97-150, dated August 26, 1997; DCL-97-177, dated October 14, 1997; DCL-97-191, dated November 13, 1997; and DCL-98-013, dated January 29, 1998.
49. NRC Letter to PG&E dated March 26, 1999, granting License Amendment No. 131 to Unit 1 and No. 129 to Unit 2.

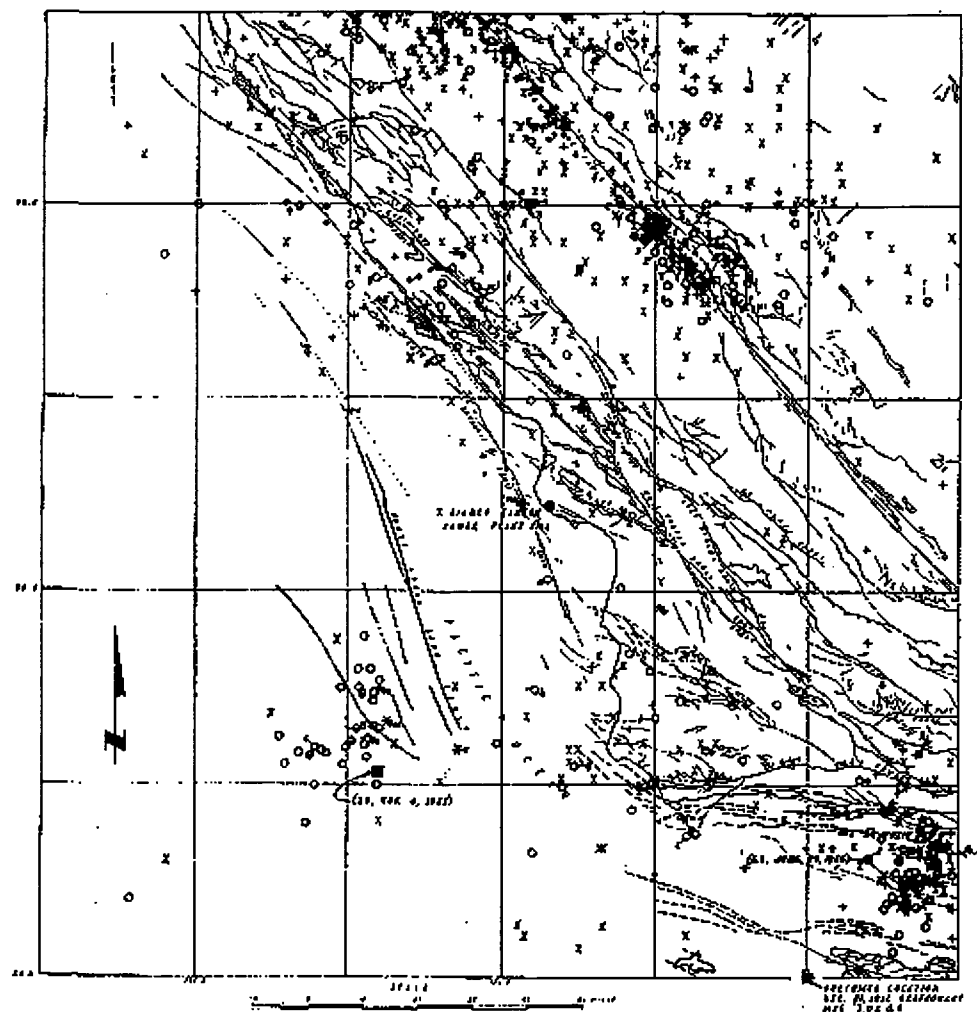


FSAR UPDATE

**UNITS 1 AND 2
DIABLO CANYON SITE**

**FIGURE 2.5-2
EARTHQUAKE EPICENTERS
WITHIN 200 MILES OF PLANT SITE**

Revision 11 November 1996



EXPLANATION

EARTHQUAKE EPICENTER DATA

INTERPOLATED LOCATION AND ASSIGNED MAGNITUDE
SELECTED EARTHQUAKE EPICENTERS WITHIN 75 MILES
OF THE DIABLO CANYON POWER PLANT SITE, 1940-1972

| SYMBOL | MAGNITUDE |
|--------|---|
| ■ | 7.0 2 M 2.5.0 } MAGNITUDE AND DATE ASSIGNED |
| ● | 6.5 2 M 2.4.0 |
| ○ | 5.5 2 M 2.3.0 |
| □ | 4.5 2 M 2.2.0 |
| × | 3.5 2 M 2.1.0 |
| + | 2.5 2 M 2.0.0 |

(SYMBOLS OF UNKNOWN NUMBER OF EARTHQUAKES OCCURRED AT SAME LOCATION)

INDICES FOR FAULTS AND EARTHQUAKE EPICENTERS ARE AS FOLLOWS:

1. FAULT DATA FROM JENSEN, C. W., 1972, GEOLOGIC MAP OF CALIFORNIA, 1:500,000, (1972).
2. THE EARTHQUAKES OF 2.0 MAGNITUDE OCCURRING DURING THE TIME INTERVAL 1934-1972, 1972, CALIFORNIA DIVISION OF MINES AND GEOLOGY, (1972), (1972).
3. THE EARTHQUAKES OF 2.0 MAGNITUDE OCCURRING DURING THE TIME INTERVAL 1934-1972, 1972, CALIFORNIA DIVISION OF MINES AND GEOLOGY, (1972), (1972).
4. THE LARGE EARTHQUAKES OCCURRING DURING THE TIME INTERVAL 1934-1972, 1972, CALIFORNIA DIVISION OF MINES AND GEOLOGY, (1972), (1972).
5. THE EARTHQUAKES OF 2.0 MAGNITUDE OCCURRING DURING THE TIME INTERVAL 1934-1972, 1972, CALIFORNIA DIVISION OF MINES AND GEOLOGY, (1972), (1972).
6. THE EARTHQUAKES OF 2.0 MAGNITUDE OCCURRING DURING THE TIME INTERVAL 1934-1972, 1972, CALIFORNIA DIVISION OF MINES AND GEOLOGY, (1972), (1972).

NOTES FOR REVISIONS AND EARTHQUAKE DATA

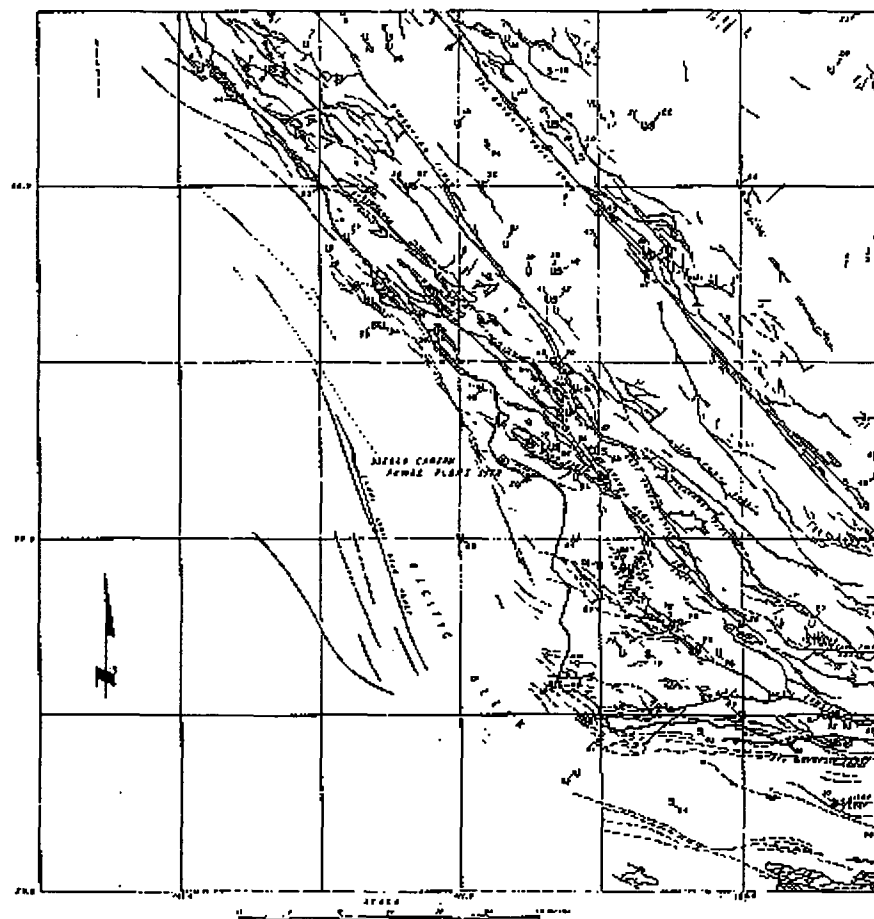
- A. FAULT DATA REVISED IN ACCORDANCE WITH NOTE 6, FIGURE 5, APPENDIX 2.50
- B. EARTHQUAKES OF 2.0 MAGNITUDE OCCURRING DURING THE TIME INTERVAL 1934-1972, 1972, CALIFORNIA DIVISION OF MINES AND GEOLOGY, (1972), (1972).
- C. EARTHQUAKES OF 2.0 MAGNITUDE OCCURRING DURING THE TIME INTERVAL 1934-1972, 1972, CALIFORNIA DIVISION OF MINES AND GEOLOGY, (1972), (1972).

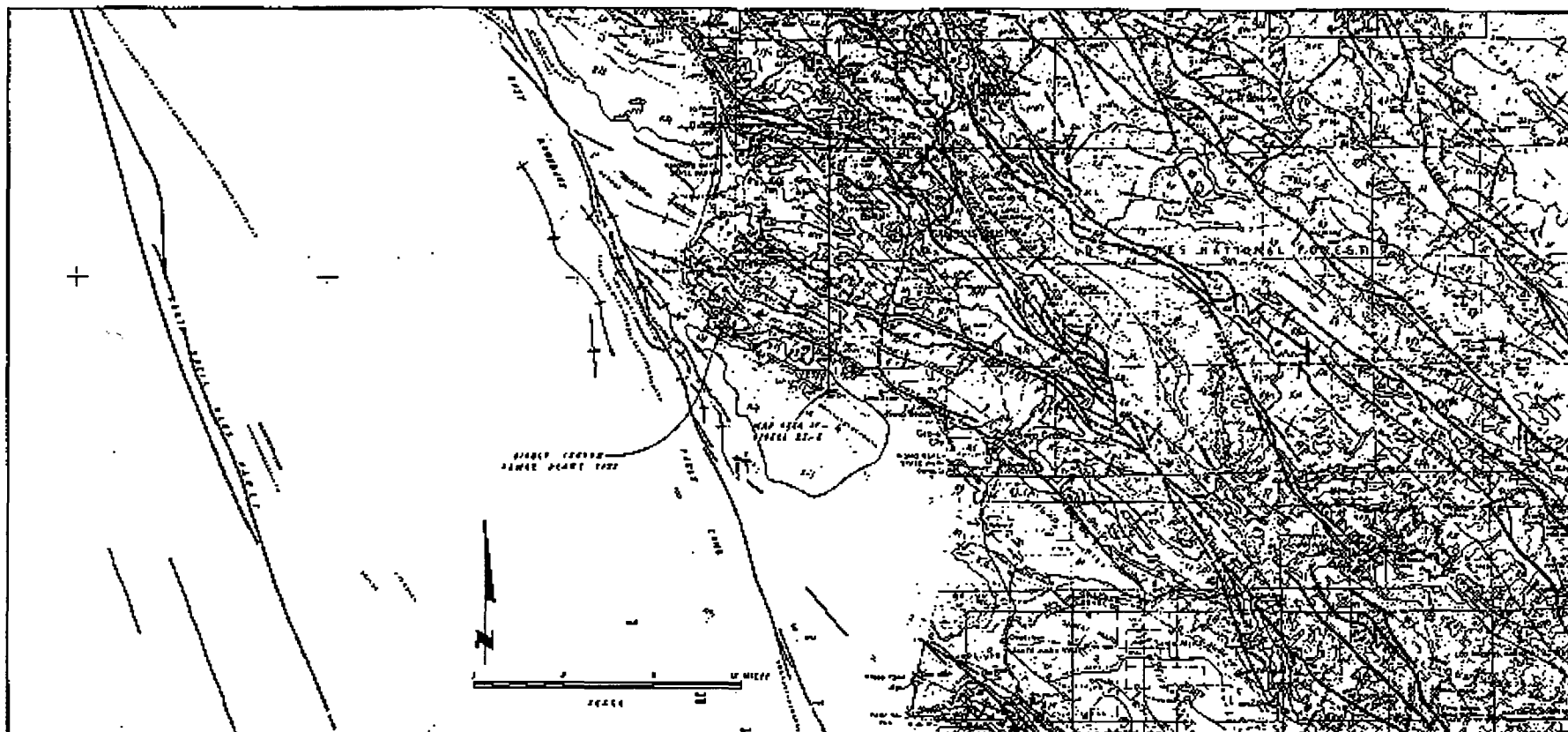
FSAR UPDATE

UNITS 1 AND 2 DIABLO CANYON SITE

FIGURE 2.5-3 FAULTS AND EARTHQUAKE EPICENTERS WITHIN 75 MILES OF PLANT SITE (FOR EARTHQUAKES WITH ASSIGNED MAGNITUDES)

Revision 11 November 1996





FSAR UPDATE

**UNITS 1 AND 2
DIABLO CANYON SITE**

**FIGURE 2.5-5
GEOLOGIC AND TECTONIC MAP OF
SOUTHERN COAST RANGES IN THE
REGION OF PLANT SITE
(SHEET 1 OF 2)**

Revision 11 November 1996

EXPLANATION

GEOLOGIC UNITS

CEHOZOTIC

QUATERNARY DEPOSITS AND ROCKS

- Q HOLOCENE AND PLISTOCENE NONMARINE (THINLY ACCUMULATED AND MARINE DEPOSITS, UNDIVIDED)
- Qz LARGE LANDSLIDES, WHEN MAPPED SEPARATELY
- Qs OVER SAND DEPOSITS, WHEN MAPPED SEPARATELY
- Qp CLIP-PLISTOCENE AND ALLUVIAL NONMARINE
- P PLEISTOCENE MARINE
- M MIOCENE MARINE
- O OCEANIC NONMARINE
- E Eocene MARINE
- Ep PALEOCENE MARINE

Volcanic Rocks

- Tv TERTIARY VOLCANIC ROCKS
- Tv* TERTIARY PYROCLASTIC ROCKS, INCLUDING VOLCANIC HYDROGEN DEPOSITS
- Ti TERTIARY INTRUSIVE ROCKS

SYMBOLS

- GEOLOGIC CONTACT, DASHED WHERE APPROXIMATE OR WHERE QUATERNARY DEPOSITS ARE INVOLVED.
- FAULT (SOLID LINE WHERE LOCATION IS WELL DEFINED; DASHED LINE WHERE APPROXIMATE OR INFERRED; DOTTED WHERE CONCEALED)
- ANTICLINAL AXIS - WITH PLUNGE INDICATED (SOLID LINE WHERE LOCATION IS WELL DEFINED; DASHED WHERE APPROXIMATE OR INFERRED; DOTTED WHERE CONCEALED)
- SYNCLINAL AXIS - WITH PLUNGE INDICATED (SOLID LINE WHERE LOCATION IS WELL DEFINED; DASHED WHERE APPROXIMATE OR INFERRED; DOTTED WHERE CONCEALED)

MEZOTIC

SEDIMENTARY AND METAMORPHIC ROCKS

- Ku UPPER CRETACEOUS MARINE ROCKS
 - Ks LOWER CRETACEOUS MARINE ROCKS
 - Ksf FRANCISCAN ASSEMBLAGE (PREDOMINANTLY SEDIMENTARY AND METAMORPHIC ROCKS, INCLUDING FRANCISCAN MELANGE)
 - J JURASSIC MARINE ROCKS (INCLUDES WHITEVILLE FORMATION)
 - M METAMORPHIC ROCKS OF PRE-TERTIARY AGE, UNDIVIDED
- METAVOLCANIC ROCKS
- Mzv METAVOLCANIC ROCKS (INCLUDING FRANCISCAN VOLCANIC ROCKS)
- PLUTONIC ROCKS
- GtMc MEZOTIC GRANITIC ROCKS
 - Uv MEZOTIC ULTRAMAFIC ROCKS

NOTES

1. MAP BASE FROM PARTS OF SAN LUIS GRIST AND TEMPA MAPS TRACTS, U.S. GEOLOGICAL SURVEY 1:250,000 SCALE TERRAIN MAP SERIES

2. GEOLOGIC DATA FROM:

"GEOLOGIC MAP OF CALIFORNIA" 1932, SCALE 1:500,000; PRELIMINARY, UNPUBLISHED, CALIFORNIA DIVISION OF MINES AND GEOLOGY (COMPILED BY C. W. FENNINGS)

LOCALLY SUPPLEMENTED WITH DATA FROM:

BEAVER, L.S., 1945, GEOLOGY OF THE COASTAL PORTION OF THE SAN LUIS RANGE, SAN LUIS OBISPO COUNTY, CALIF., UNPUBLISHED M.S. THESIS, UNIV. OF CALIF.

JARRIS, R.A., 1946, GEOLOGY OF THE DIABLO CANYON POWER PLANT SITE, SAN LUIS OBISPO COUNTY, CALIFORNIA; 1947 SUPPLEMENTARY REPORTS I AND II, 1948 SUPPLEMENTARY REPORT III, UNPUBLISHED REPORT TO THE PACIFIC GAS AND ELECTRIC COMPANY.

HALL, C.A., 1975, U.S.G. MAP OF SO.

EARTH SCIENCES ASSOCIATES, 1974, OFFSHORE INVESTIGATION.

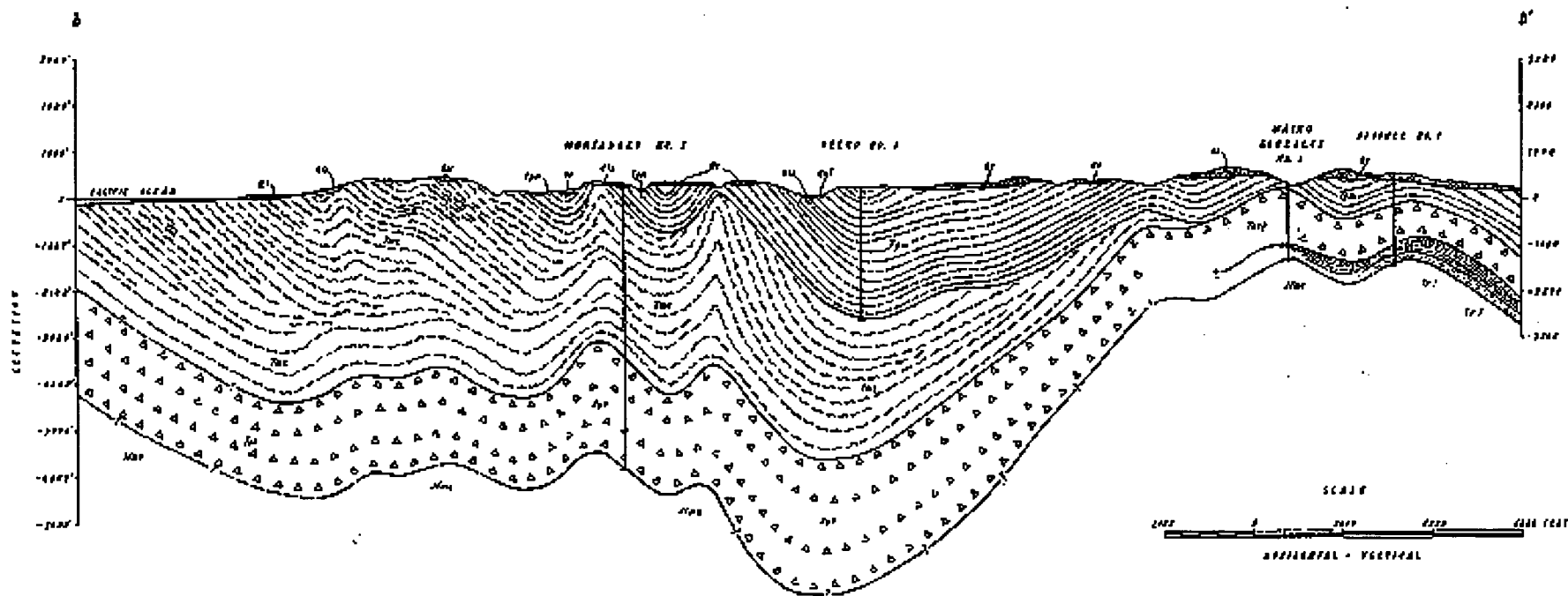
FSAR UPDATE

UNITS 1 AND 2 DIABLO CANYON SITE

FIGURE 2.5-5 GEOLOGIC AND TECTONIC MAP OF SOUTHERN COAST RANGES IN THE REGION OF PLANT SITE (SHEET 2 OF 2)

(0886) 2 OF 2

Revision 11 November 1996



SECTION A-A'
SHOWING EXPLORATORY OIL WELLS AND
GEOLOGIC RELATIONSHIPS IN THE SAN LUIS RANGE
VIEW WEST-NORTHWEST

NOTE: THE SYMBOL S.S.-G. INDICATES THE LOCATION OF THE
SECTION, AND ORIENTATION OF STRUCTURE.

| |
|--|
| FSAR UPDATE |
| UNITS 1 AND 2 DIABLO CANYON SITE |
| FIGURE 2.5-7 GEOLOGIC SECTION THROUGH EXPLORATORY OIL WELLS IN THE SAN LUIS RANGE |

Revision 11 November 1996

GEOLOGIC MAP OF DIABLO CANYON COASTAL AREA

EXPLANATION

0-10
0-11
0-12
0-13
0-14
0-15
0-16
0-17
0-18
0-19
0-20
0-21
0-22
0-23
0-24
0-25
0-26
0-27
0-28
0-29
0-30
0-31
0-32
0-33
0-34
0-35
0-36
0-37
0-38
0-39
0-40
0-41
0-42
0-43
0-44
0-45
0-46
0-47
0-48
0-49
0-50
0-51
0-52
0-53
0-54
0-55
0-56
0-57
0-58
0-59
0-60
0-61
0-62
0-63
0-64
0-65
0-66
0-67
0-68
0-69
0-70
0-71
0-72
0-73
0-74
0-75
0-76
0-77
0-78
0-79
0-80
0-81
0-82
0-83
0-84
0-85
0-86
0-87
0-88
0-89
0-90
0-91
0-92
0-93
0-94
0-95
0-96
0-97
0-98
0-99
1-00
1-01
1-02
1-03
1-04
1-05
1-06
1-07
1-08
1-09
1-10
1-11
1-12
1-13
1-14
1-15
1-16
1-17
1-18
1-19
1-20
1-21
1-22
1-23
1-24
1-25
1-26
1-27
1-28
1-29
1-30
1-31
1-32
1-33
1-34
1-35
1-36
1-37
1-38
1-39
1-40
1-41
1-42
1-43
1-44
1-45
1-46
1-47
1-48
1-49
1-50
1-51
1-52
1-53
1-54
1-55
1-56
1-57
1-58
1-59
1-60
1-61
1-62
1-63
1-64
1-65
1-66
1-67
1-68
1-69
1-70
1-71
1-72
1-73
1-74
1-75
1-76
1-77
1-78
1-79
1-80
1-81
1-82
1-83
1-84
1-85
1-86
1-87
1-88
1-89
1-90
1-91
1-92
1-93
1-94
1-95
1-96
1-97
1-98
1-99
2-00
2-01
2-02
2-03
2-04
2-05
2-06
2-07
2-08
2-09
2-10
2-11
2-12
2-13
2-14
2-15
2-16
2-17
2-18
2-19
2-20
2-21
2-22
2-23
2-24
2-25
2-26
2-27
2-28
2-29
2-30
2-31
2-32
2-33
2-34
2-35
2-36
2-37
2-38
2-39
2-40
2-41
2-42
2-43
2-44
2-45
2-46
2-47
2-48
2-49
2-50
2-51
2-52
2-53
2-54
2-55
2-56
2-57
2-58
2-59
2-60
2-61
2-62
2-63
2-64
2-65
2-66
2-67
2-68
2-69
2-70
2-71
2-72
2-73
2-74
2-75
2-76
2-77
2-78
2-79
2-80
2-81
2-82
2-83
2-84
2-85
2-86
2-87
2-88
2-89
2-90
2-91
2-92
2-93
2-94
2-95
2-96
2-97
2-98
2-99
3-00
3-01
3-02
3-03
3-04
3-05
3-06
3-07
3-08
3-09
3-10
3-11
3-12
3-13
3-14
3-15
3-16
3-17
3-18
3-19
3-20
3-21
3-22
3-23
3-24
3-25
3-26
3-27
3-28
3-29
3-30
3-31
3-32
3-33
3-34
3-35
3-36
3-37
3-38
3-39
3-40
3-41
3-42
3-43
3-44
3-45
3-46
3-47
3-48
3-49
3-50
3-51
3-52
3-53
3-54
3-55
3-56
3-57
3-58
3-59
3-60
3-61
3-62
3-63
3-64
3-65
3-66
3-67
3-68
3-69
3-70
3-71
3-72
3-73
3-74
3-75
3-76
3-77
3-78
3-79
3-80
3-81
3-82
3-83
3-84
3-85
3-86
3-87
3-88
3-89
3-90
3-91
3-92
3-93
3-94
3-95
3-96
3-97
3-98
3-99
4-00
4-01
4-02
4-03
4-04
4-05
4-06
4-07
4-08
4-09
4-10
4-11
4-12
4-13
4-14
4-15
4-16
4-17
4-18
4-19
4-20
4-21
4-22
4-23
4-24
4-25
4-26
4-27
4-28
4-29
4-30
4-31
4-32
4-33
4-34
4-35
4-36
4-37
4-38
4-39
4-40
4-41
4-42
4-43
4-44
4-45
4-46
4-47
4-48
4-49
4-50
4-51
4-52
4-53
4-54
4-55
4-56
4-57
4-58
4-59
4-60
4-61
4-62
4-63
4-64
4-65
4-66
4-67
4-68
4-69
4-70
4-71
4-72
4-73
4-74
4-75
4-76
4-77
4-78
4-79
4-80
4-81
4-82
4-83
4-84
4-85
4-86
4-87
4-88
4-89
4-90
4-91
4-92
4-93
4-94
4-95
4-96
4-97
4-98
4-99
5-00
5-01
5-02
5-03
5-04
5-05
5-06
5-07
5-08
5-09
5-10
5-11
5-12
5-13
5-14
5-15
5-16
5-17
5-18
5-19
5-20
5-21
5-22
5-23
5-24
5-25
5-26
5-27
5-28
5-29
5-30
5-31
5-32
5-33
5-34
5-35
5-36
5-37
5-38
5-39
5-40
5-41
5-42
5-43
5-44
5-45
5-46
5-47
5-48
5-49
5-50
5-51
5-52
5-53
5-54
5-55
5-56
5-57
5-58
5-59
5-60
5-61
5-62
5-63
5-64
5-65
5-66
5-67
5-68
5-69
5-70
5-71
5-72
5-73
5-74
5-75
5-76
5-77
5-78
5-79
5-80
5-81
5-82
5-83
5-84
5-85
5-86
5-87
5-88
5-89
5-90
5-91
5-92
5-93
5-94
5-95
5-96
5-97
5-98
5-99
6-00
6-01
6-02
6-03
6-04
6-05
6-06
6-07
6-08
6-09
6-10
6-11
6-12
6-13
6-14
6-15
6-16
6-17
6-18
6-19
6-20
6-21
6-22
6-23
6-24
6-25
6-26
6-27
6-28
6-29
6-30
6-31
6-32
6-33
6-34
6-35
6-36
6-37
6-38
6-39
6-40
6-41
6-42
6-43
6-44
6-45
6-46
6-47
6-48
6-49
6-50
6-51
6-52
6-53
6-54
6-55
6

EXPLANATION

- | | |
|-----|---------------------------------------|
| 001 | Stegonolepis olivaceum. |
| 002 | Telus and beach deposits. |
| 003 | Stream silt and clay - near deposits. |
| 004 | Lenticular deposits. |
| 005 | Stream - terrace deposits. |
| 006 | Cliff - beach deposits. |
| 007 | Older beach deposits. |
| 008 | Deposits in Marine terrace - terrace. |
| 009 | Late - bottom (P) deposits. |
| 010 | Beach - (P) deposits. |
| 011 | Marine terrace. |
| 012 | Beach terrace. |
| 013 | Beach terrace. |
| 014 | Beach terrace. |
| 015 | Beach terrace. |
| 016 | Beach terrace. |
| 017 | Beach terrace. |
| 018 | Beach terrace. |
| 019 | Beach terrace. |
| 020 | Beach terrace. |
| 021 | Beach terrace. |
| 022 | Beach terrace. |
| 023 | Beach terrace. |
| 024 | Beach terrace. |
| 025 | Beach terrace. |
| 026 | Beach terrace. |
| 027 | Beach terrace. |
| 028 | Beach terrace. |
| 029 | Beach terrace. |
| 030 | Beach terrace. |
| 031 | Beach terrace. |
| 032 | Beach terrace. |
| 033 | Beach terrace. |
| 034 | Beach terrace. |
| 035 | Beach terrace. |
| 036 | Beach terrace. |
| 037 | Beach terrace. |
| 038 | Beach terrace. |
| 039 | Beach terrace. |
| 040 | Beach terrace. |
| 041 | Beach terrace. |
| 042 | Beach terrace. |
| 043 | Beach terrace. |
| 044 | Beach terrace. |
| 045 | Beach terrace. |
| 046 | Beach terrace. |
| 047 | Beach terrace. |
| 048 | Beach terrace. |
| 049 | Beach terrace. |
| 050 | Beach terrace. |
| 051 | Beach terrace. |
| 052 | Beach terrace. |
| 053 | Beach terrace. |
| 054 | Beach terrace. |
| 055 | Beach terrace. |
| 056 | Beach terrace. |
| 057 | Beach terrace. |
| 058 | Beach terrace. |
| 059 | Beach terrace. |
| 060 | Beach terrace. |
| 061 | Beach terrace. |
| 062 | Beach terrace. |
| 063 | Beach terrace. |
| 064 | Beach terrace. |
| 065 | Beach terrace. |
| 066 | Beach terrace. |
| 067 | Beach terrace. |
| 068 | Beach terrace. |
| 069 | Beach terrace. |
| 070 | Beach terrace. |
| 071 | Beach terrace. |
| 072 | Beach terrace. |
| 073 | Beach terrace. |
| 074 | Beach terrace. |
| 075 | Beach terrace. |
| 076 | Beach terrace. |
| 077 | Beach terrace. |
| 078 | Beach terrace. |
| 079 | Beach terrace. |
| 080 | Beach terrace. |
| 081 | Beach terrace. |
| 082 | Beach terrace. |
| 083 | Beach terrace. |
| 084 | Beach terrace. |
| 085 | Beach terrace. |
| 086 | Beach terrace. |
| 087 | Beach terrace. |
| 088 | Beach terrace. |
| 089 | Beach terrace. |
| 090 | Beach terrace. |
| 091 | Beach terrace. |
| 092 | Beach terrace. |
| 093 | Beach terrace. |
| 094 | Beach terrace. |
| 095 | Beach terrace. |
| 096 | Beach terrace. |
| 097 | Beach terrace. |
| 098 | Beach terrace. |
| 099 | Beach terrace. |
| 100 | Beach terrace. |

FSAR UPDATE

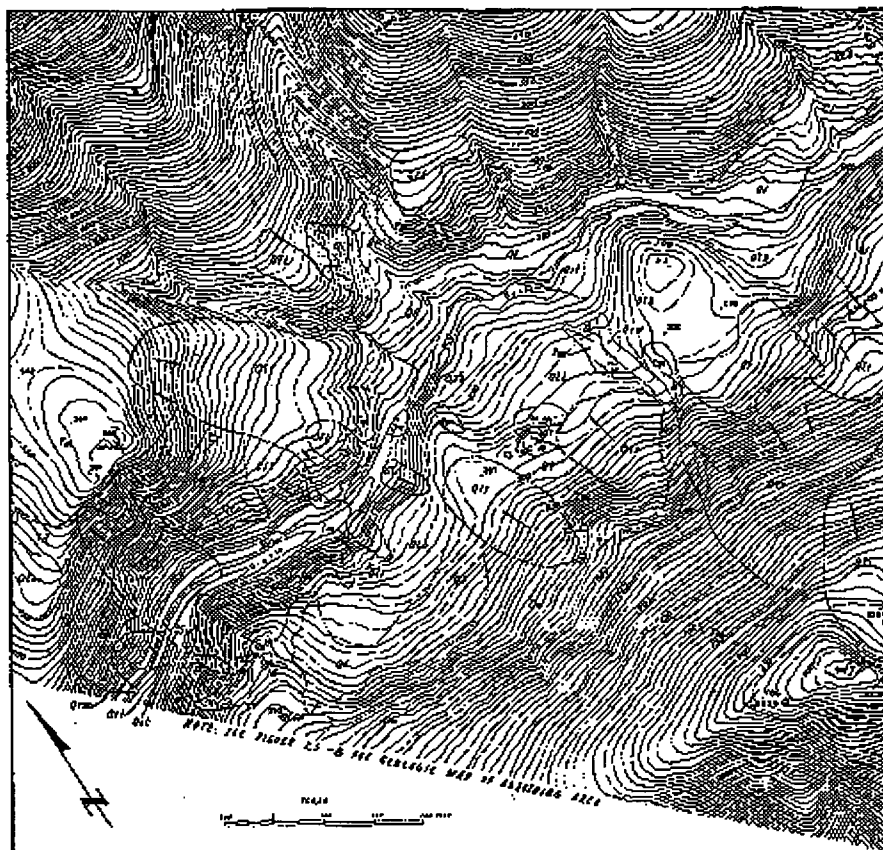
**UNITS 1 AND 2
DIABLO CANYON SITE**

**FIGURE 2.5-8
GEOLOGIC MAP OF DIABLO CANYON
COASTAL AREA**

FIGURE 2.5-8

Revised 11 November 1996.

Revision 11 November 1996



EXPLANATION

| | | |
|---------------------|------|--------------------------------------|
| PLISTOCENE - RECENT | Qal | STREAM-LAIN ALLUVIUM |
| | Qsu | SLOPE-SCARP AND SLOPE-WASH DEPOSITS |
| | Qls | LANDSLIDE DEPOSITS |
| | Qst | STRAIN-TERRACE DEPOSITS |
| | Qf | ALLUVIAL-FAN DEPOSITS |
| | Qft | OLDER FAN-TERRACE DEPOSITS |
| MIOCENE | Qlor | DEPOSITS ON MARINE WAVE-CUT TERRACES |
| | Qlb | LAKE-BOTTOM (?) DEPOSITS |
| | Td | DIABASE INTRUSIVE ROCK |
| | Im | MONTANEY FORMATION |

- CONTACT INVOLVING JURASSIC DEPOSITS.
- CONTACT BETWEEN DEBROCA UNIT. DASHED WHERE APPROX. LOCATED, DOTTED WHERE CONCEALED BY SCARP.
- 70° S. STRIKE AND DIP OF BEAR
- 40-70° TREND AND RANGE IN DIP OF SCARP FOLDED OR WIPPED ON A SMALL SCALE.

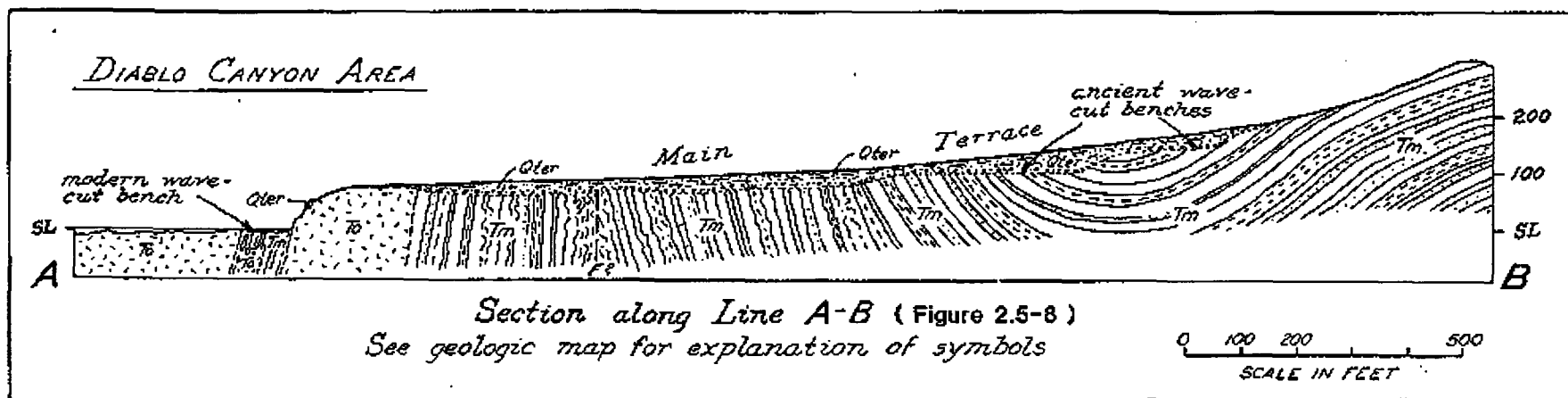
GEOLOGY MAPS BY E. H. JAMES AND A. M. JOHNSON, 1967, SUPPLEMENTED BY E. H. JAMES, 1969.

FSAR UPDATE

**UNITS 1 AND 2
DIABLO CANYON SITE**

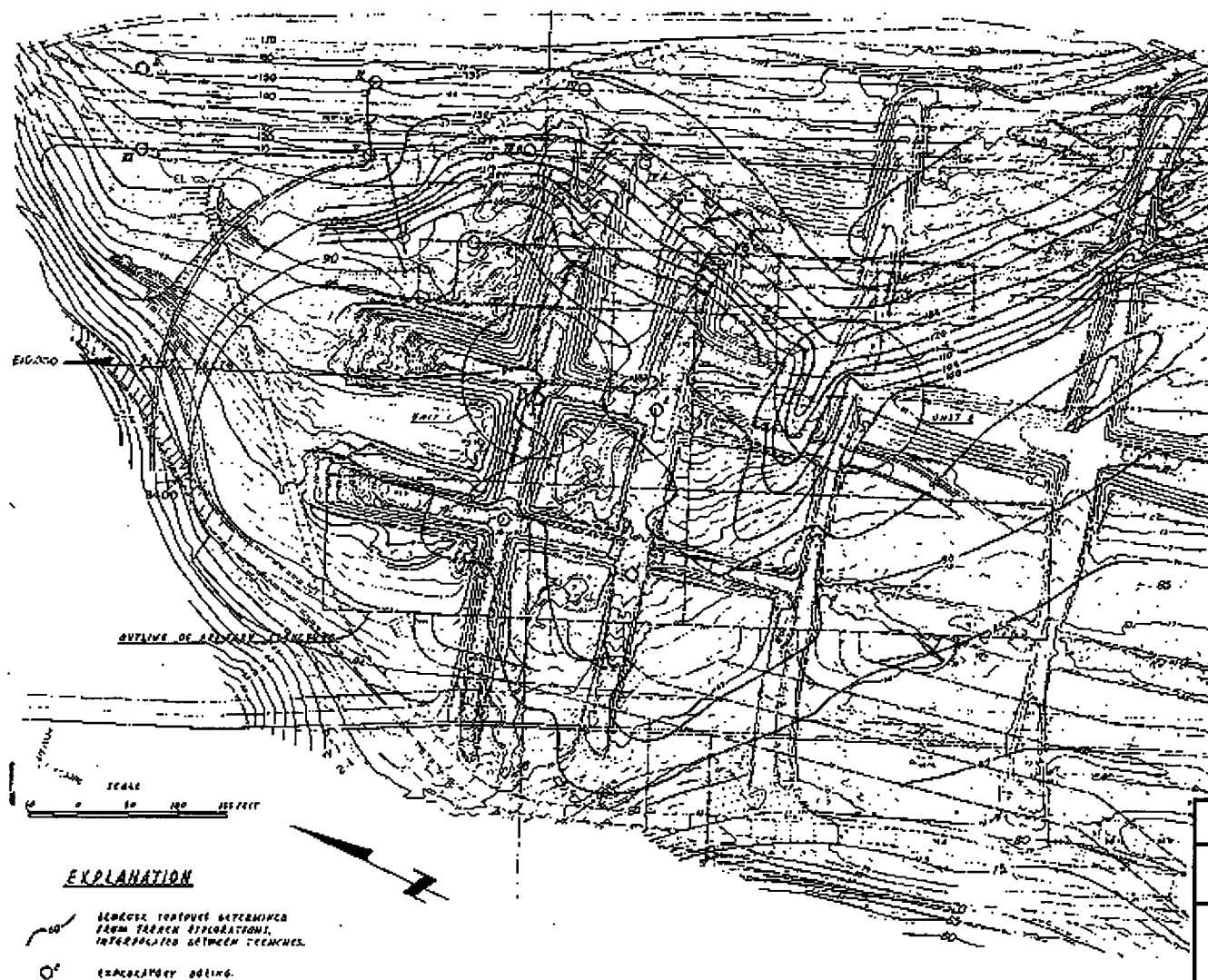
**FIGURE 2.5-9
GEOLOGIC MAP OF SWITCHYARD AREA**

Revision 11 November 1996



| |
|---|
| FSAR UPDATE |
| UNITS 1 AND 2 DIABLO CANYON SITE |
| FIGURE 2.5-10 GEOLOGIC SECTION THROUGH THE PLANT SITE |

Revision 11 November 1996

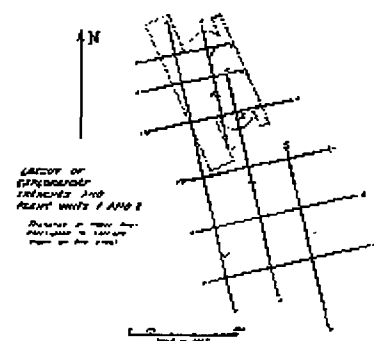
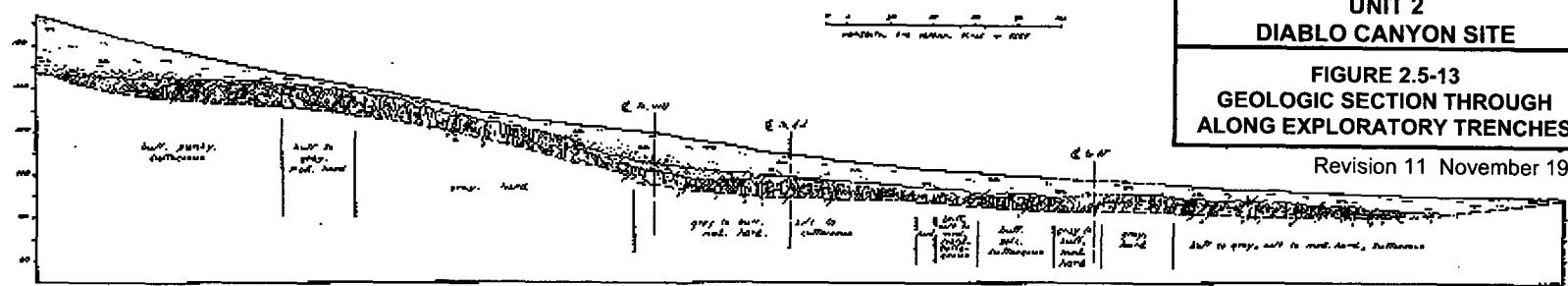
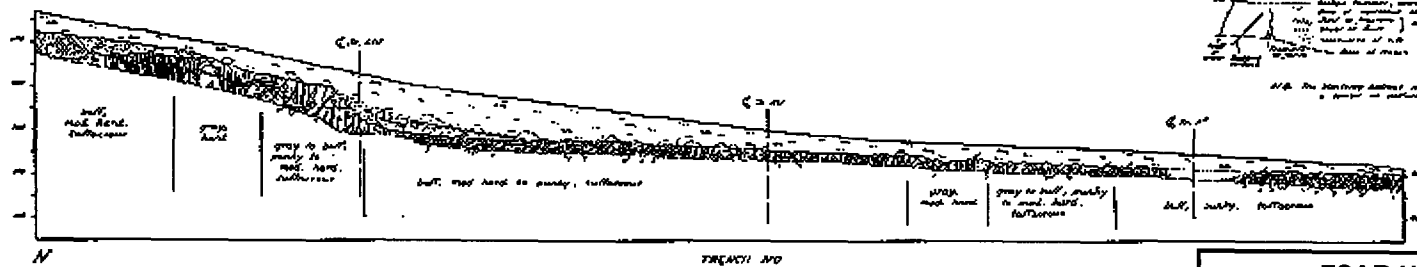
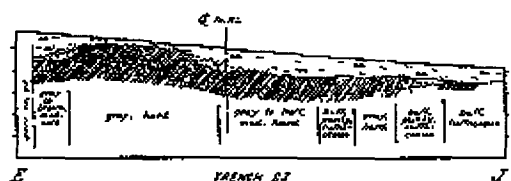
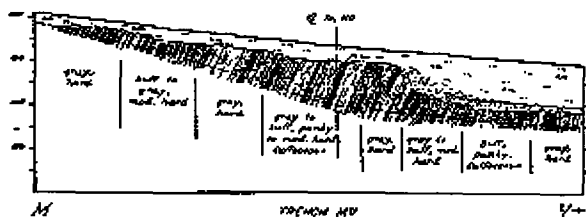
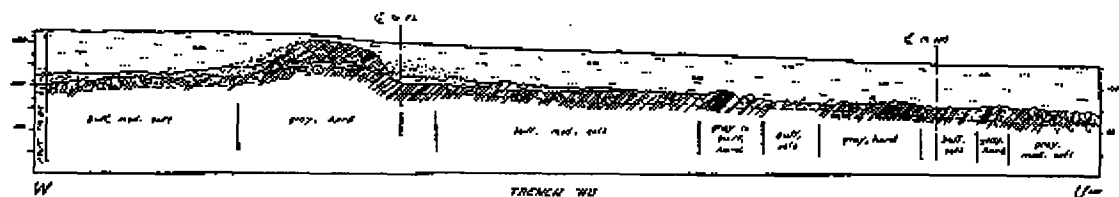


FSAR UPDATE

UNITS 1 AND 2
DIABLO CANYON SITE

FIGURE 2.5-11
SITE EXPLORATION FEATURES
AND BEDROCK CONTOURS

Revision 11 November 1996



EXPLANATION

Legend for the geologic section:

- Buff. med. soft: Buff. med. soft
- Gray, hard: Gray, hard
- Buff. med. soft: Buff. med. soft
- Gray to buff. med. hard: Gray to buff. med. hard
- Buff. med. soft: Buff. med. soft
- Buff. med. soft to buff. med. hard: Buff. med. soft to buff. med. hard
- Buff. med. soft: Buff. med. soft

FSAR UPDATE

UNIT 2

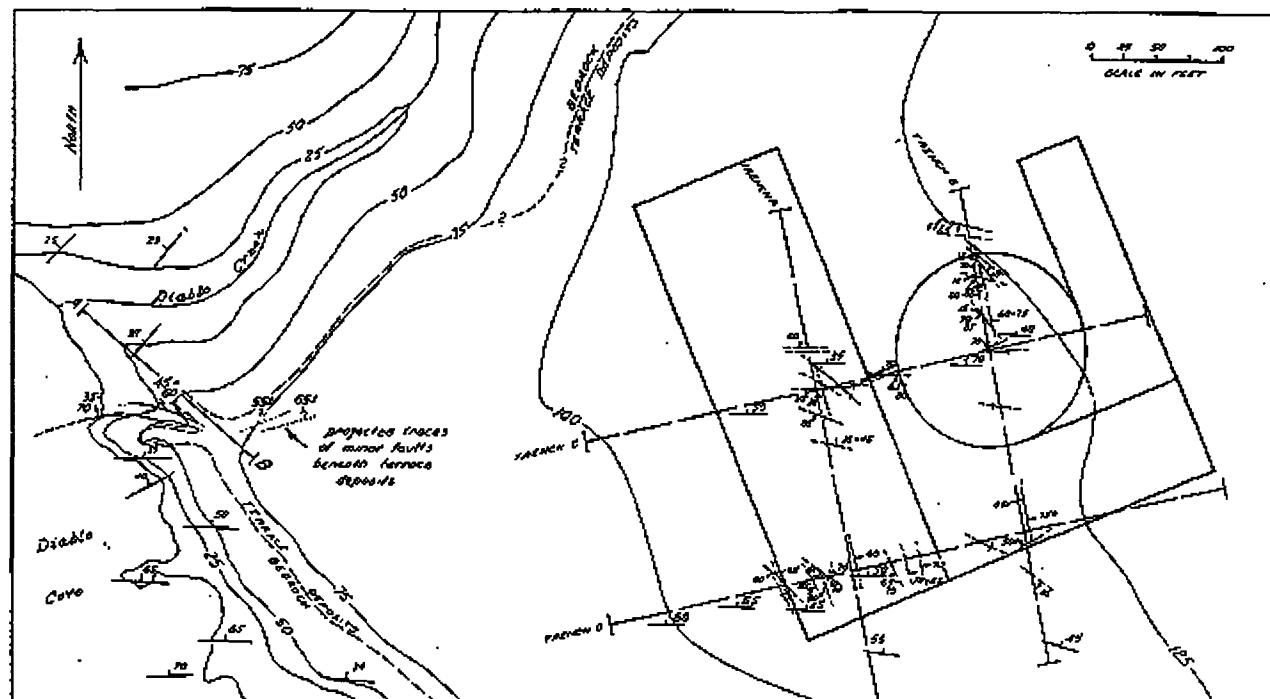
DIABLO CANYON SITE

FIGURE 2.5-13

GEOLOGIC SECTION THROUGH

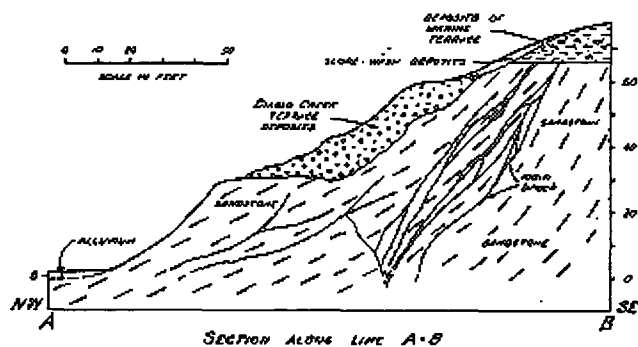
ALONG EXPLORATORY TRENCHES

Revision 11 November 1996



EXPLANATION

- 1:20 Strike and dip of beds
- Generalized trace of bedding (in section only)
- Fault or shear, showing dip and trend and plunge of strata
- Vertical fault or shear
- Center line of exploratory trench
- Outline of power plant structure



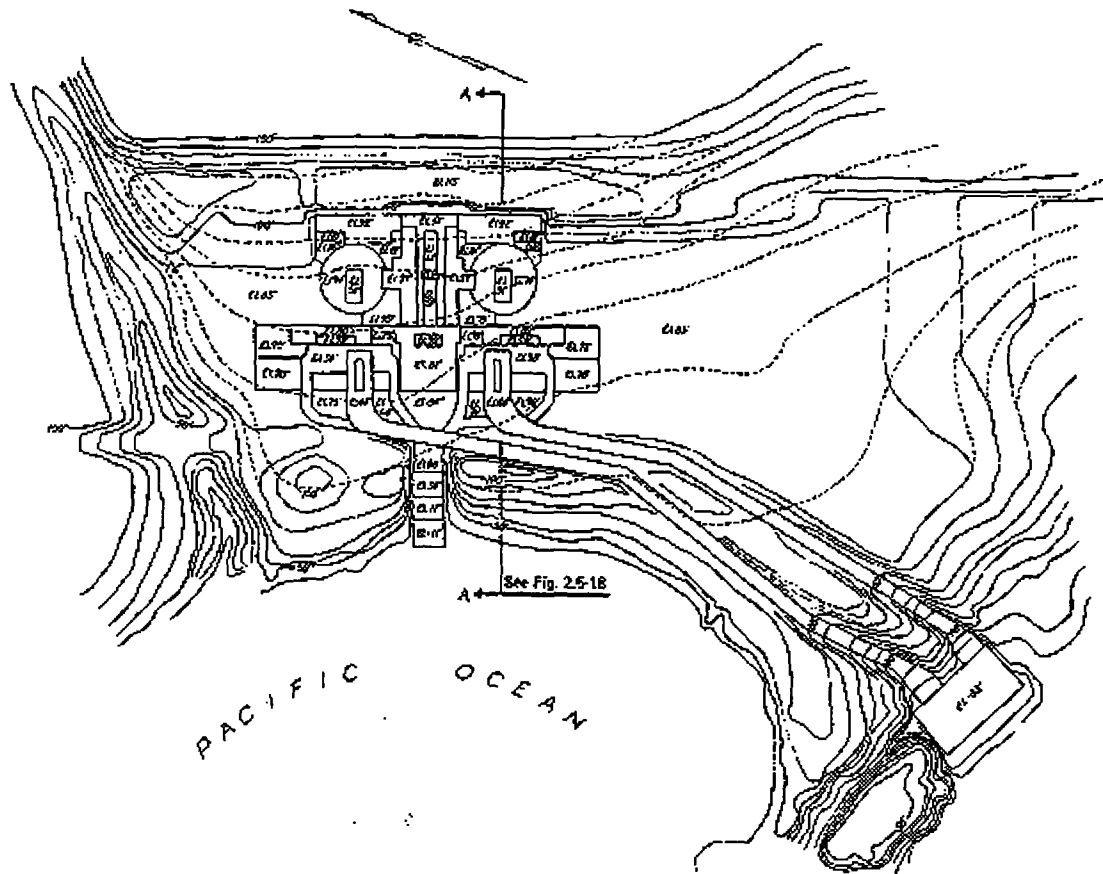
SECTION ALONG LINE A-B

FSAR UPDATE

UNITS 1 AND 2 DIABLO CANYON SITE

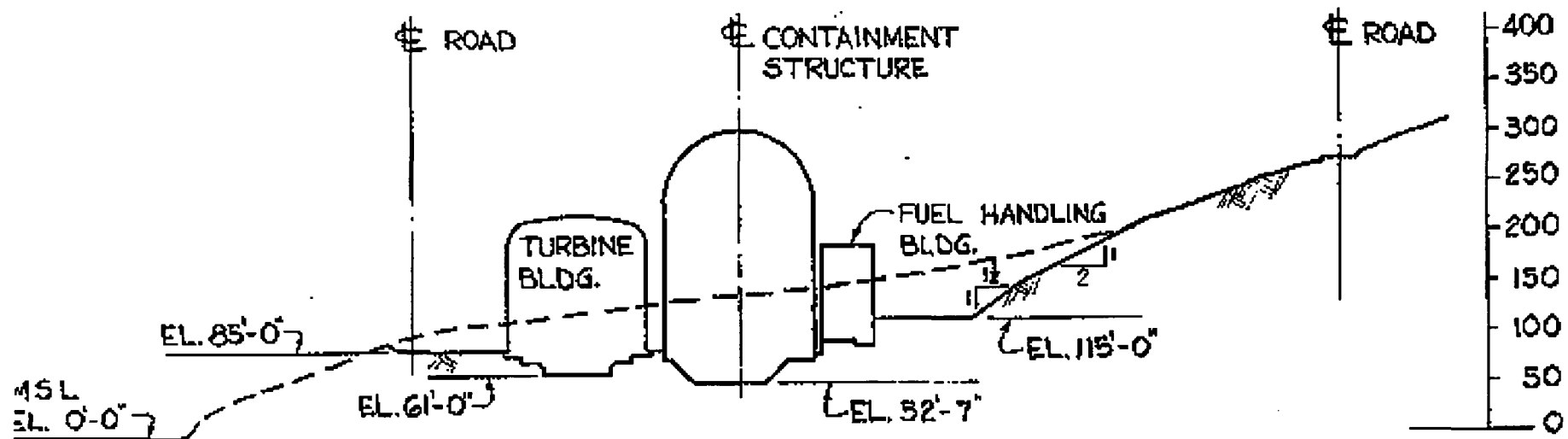
FIGURE 2.5-14 RELATIONSHIPS OF FAULTS AND SHEARS AT PLANT SITE

Revision 11 November 1996



| |
|--|
| FSAR UPDATE |
| UNITS 1 AND 2 DIABLO CANYON SITE |
| FIGURE 2.5-17 PLAN OF EXCAVATION AND BACKFILL |

Revision 11 November 1996

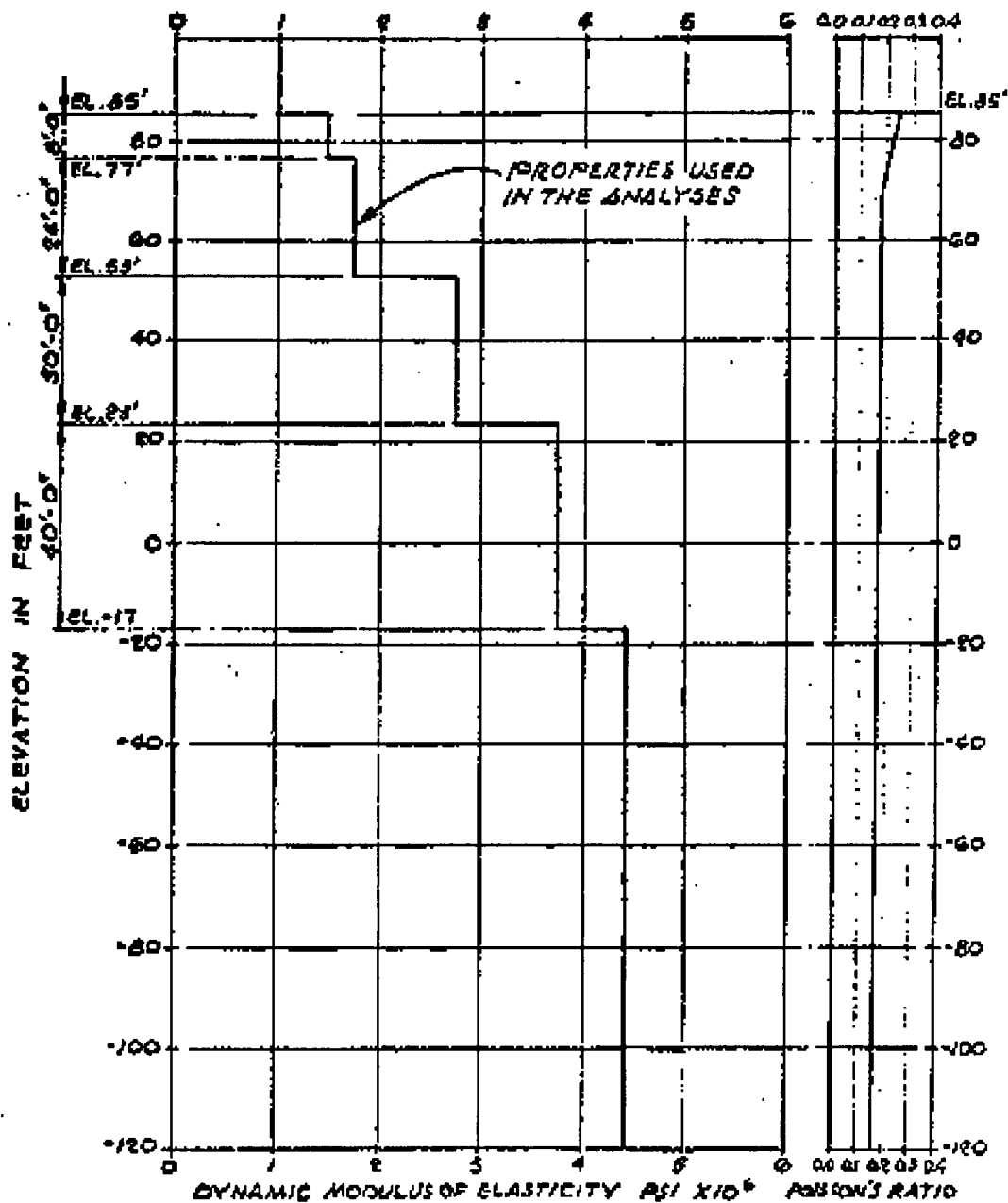


SECTION A-A

FROM FIGURE 2.5-17

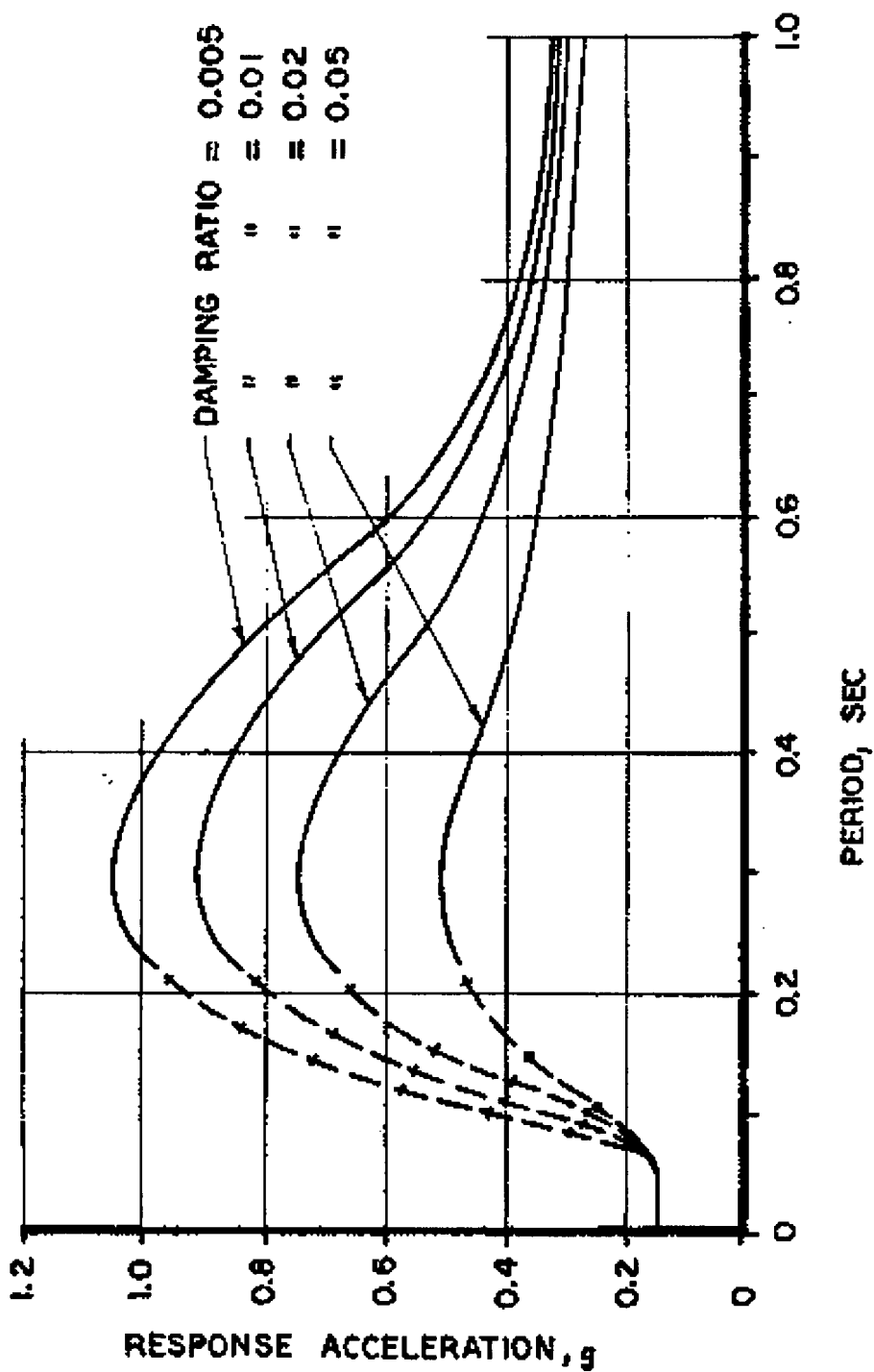
| |
|---|
| FSAR UPDATE |
| UNITS 1 AND 2 DIABLO CANYON SITE |
| FIGURE 2.5-18 SECTION A-A EXCAVATION AND BACKFILL |

Revision 11 November 1996



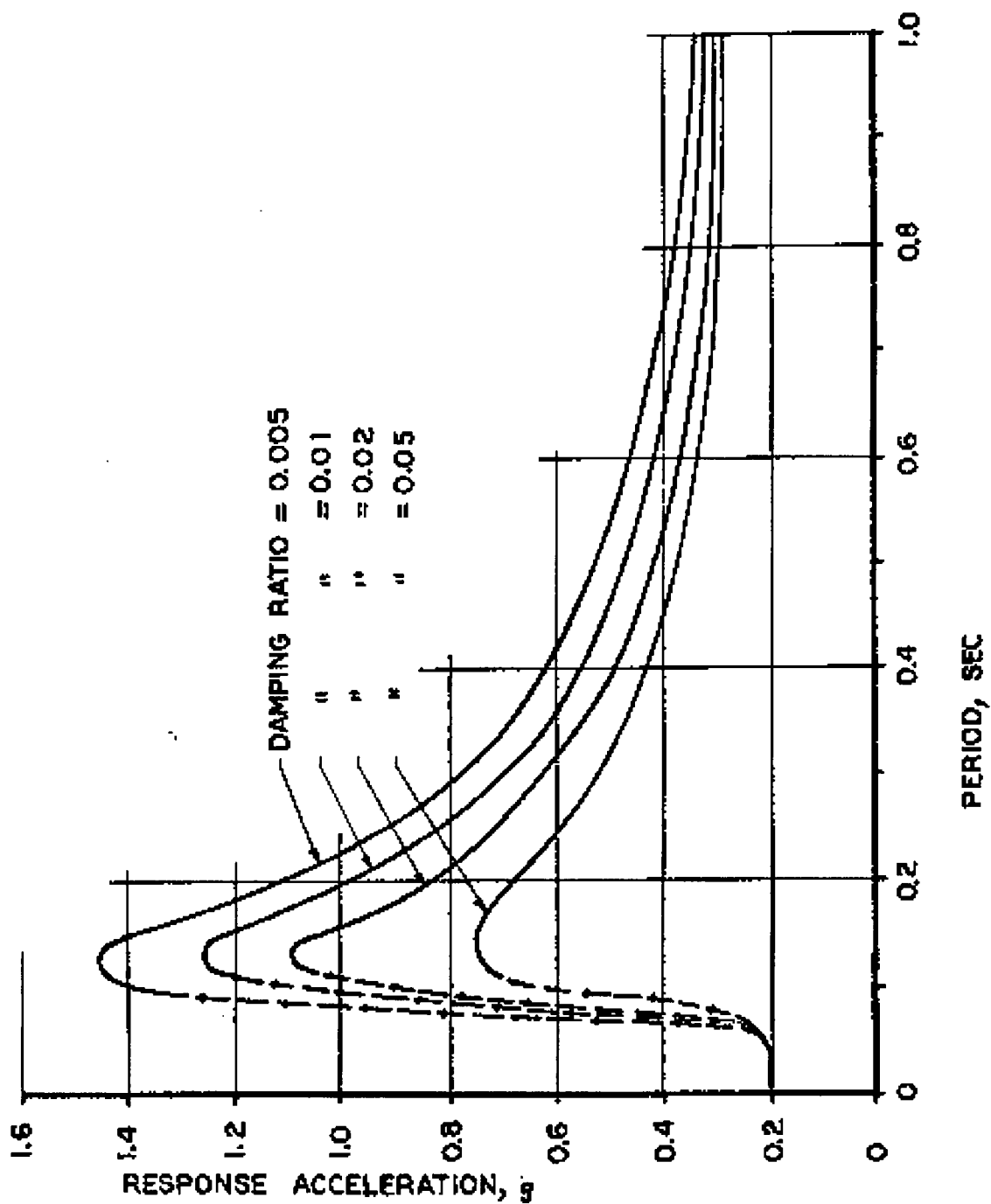
| |
|--|
| FSAR UPDATE |
| UNITS 1 AND 2 DIABLO CANYON SITE |
| FIGURE 2.5-19 SOIL MODULE OF ELASTICITY AND POISSON'S RATIO |

Revision 11 November 1996



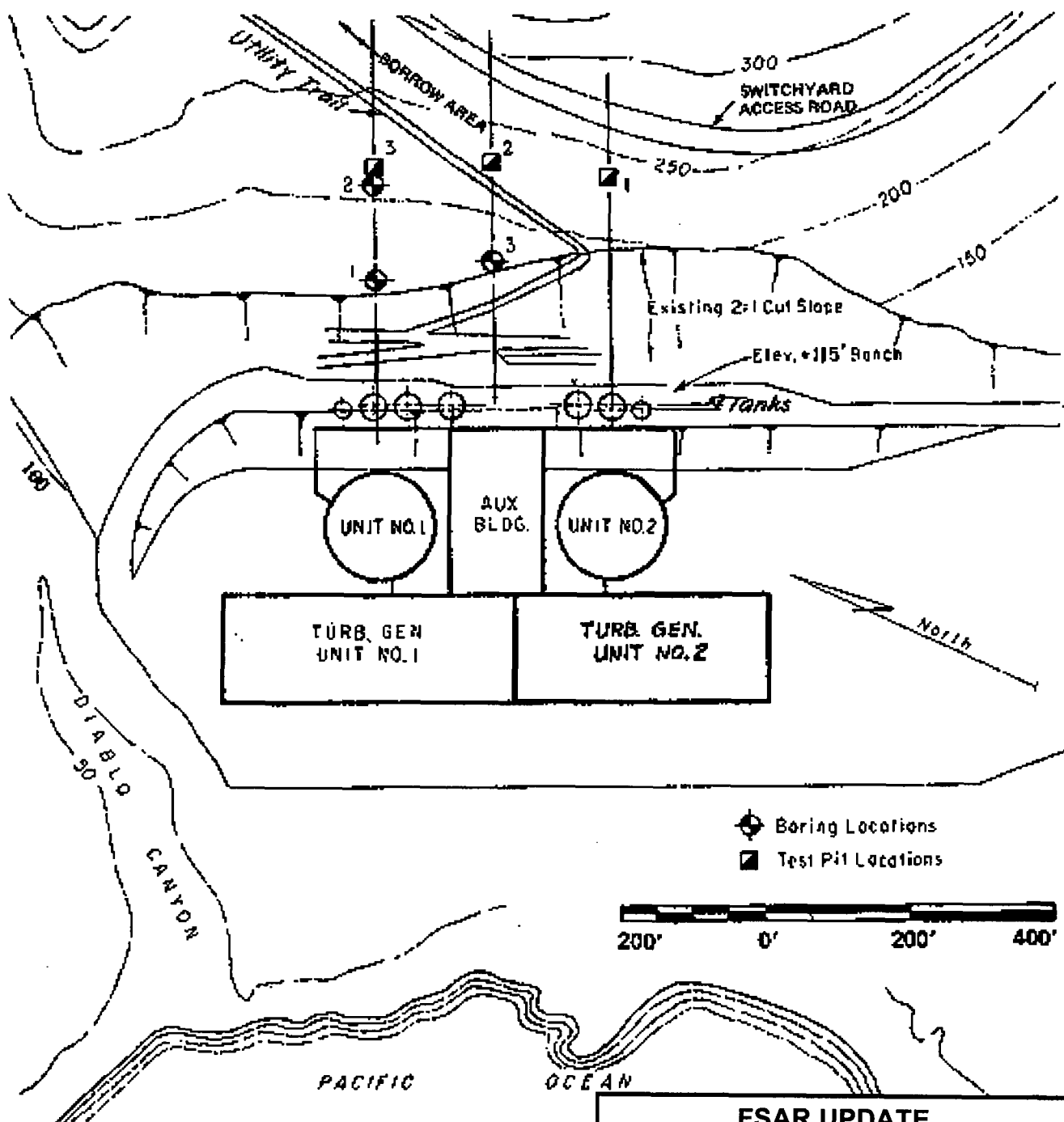
| |
|---|
| FSAR UPDATE |
| UNITS 1 AND 2 DIABLO CANYON SITE |
| FIGURE 2.5-20 SMOOTH RESPONSE ACCELERATION SPECTRA - EARTHQUAKE "B" |

Revision 11 November 1996



| |
|--|
| FSAR UPDATE |
| UNITS 1 AND 2 DIABLO CANYON SITE |
| FIGURE 2.5-21 SMOOTH RESPONSE ACCELERATION SPECTRA – EARTHQUAKE "D" MODIFIED |

Revision 11 November 1996



FSAR UPDATE

**UNITS 1 AND 2
DIABLO CANYON SITE**

**FIGURE 2.5-22
POWER PLANT SLOPE
PLAN**

Revision 11 November 1996

Shear Strength (lbs/sq ft)

Moisture
Content (%)

Dry
Density (pcf)

Depth (ft)

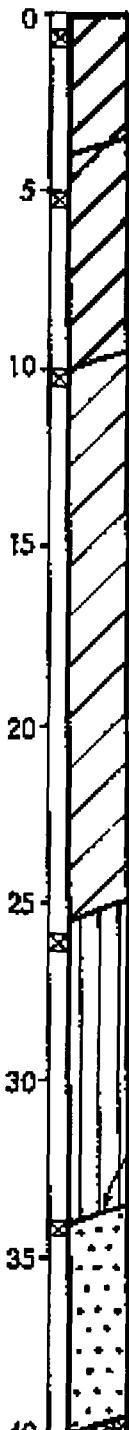
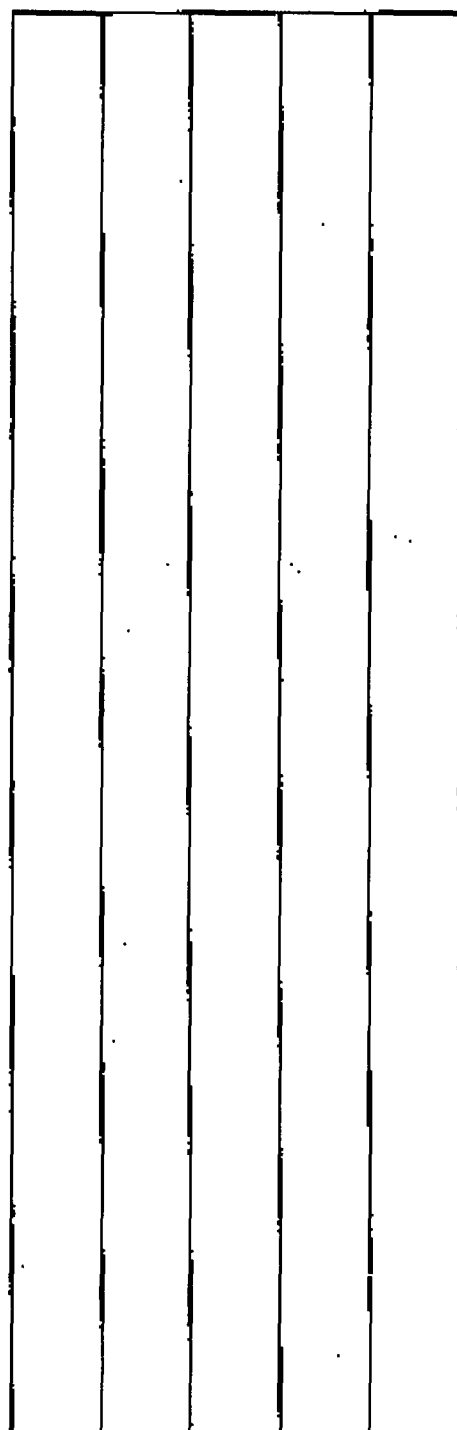
Sample

LOG OF BORING 1

Equipment 24" Flight Auger

Elevation 170.0

Date 4/7/70



BLACK SILTY CLAY (CH)
soft, moist
change to medium stiff at 3"

GRAY BROWN SANDY SILTY CLAY
(CH) - medium stiff, moist

BROWN SANDY CLAY (CL)
stiff, moist

BROWN SANDY SILT (ML)
medium stiff, moist

BROWN GRAVELLY SAND (SP)
loose, moist, well rounded

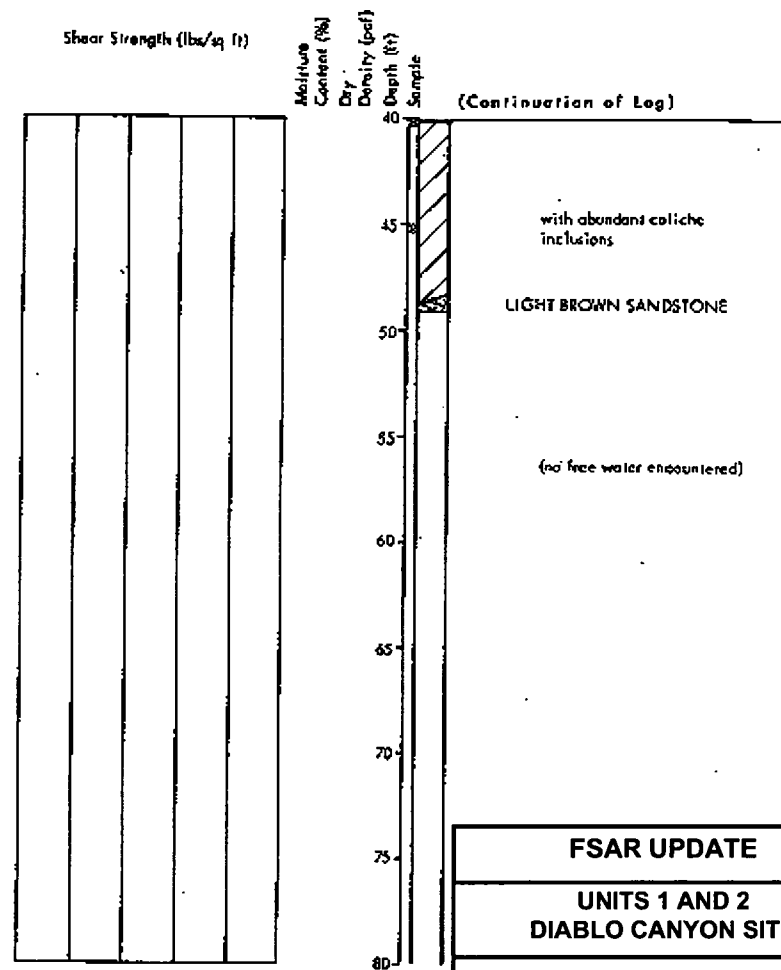
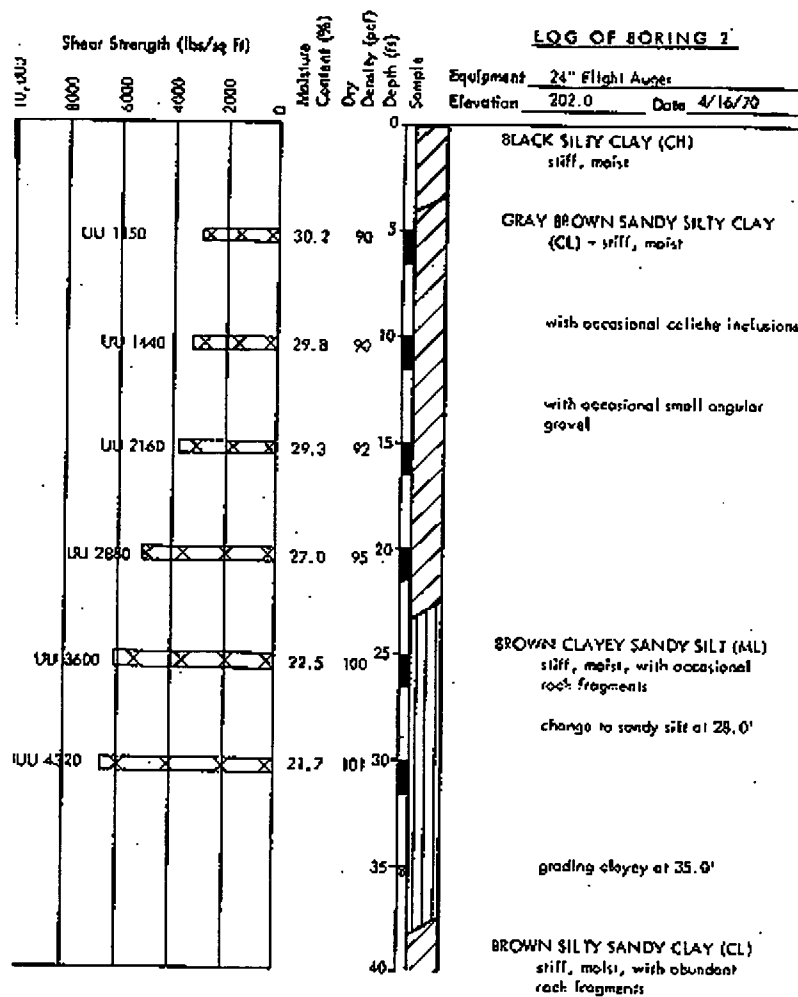
(no free water encountered) BROWN SANDSTONE

FSAR UPDATE

**UNITS 1 AND 2
DIABLO CANYON SITE**

**FIGURE 2.5-23
POWER PLANT SLOPE
LOG OF BORING 1**

Revision 11 November 1996



FSAR UPDATE

UNITS 1 AND 2
DIABLO CANYON SITE

FIGURE 2.5-24
POWER PLANT SLOPE
LOG OF BORING 2

Revision 11 November 1996

Shear Strength (lbs/sq ft)

Moisture
Content (%)

Dry

Density (pcf)

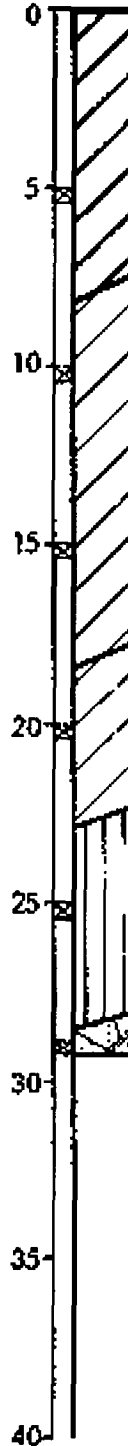
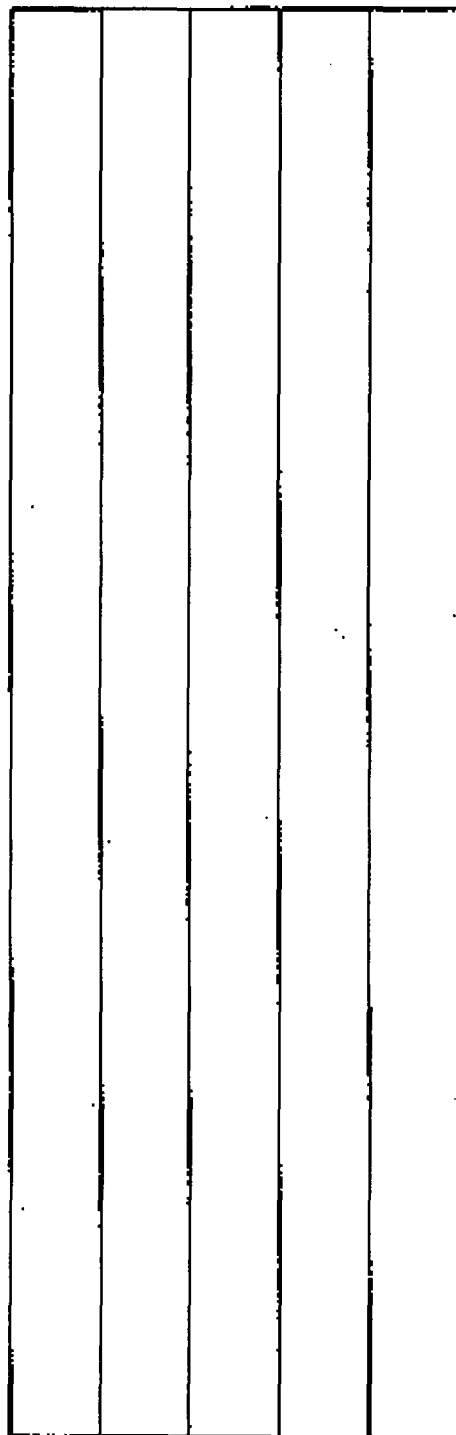
Depth (ft)

Sample

LOG OF BORING 3

Equipment 24" Flight Auger

Elevation 178.0 Date 4/16 70



DARK BROWN SANDY CLAY (CH)
stiff, dry

change to medium stiff at 4'

BROWN SANDY CLAY (CL)
stiff, moist, with occasional
angular gravel

BROWN SANDY CLAYEY SILT (ML)
medium stiff, moist

BROWN CLAYEY SANDY SILT (ML)
medium stiff, moist, with
occasional rock fragments

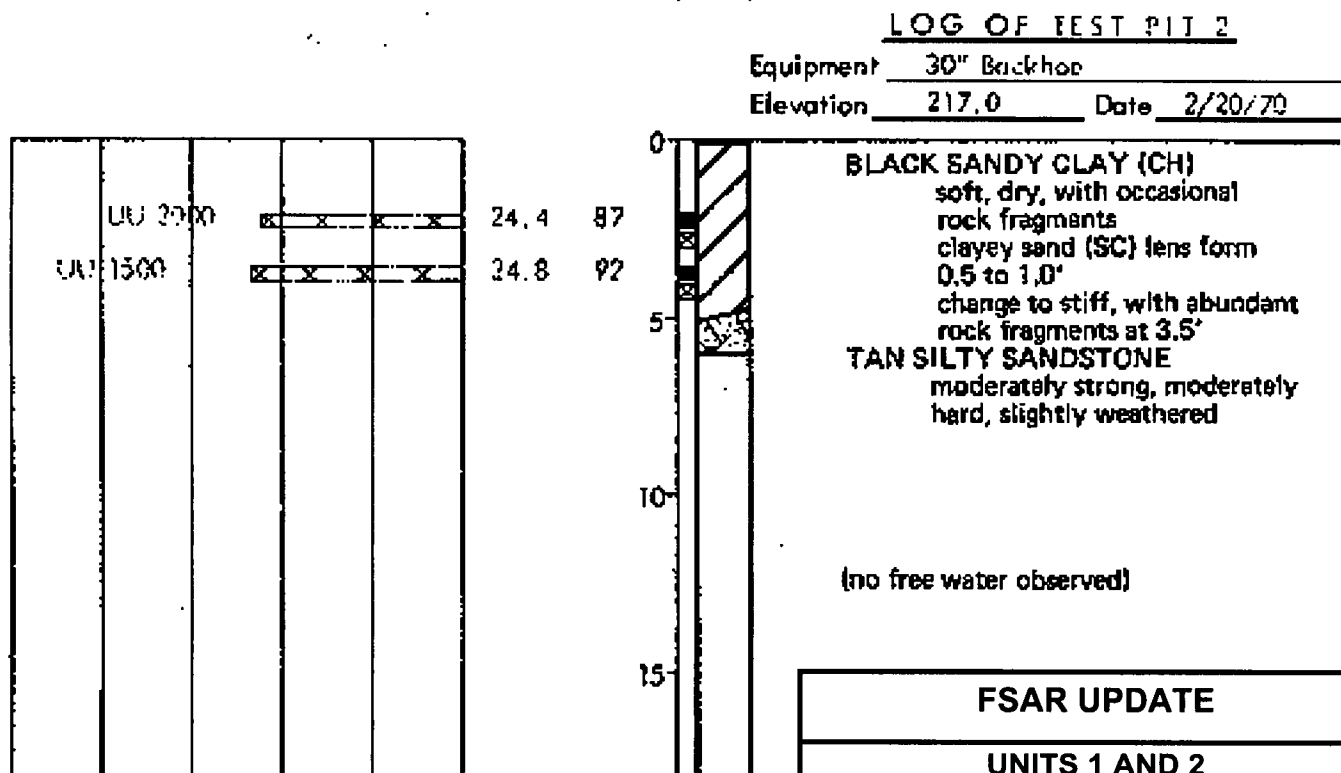
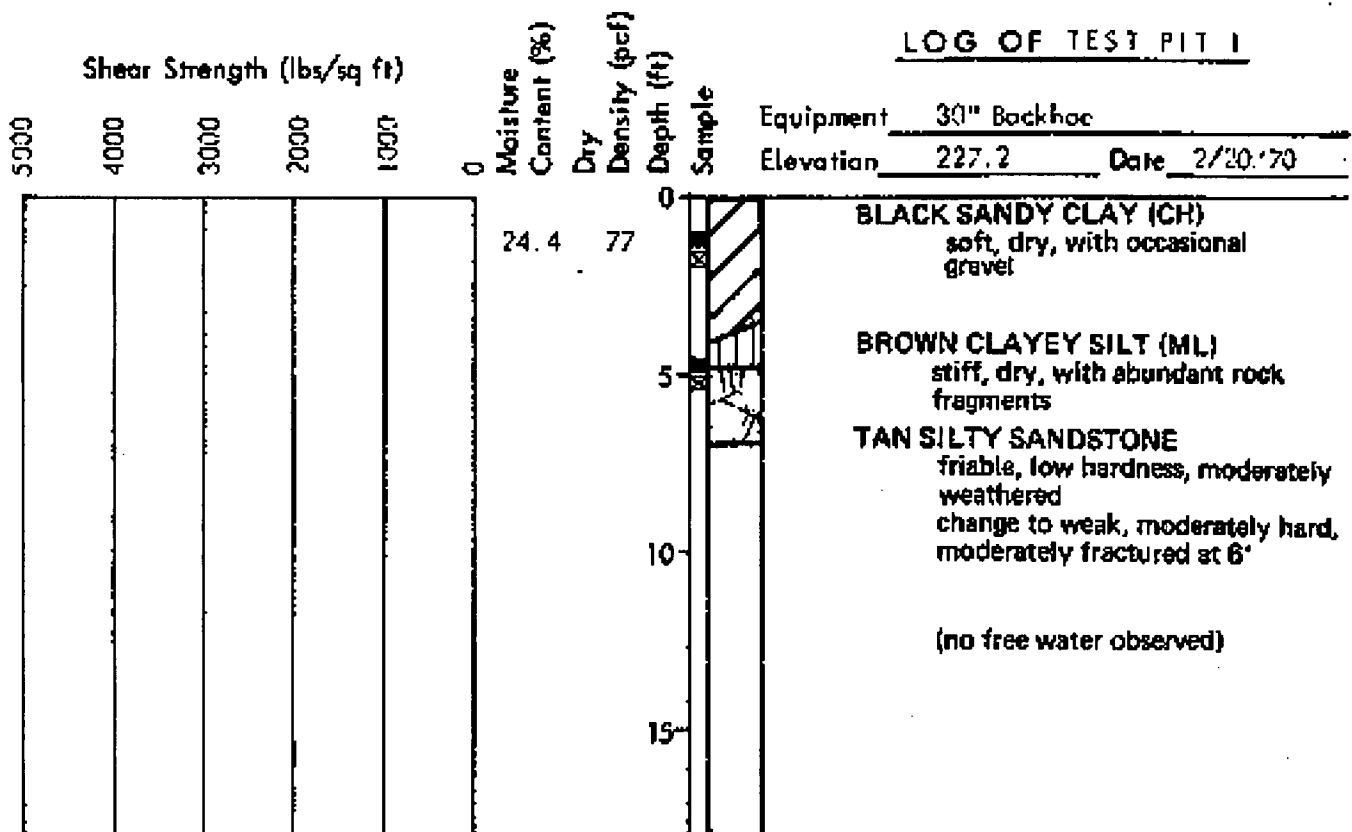
LIGHT BROWN SANDSTONE
moderately fractured, hard,
strong

(no free water encountered)

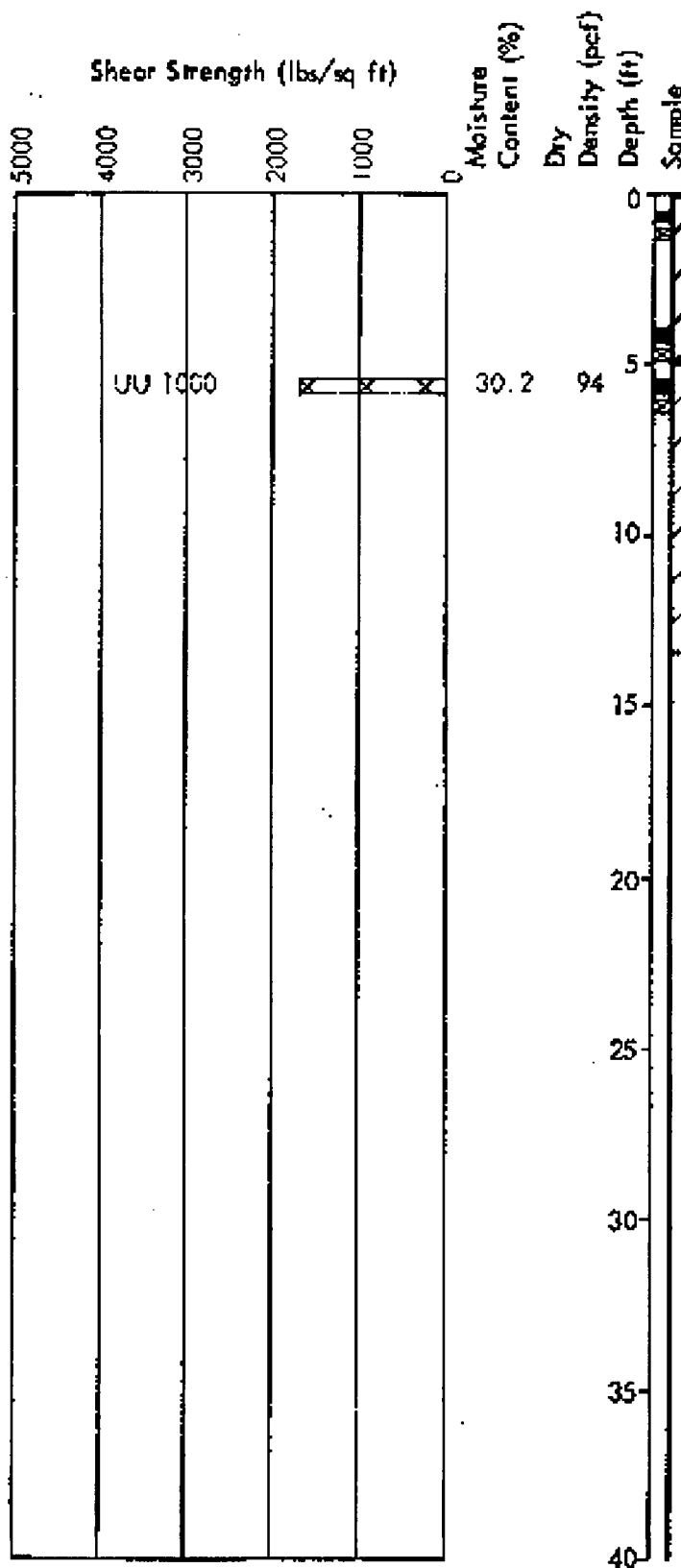
FSAR UPDATE

**UNITS 1 AND 2
DIABLO CANYON SITE**

**FIGURE 2.5-25
POWER PLANT SLOPE
LOG OF BORING 3**



| |
|---|
| FSAR UPDATE |
| UNITS 1 AND 2 DIABLO CANYON SITE |
| FIGURE 2.5-26 POWER PLANT SLOPE LOG OF TEST PITS 1 & 2 |



LOG OF TEST PIT 3

Equipment 30" Backhoe
 Elevation 204.6 Date 2/20/70

BLACK SILTY CLAY (CH)
 stiff, moist, with occasional
 angular gravel

BROWN SANDY SILTY CLAY (CL)
 soft to stiff, wet, with
 occasional gravel
 abundant caliche inclusions
 from 5.5 to 7'

abundant large angular gravel
 at 12'
 (depth limit of backhoe)

(no free water encountered)

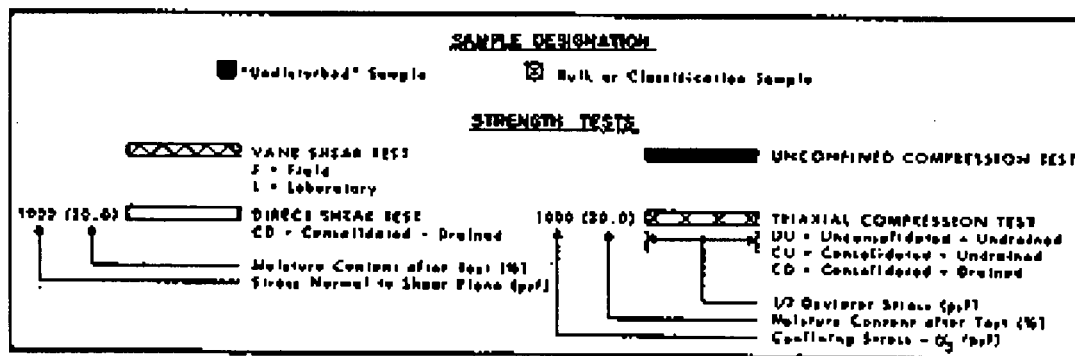
FSAR UPDATE

**UNITS 1 AND 2
 DIABLO CANYON SITE**

**FIGURE 2.5-27
 POWER PLANT SLOPE
 LOG OF TEST PIT 3**

| MAJOR DIVISIONS | | | TYPICAL NAMES | |
|--|---|---------------------------------------|---|---|
| COARSE GRAINED SOILS MORE THAN HALF IS LARGER THAN #200 SIEVE | GRAVELS MORE THAN HALF COARSEST FRACTION IS LARGER THAN NO. 4 SIEVE SIZE | CLEAN GRAVELS WITH LITTLE OR NO FINES | GW | WELL GRADED GRAVELS, GRAVEL - SAND MIXTURES |
| | | | GP | POORLY GRADED GRAVELS, GRAVEL - SAND MIXTURES |
| | | GRAVELS WITH OVER 12% FINES | GM | SILTY GRAVELS, POORLY GRADED GRAVEL - SAND - SILT MIXTURES |
| | | | GC | CLAYEY GRAVELS, POORLY GRADED GRAVEL - SAND - CLAY MIXTURES |
| | SANDS MORE THAN HALF COARSE FRACTION IS SMALLER THAN NO. 4 SIEVE SIZE | CLEAN SANDS WITH LITTLE OR NO FINES | SW | WELL GRADED SANDS, GRAVELLY SANDS |
| | | | SP | POORLY GRADED SANDS, GRAVELLY SANDS |
| | | SANDS WITH OVER 12% FINES | SM | SILTY SANDS, POORLY GRADED SAND - SILT MIXTURES |
| | | | SC | CLAYEY SANDS, POORLY GRADED SAND - CLAY MIXTURES |
| FINE GRAINED SOILS MORE THAN HALF IS SMALLER THAN #200 SIEVE | SILTS AND CLAYS LIQUID LIMIT LESS THAN 50 | ML | INORGANIC SILTS AND VERY FINE SANDS, EDGE FLOES, SILTY OR CLAYEY FINE SANDS, OR CLAYEY SILTS WITH SLIGHT PLASTICITY | |
| | | CL | INORGANIC CLAYS OF LOW TO MEDIUM PLASTICITY, GRAVELLY CLAYS, SANDY CLAYS, SILTY CLAYS, LEAN CLAYS | |
| | | OL | ORGANIC CLAYS AND ORGANIC SILTY CLAYS OF LOW PLASTICITY | |
| | SILTS AND CLAYS LIQUID LIMIT GREATER THAN 50 | MH | INORGANIC SILTS, MICACEOUS OR ORBITACIOUS FINE SANDY OR SILTY SILTS, PLASTIC SILTS | |
| | | CH | INORGANIC CLAYS OF HIGH PLASTICITY, FAT CLAYS | |
| | | OH | ORGANIC CLAYS OF MEDIUM TO HIGH PLASTICITY, ORGANIC SILTS | |
| | HIGHLY ORGANIC SOILS | | PI | PEAT AND OTHER HIGHLY ORGANIC SOILS |

UNIFIED SOIL CLASSIFICATION SYSTEM

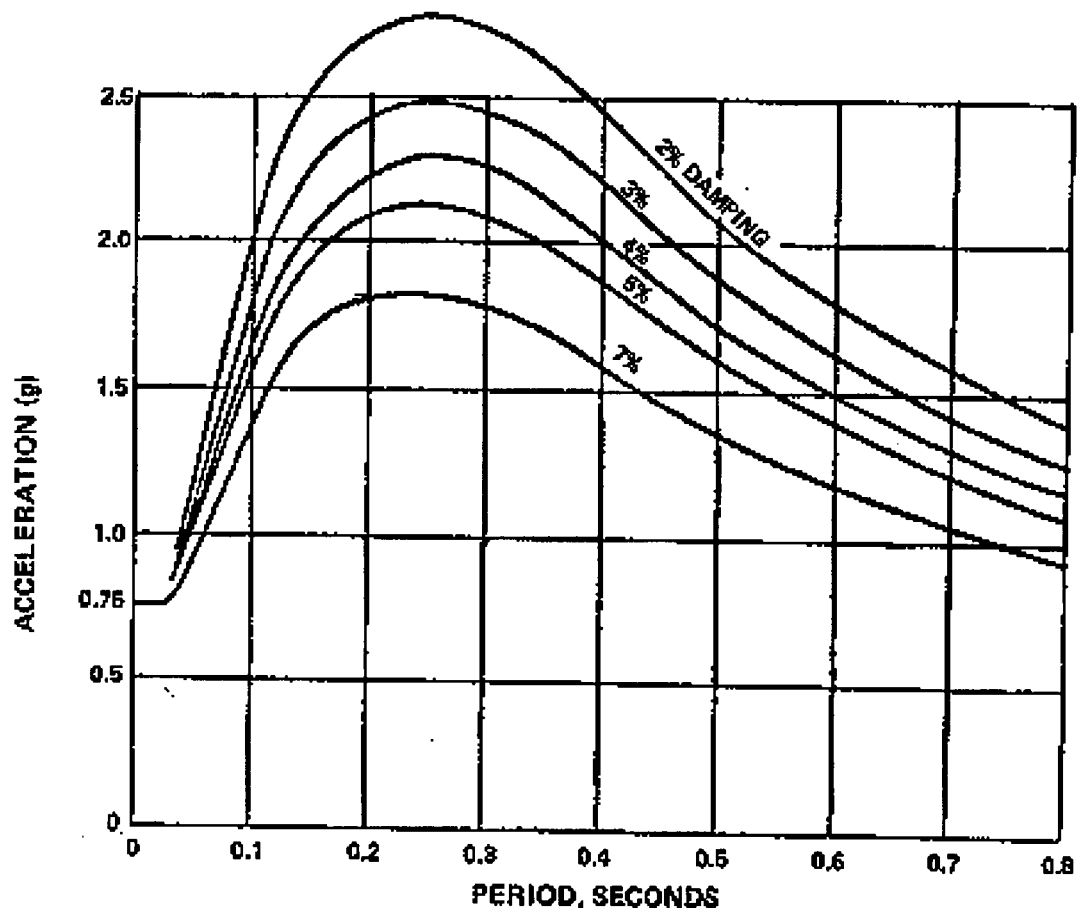


KEY TO TEST DATA

FSAR UPDATE

UNITS 1 AND 2 DIABLO CANYON SITE

FIGURE 2.5-28 POWER PLANT SLOPE SOIL CLASSIFICATION CHART AND KEY TO TEST AREA

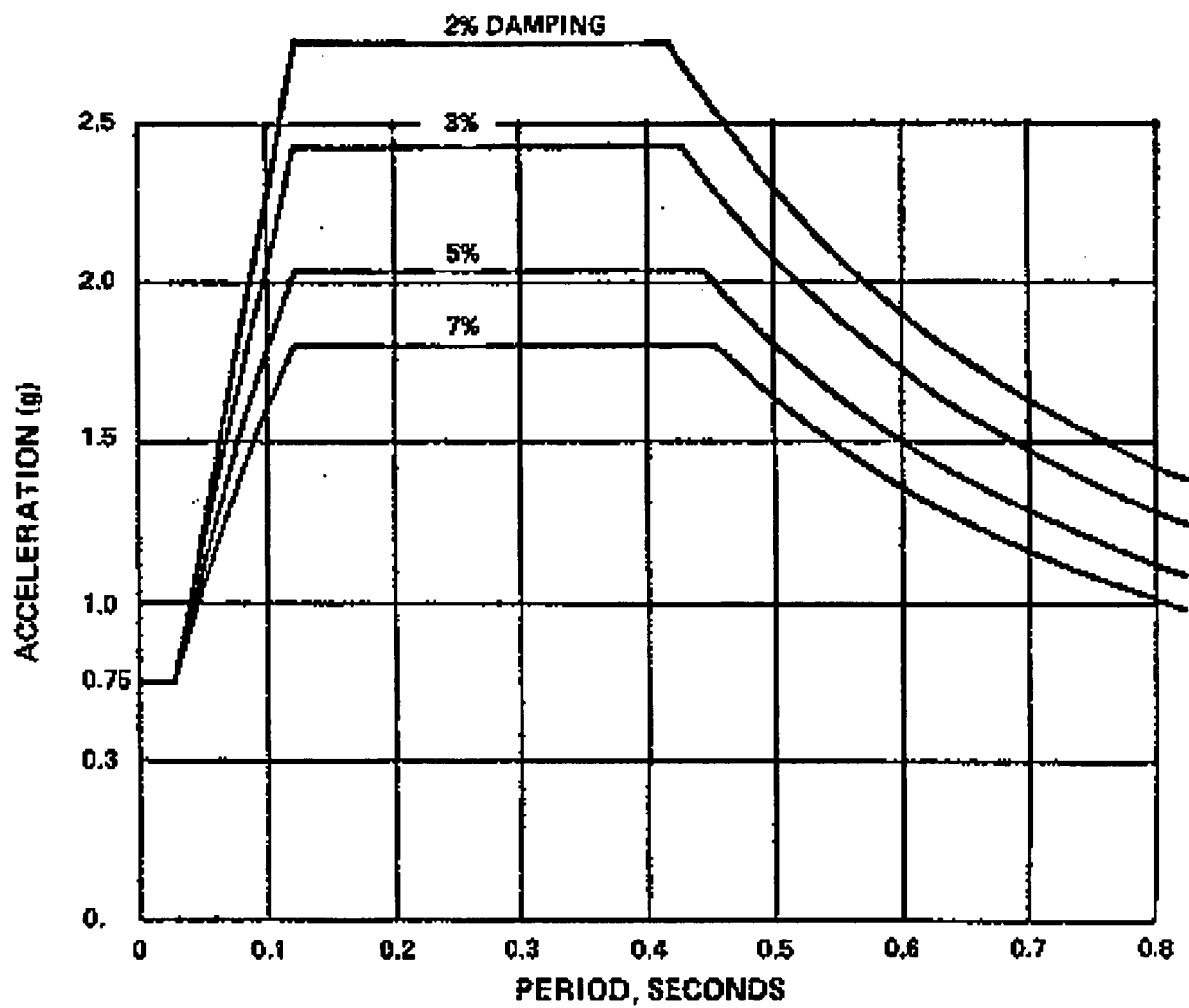


FSAR UPDATE

**UNITS 1 AND 2
DIABLO CANYON SITE**

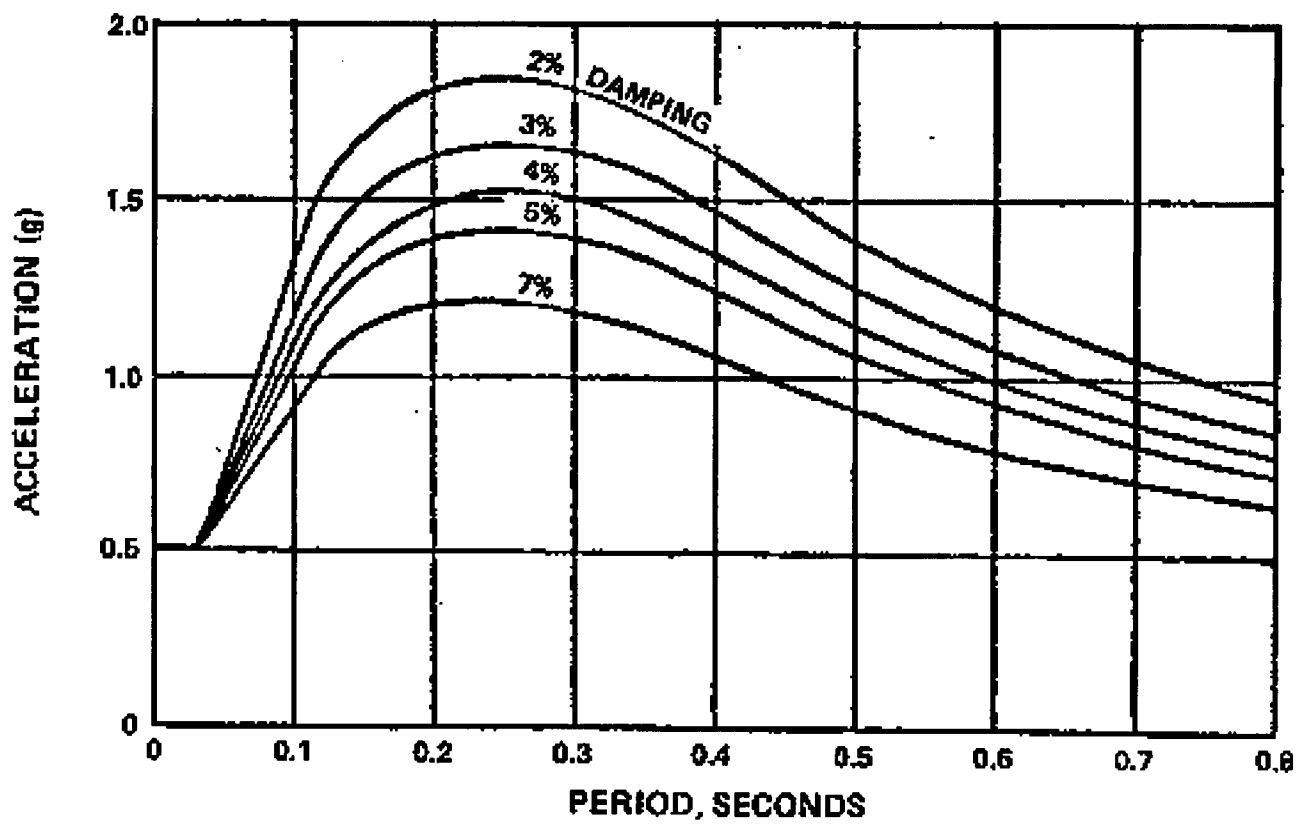
**FIGURE 2.5-29
FREE FIELD SPECTRA
HORIZONTAL
HOSGRI 7.5M/BLUME**

Revision 11 November 1996



| |
|--|
| FSAR UPDATE |
| UNITS 1 AND 2 DIABLO CANYON SITE |
| FIGURE 2.5-30 FREE FIELD SPECTRA HORIZONTAL HOSGRI 7.5M/NEWMARK |

Revision 11 November 1996

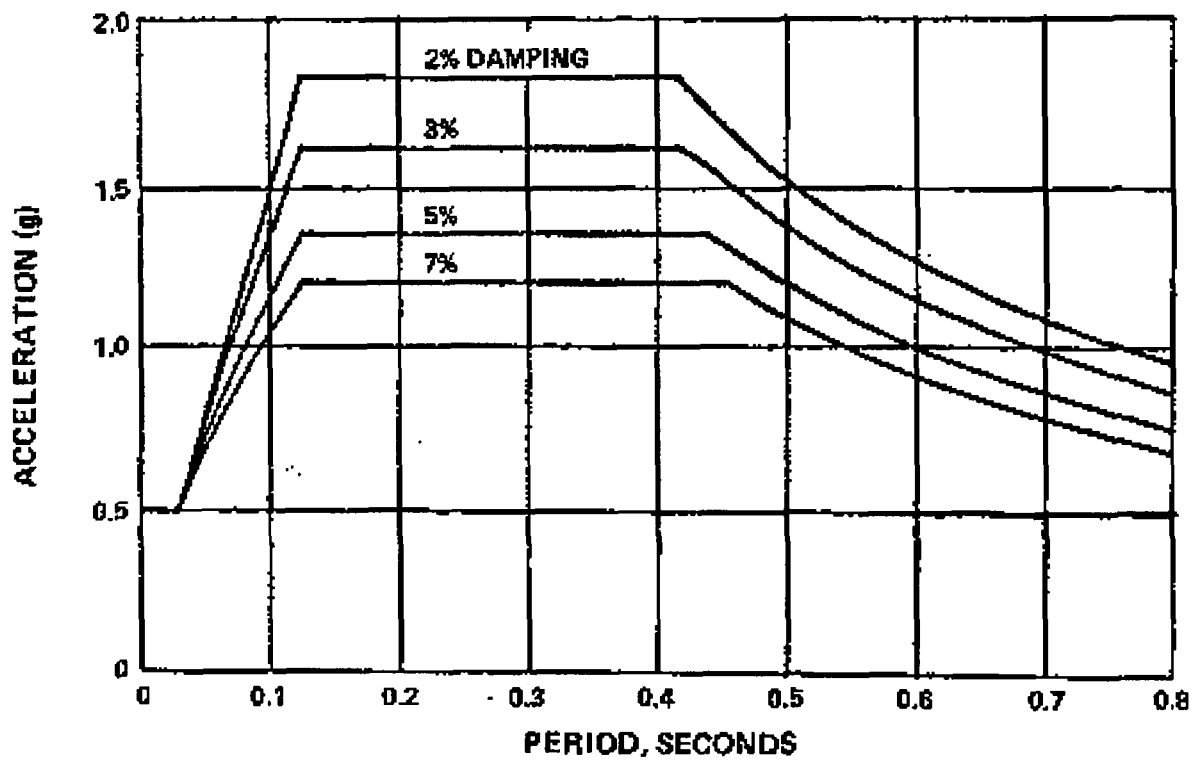


FSAR UPDATE

**UNITS 1 AND 2
DIABLO CANYON SITE**

**FIGURE 2.5-31
FREE FIELD SPECTRA
VERTICAL
HOSGRI 7.5M/BLUME**

Revision 11 November 1996



| |
|--|
| FSAR UPDATE |
| UNITS 1 AND 2 DIABLO CANYON SITE |
| FIGURE 2.5-32 FREE FIELD SPECTRA VERTICAL HOSGRI 7.5M/NEWMARK |

Revision 11 November 1996